

**Building Energy Calculator:
A Design Tool for Energy Analysis of Residential Buildings in
Developing Countries**

by

Jonathan Y. Smith

B.S., Mechanical Engineering
Georgia Institute of Technology, 2002

Submitted to the Department of Mechanical Engineering
in Partial Fulfillment of the Requirements for the Degree of

Master of Science in Mechanical Engineering
at the
Massachusetts Institute of Technology

June 2004

© 2004 Massachusetts Institute of Technology
All rights reserved

Signature of Author _____
Department of Mechanical Engineering
May 3, 2004

Certified by _____
Leon R. Glicksman
Professor of Architecture and Mechanical Engineering
Thesis Supervisor

Accepted by _____
Ain A. Sonin
Professor of Mechanical Engineering
Chairman, Department Committee on Graduate Studies

This page is intentionally left blank.

Building Energy Calculator: A Design Tool for Energy Analysis of Residential Buildings in Developing Countries

by

Jonathan Y. Smith

Submitted to the Department of Mechanical Engineering
on May 3, 2004 in Partial Fulfillment of the
Requirements for the Degree of
Master of Science in Mechanical Engineering

ABSTRACT

Buildings are one of the world's largest consumers of energy, yet measures to reduce energy consumption are often ignored during the building design process. In developing countries, enormous numbers of new residential buildings are being constructed each year, and many of these buildings perform very poorly in terms of energy efficiency. One of the major barriers to better building designs is the lack of tools to aid architects during the preliminary design stages.

In order to address the need for feedback about building energy use early in the design process, a simplified model was developed and implemented as a software design tool using the C++ programming language. The new program requires a limited amount of input from the user and runs simulations to predict heating and cooling loads for residential buildings. The user interface was created with the architect in mind, and it results in direct graphical comparisons of the energy requirements for different building designs. The simulations run hour by hour for the entire year using measured weather data. They typically complete in less than two seconds, allowing for very fast comparisons of different scenarios.

A set of simulations was run to perform a comparison between the new program and an existing tool called Energy-10. Overall, the loads predicted by the two programs were in good agreement.

Thesis Supervisor: Leon R. Glicksman

Title: Professor of Architecture and Mechanical Engineering

This page is intentionally left blank.

Acknowledgments

I am grateful to my thesis supervisor, Professor Leon Glicksman, for his valuable insight and guidance throughout the project. I also appreciate his patience and understanding as I learned a new programming language.

I am indebted to the Alliance for Global Sustainability and Emeritus Professor Warren Rohsenow for financially supporting my graduate studies.

This page is intentionally left blank.

Table of Contents

Chapter 1 Introduction	11
Chapter 2 Background	15
2.1 Introduction.....	15
2.2 Energy Consumption.....	16
2.3 Existing Software Design Tools	19
2.4 Characterization of Housing	21
2.5 Building Standards	23
2.6 Conclusions.....	27
Chapter 3 Model of a General Building Component.....	29
3.1 Introduction.....	29
3.2 Finite Difference Methods for Transient Heat Conduction.....	31
3.3 Model for Thermally Massive Building Components.....	34
3.4 Simplified Model for Lightweight Building Components	36
3.5 General Boundary Conditions	38
3.6 Assumptions Used in the General Model.....	40
3.7 Summary.....	42
Chapter 4 Outdoor Boundary Conditions	43
4.1 Introduction.....	43
4.2 Weather Data	43
4.3 Solar Angles.....	44
4.4 Incident Solar Flux	47
4.5 Assumptions.....	48
Chapter 5 Building Component Models	49
5.1 Introduction.....	49
5.2 Exterior Walls	49
5.2.1 Thermal Model.....	50
5.2.2 Assumptions.....	51

5.3 Ground Floor.....	52
5.3.1 Thermal Model.....	53
5.3.2 Assumptions.....	55
5.4 Internal Floors.....	56
5.4.1 Thermal Model.....	56
5.4.2 Assumptions.....	57
5.5 Roof.....	57
5.5.1 Thermal Model.....	58
5.5.2 Assumptions.....	59
5.6 Glazing System.....	59
5.6.1 Thermal Model.....	59
5.6.2 Assumptions.....	65
5.7 Indoor Air.....	66
5.7.1 Thermal Model.....	67
5.7.2 Assumptions.....	68
5.8 Convection and Radiation Coefficients.....	68
5.8.1 Thermal Model.....	69
5.8.2 Assumptions.....	70
5.9 Simulation Using the Model Components.....	71
5.10 Summary.....	74
Chapter 6 Model Parameters and the User Interface.....	75
6.1 Introduction.....	75
6.2 Location Group—Select a City.....	77
6.3 Building Geometry Group.....	77
6.3.1 Variables Defining Building Size: Width, Depth, Height per Floor, and Number of Floors.....	77
6.3.2 Number of Apartments per Floor.....	78
6.3.3 Wall 1 Orientation.....	79
6.4 Windows Group.....	79
6.4.1 Window Type.....	79
6.4.2 Quality of Installation and Materials.....	80

6.4.3 Overhangs above S, SE, and SW Windows.....	81
6.4.4 Wall 1-4 Window Percentage	82
6.5 Wall Construction Group.....	82
6.5.1 Main Wall Components.....	82
6.5.2 Insulation Type.....	83
6.5.3 Wall Insulation Thickness.....	83
6.5.4 Roof Insulation Thickness	84
6.6 Other Model Parameters.....	84
6.7 Program Output.....	84
Chapter 7 Simulation Results and Model Validation	87
7.1 Sample Simulation Results	87
7.1.1 Base Case Building.....	87
7.1.2 Simulation Set 1: Varied Window Types	88
7.1.3 Simulation Set 2: Varied Quality of Window Installation and Materials.....	88
7.1.4 Simulation Set 3: Varied Wall Insulation Thickness	89
7.2 Model Validation: Comparison to Energy-10 Simulations	90
7.2.1 Base Case Building in Energy-10	91
7.2.2 Description of Buildings Simulated	92
7.2.3 Simulation Results.....	93
Chapter 8 Conclusions and Recommendations for Future Work.....	95
References	99
Appendix A Nomenclature.....	101
Appendix B Summary of Parameter Values	107
Appendix C Program Flowchart.....	111
Appendix D Notes on Program Source Code.....	115

This page is intentionally left blank.

Chapter 1

Introduction

Although buildings account for roughly one third of the world's energy consumption, energy efficiency is often an afterthought in the building design process. It is common practice for an architect to virtually complete the design of a building without concern for energy use and then bring in an engineer to design the HVAC system. When this course of action is taken, the building will not perform as well as it could in terms of energy consumption because the engineer has extremely limited flexibility in making improvements. As a result, unnecessary energy costs and negative environmental effects will be incurred.

The primary goal of the project presented in this thesis has been the development of a software design tool called Building Energy Calculator (often referred to as “the program” or “the new program”) to guide architects toward more energy-efficient building designs. The program performs hourly simulations and approximates the annual heating and cooling loads for different buildings input by the user. Chinese residential buildings have been targeted specifically because of the current growth in the sector, which is one important factor driving the recent increases in both energy production and carbon dioxide emissions in China. Architects face a plethora of issues when designing buildings, and energy tends to be an area that lacks focus in their training. The new software can help them see how some of their important design decisions impact building energy performance. The hope of this work is that by providing such a tool, energy performance will be considered as an important part of a project from its inception. Early consideration of these issues is one of the keys to achieving more efficient buildings because there is still a great deal of flexibility to incorporate sustainable features into the design.

If the program is to be used in the manner described, it must appeal to its intended user—the architect in the conceptual design phase of a project. Taking this fact into account, the program was created using several guiding principles: (1) ease of use, (2) minimal required input, and (3) output that is simple, graphical, and quantitative. Problems in any of these areas can quickly lead to frustration, likely resulting in abandonment of the program. Ease of use is especially important for this tool since it is intended for use early in the design process. An

interface that can be learned very quickly is necessary since a designer will not be willing to invest a large amount of time for basic information about energy at a point when so many issues need to be addressed. It is also important not to bombard the designer with all kinds of detailed questions to which they do not yet know the answers. Input to the program should be restricted to variables that can be considered at the early design stages, and a limited number of choices for each variable should be presented. Finally, the results of the program must be easy to understand. To that end, the program should produce graphical results that allow for side-by-side comparison of different scenarios. The relative strength of one design compared to another in terms of energy efficiency should be readily apparent from the output of the program. Creating a program following these guiding principles requires making simplifying assumptions and using typical values for many parameters. Simplifications of this sort are appropriate since the goal of the program is to provide rough estimates that guide the user by indicating which of their decisions have the greatest impact on building energy use.

The approach described above is fundamentally different from that taken by most other programs that work in a similar way. Typically, programs that do energy simulations are extremely detailed in nature and are useful late in the design process or after a design is complete. The new program that has been developed makes many more assumptions and limits the input of the user to a several basic choices. By tailoring the options for materials, cities, etc. and appropriately setting model parameters, it targets Chinese residential buildings. More advanced input options could be realized by changing assumptions in the source code and rebuilding the program or by developing a new user interface that is more detailed. Since the model used is general, most of the calculation engine could be used in a more advanced simulation tool. However, many advanced tools already exist, so the need for more simple tools is addressed by this project.

The remainder of this thesis is divided into several chapters. Chapter 2 gives some relevant background on energy consumption and housing in China, building codes, and existing software design tools. The trends in energy consumption that are presented motivate focusing attention on the Chinese residential sector, and the overview of existing design tools demonstrates the need for more simplified energy simulation software.

The thermal model used in the simulation program is presented in three chapters. Chapter 3 presents the general modeling approach used for building components and boundary

conditions. Chapter 4 then describes how the outdoor boundary conditions are determined using weather data. Included in this discussion is the calculation of solar position and incident solar radiation. Chapter 5 then presents the details of specific building component models, many of which are derived from the general model from Chapter 3.

Chapter 6 explains the input options found in the user interface of the program and the way in which they affect the model parameters. Chapter 7 first demonstrates a typical use of the new software by presenting simulation results for a set of building scenarios. Then, simulation results for a few base case buildings using the new program are compared with those for the same buildings using an existing program called Energy-10. Finally, Chapter 8 makes some concluding remarks and recommendations for future work.

This page is intentionally left blank.

Chapter 2

Background

2.1 Introduction

The Chinese economy has experienced rapid growth in recent years, and this economic prosperity has spawned the first generation of homeowners in the country. The higher standard of living has resulted in a significant increase in energy consumption from the residential sector, and this trend is expected to continue into the future. Since millions of new dwelling units are being built each year, their energy efficiency is becoming increasingly important on a national as well as a global scale. Many of the new buildings being constructed do not perform nearly as well as they could with today's technology in terms of energy efficiency, and improvements must be made in this area if China is to continue to develop in a sustainable manner.

Several software tools exist to help architects understand how their design decisions will impact the energy performance of their buildings. Some of these tools take input from the user about their building, make simplifying assumptions, and run some sort of energy simulation. The reported results are supposed to give the user some information about how well the building he or she described will perform. A common problem among these programs is that they require extensive input from the user, and much of the required information is not known during the preliminary design stages of the building. In addition, the results of these programs are often difficult to interpret for someone without a thorough technical background. If either of these problems is present, the tool is of limited use to the building designer, and it is more likely that sustainability issues in the building will go unaddressed.

The Chinese Ministry of Construction recently issued a document called *Green Guidelines for Sustainable Housing in China*, which is an important attempt to bring sustainability into the foreground during the building design process. The guidelines highlight important issues in several areas of sustainability, including energy use, site selection, materials, water management, and others. The document addresses areas very similar to the Leadership in Energy & Environmental Design (LEED) building rating system issued by the United States Green Building Council. LEED is a well-known system that assigns an overall rating to a

building based on points it receives for meeting sustainability criteria in several different categories. Although not mandatory, rating systems such as LEED are important because they establish a mark at which people can aim to make their building designs sustainable. A standard imposing constraints on the energy consumption of new Chinese residential buildings is necessary to limit their negative environmental impact. There are many things that need to be given careful consideration in creating fair standards specific to China, but existing systems in the United States and elsewhere can provide a good starting point.

2.2 Energy Consumption

Figure 2.1 shows estimates of the total energy consumption in China over the past several years from three different sources—the Energy Information Association [8], British Petroleum [3], and the *China Statistical Yearbook* [5]. There is some variation between the sources, but the general upward trends in energy consumption are the same in each case. Looking at the numbers from the Energy Information Association, China’s 42 EJ of energy consumption in 2001 was second only to the United States, and it accounted for approximately 9.8% of the world’s total 430 EJ. The slight downward trend from 1997 to 2000 was affected by many factors, most importantly the gradual slowdown of the economic boom in the industrial sector. The recent reversal of this trend is seen in all three data sets, and the upward trend is expected to continue. The per capita energy consumption follows a pattern very similar to the total energy

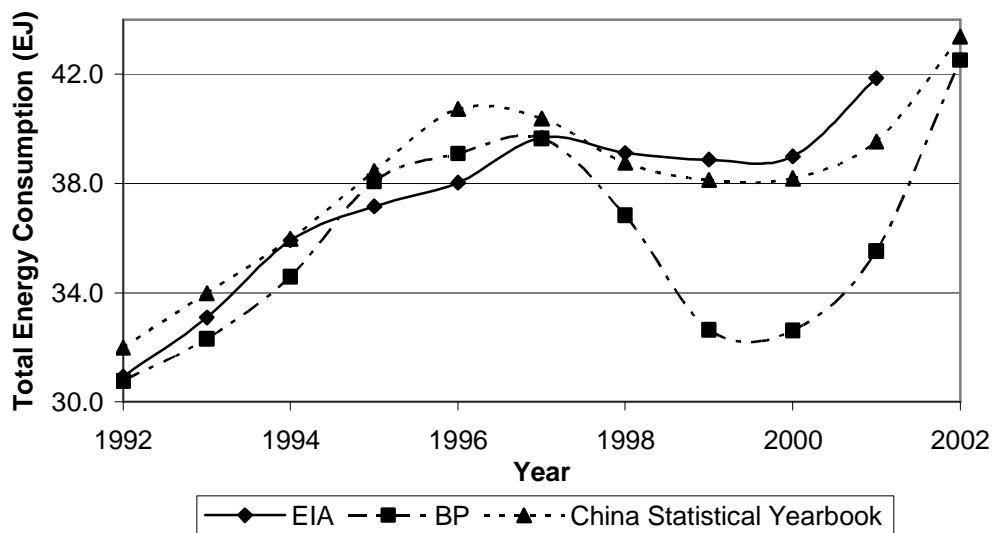


Figure 2.1: China’s annual energy consumption since 1992 (1 EJ = 10^{18} J)

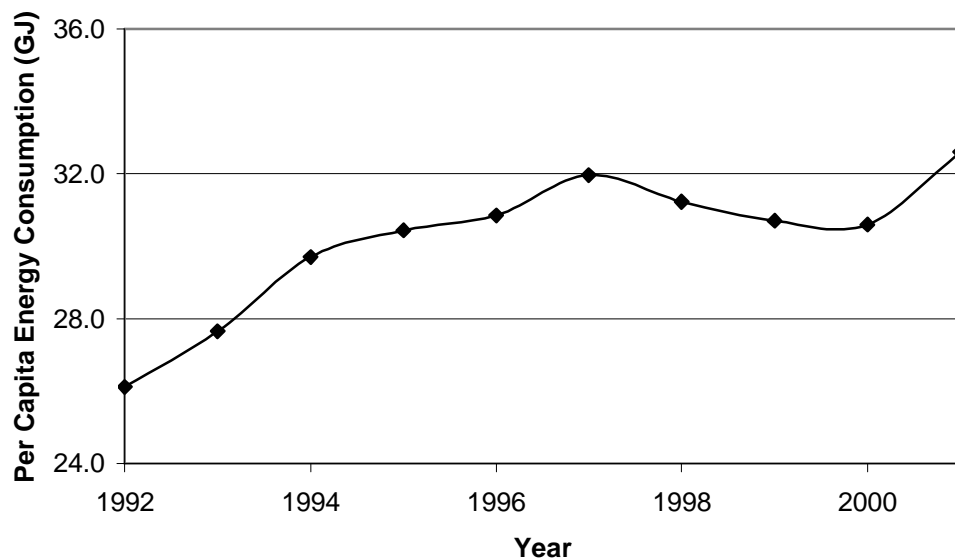


Figure 2.2: China's per capita energy consumption since 1992 (EIA data)

consumption, as shown in Figure 2.2, which uses the Energy Information Association's data. The population in 2001 was 1.29 billion, yielding a per capita energy consumption of 33 GJ. This figure is much lower than the world average per capita energy consumption of 69 GJ for the same year.

Table 2.1 shows a breakdown of China's energy consumption by sector for 2001 [5]. The manufacturing sector still accounts for the majority of energy consumption, but the residential and transportation sectors are growing rapidly. The standard of living in China has increased considerably, and many people are buying their own homes for the first time. Consequently, the demand for new residential buildings is high, and construction of these buildings is occurring at an incredible rate—about ten million new units per year. Previously, employers provided housing to employees that was very close to work, but that has changed with the move to individual home ownership. As a result, people have to travel farther, and the transportation sector is expanding rapidly and consuming an increasing proportion of the nation's energy. The recent economic prosperity in China has resulted in a fundamental switch from employer-provided housing to employee-owned housing, which has caused growth in both the residential and transportation sectors.

Because of the large-scale construction of new residential buildings, energy consumption in the residential sector has become an important issue. Glicksman, Norford, and Greden list

Table 2.1: Chinese energy consumption by sector for 2001 [5]

Sector	Energy Consumption (EJ)	Energy Consumption Per Capita (GJ)	Percentage of Total (%)
Manufacturing	21.1	16.5	55.9
Residential	4.5	3.5	12.0
Power, Gas, & Water Supply	3.2	2.5	8.4
Transportation	3.0	2.4	8.0
Mining and Quarrying	2.8	2.2	7.5
Wholesale and Retail	0.9	0.7	2.5
Construction	0.4	0.3	1.1
Others	1.8	1.4	4.7
Totals	38	30	100

three key economic factors that impact residential energy efficiency—increased consumer spending capacity, economic disincentives for investment in energy efficiency, and limited capital. The increased consumer spending capacity has led to the demand for new and bigger residential buildings, air conditioners, and major electrical appliances. Although air conditioners and appliances are big energy consumers, space heating accounts for roughly 80-90% of the total energy consumed in Chinese residential buildings [9]. The average size of dwelling units is increasing, which substantially increases energy consumption required for both heating and cooling. In addition to increased energy consumption due to the growing number of residential buildings, these trends resulting from the increased consumer spending capacity tend to increase the *rate* of energy consumption in each new building.

According to Glicksman, Norford, and Greden, energy efficiency and other sustainability issues in the new housing market take the back seat to the issue of affordability. Chinese people typically spend a much higher proportion of their income on housing than their western counterparts, and sources of financing are limited. The affordability issue combined with the fact that the huge market has attracted numerous developers who are primarily concerned with making money has caused limited attention to be focused on sustainability. Despite the fact that the scale of the construction will have global impacts on energy and the environment, governmental regulations do little to encourage investment in energy efficiency, and it is usually very difficult to get funds approved to make energy improvements to existing buildings and equipment. The transitioning Chinese economy facilitates consuming increased amounts of

energy through the increased spending capacity of its people, and it also presents obstacles to improving energy efficiency.

In addition to the economic factors already mentioned, several other factors contribute to the suboptimal energy performance seen in many buildings. The lack of enforced building standards allows for low quality construction without any real penalties. In developed countries, history has shown that enforced policy is usually required to make progress, although voluntary measures have had some degree of success. Enforcement is a difficult issue in China because there are simply not enough building inspectors to deal with all of the new construction, again showing that limited resources reduce the ability to make an impact in residential building energy consumption. A largely untrained construction workforce often lacks the skills to properly install windows and insulation, which can substantially degrade the performance of a building. Finally, there is a lack of both consumer and builder education in sustainability, which tends to push important issues into the background so that they never receive proper attention.

The standard of living in China has improved to such a point that it is now critical to focus on the energy efficiency of residential buildings, particularly the new buildings that are being constructed. Since China's population is so large, the increased demand for energy associated with the economic prosperity has a significant impact on energy use and the environment. Space heating still accounts for a very large proportion of residential energy consumption, and vast energy savings can be realized simply by ensuring that buildings are in compliance with standards for insulation. More efficient windows, daylighting, shading, and natural ventilation are other energy-saving strategies that should be integrated into building design. The large number of new residential buildings in China demands that attention be given to their energy consumption in order to minimize the associated negative effects. Developing good building codes, enforcing them, educating the energy consumer, and implementing voluntary programs similar to Energy Star in the United States are the best ways to ensure that energy issues are addressed.

2.3 Existing Software Design Tools

The consumption of energy in buildings involves many complicated physical processes occurring simultaneously. Models of varying degrees of complexity have been developed to approximate these processes, and the most sophisticated models are required to obtain highly

accurate results. There are a number of simulation and design tools available to aid architects in the sustainable design process. These programs vary widely in scope, including everything from very detailed hourly energy simulations using computational fluid dynamics to extremely simplified analyses that are not project-specific. Cordero gives a representative list and discussion of such tools [6]. A few tools applicable to energy simulation and energy-efficient design, including some not mentioned by Cordero, are summarized below.

Energy Plus, DOE-2, and PowerDOE are energy simulation tools released by the U.S. Department of Energy (DOE). Energy-10 is a similar tool released by the National Renewable Energy Laboratory (NREL), et al. Like many of the programs that perform a whole building energy simulation and performance analysis, they require detailed information from the user and provide fairly accurate results. Although such programs are very useful to people such as HVAC system designers, they are often of limited use during preliminary design because so much information about the building has to be known in order to run a simulation. A user would not be able to see the effects of changing specific features without doing an elaborate setup of building parameters. Energy Plus and DOE-2 do not have a user interface; instead, they work based on text file input and output. Programs like these require a significant investment of time to learn, and they are typically used by people who specialize in building energy rather than architects, who deal with a much broader range of issues. PowerDOE and Energy-10 have graphical user interfaces and are much less complicated than Energy Plus and DOE-2. However, they are still detailed enough that the required input is fairly extensive, and there is significant learning curve. Although programs that perform energy simulations are useful in many design applications, many of them do not provide much help when rough approximations of the energy impact of certain features are desired during the conceptual design of a building.

The Green Building Advisor is a program at the other end of the spectrum that has extremely limited user input and gives general recommendations that are not project-specific. It includes a variety of resources, such as case studies and technical articles, to help designers in the preliminary design phase. Cordero gives the following list of output related to energy use: building envelope, heating, cooling, ventilation, lighting, appliances, equipment, water heating, and energy sources. Information of this type is undoubtedly useful during the preliminary design of a building; however, the fact that it is not project-specific means that it cannot give a real estimate of energy savings and opportunities for a specific building in a given location.

The Building Design Advisor 3.0 is another simplified design tool that is being developed. This tool is linked to DOE-2, an established set of simulation tools for energy performance. It will also link to other tools for airflow, daylighting, and CAD modeling. The results are displayed in a graphical format that is easy to understand, but it seems that the input will still be somewhat difficult. This program shows promise of being very useful once all the bugs are worked out since it makes use of many different tools that are already available and performs a simplified building analysis.

Although there are many software packages that perform energy analysis for buildings, many of them require comprehensive input from the user and attempt to perform very accurate calculations. When a building is in its preliminary design phase, many of these required inputs are not known by the architect or building designer, rendering the software of little practical use. Other programs do not perform an analysis detailed enough to produce results that are project-specific. Although heat transfer is a complicated process, simple models can be developed with relatively little information to produce first order estimates of building performance. The development of a software package that requires minimal input from the user and produces meaningful output describing the energy consequences of various design decisions will be useful to building designers interested in sustainability. Due to the current construction trends in China, a program that specifically targets Chinese residential buildings would be particularly helpful to the architects designing these new buildings. By showing the energy and cost savings associated with construction quality, adequate insulation, double-glazed windows, and other energy-conscious design choices, the software will encourage the implementation of such features in new buildings. In order to be effective, such a program must provide output in a simple, graphical manner so that results can be easily understood and interpreted. A software package that requires minimal design information and performs project- and site-specific analyses will benefit designers by informing them of the energy-related consequences of the decisions that they have to make early in the design process.

2.4 Characterization of Housing

Characterizing housing in China is difficult because the income level and types of housing vary greatly from region to region. Recently, there has been a trend of mass movement to very large cities in China. The new housing being built consists largely of low-rise and high-

rise buildings made from concrete or steel with many separate single-family dwelling units. According to Glicksman, Norford, and Greden, a typical unit has 60-120 m² of floor space, and about 4-7 million units per year are being built in urban areas. Some typical low-rise residential buildings in Beijing are shown in Figure 2.3. Many of these units have numerous opportunities for increased energy efficiency, including better insulation, more energy-efficient windows, natural ventilation, and better site design [9]. The recent urban shift of the Chinese population has resulted in large-scale construction of residential buildings, and these buildings account for an increasingly large proportion of China's total energy consumption.

Village housing in China is extremely varied from location to location. Some poor villages have extremely small homes and no commercial power, while others have spacious homes with electrical appliances. Materials used in homes include red brick, granite, earth, reinforced concrete, and ceramics [4]. Many of the poorer villages use biomass as their primary fuel, and cooking is the major energy consumer. Figure 2.4 shows some round dwellings (yuanlou) typical in southwest China. Although the varied housing in rural China makes it difficult to make generalizations, the recent trend has been migration from villages into large urban areas and from village housing into large residential buildings.



Figure 2.3: Typical residential buildings in Beijing. Photograph courtesy of Tridib Banerjee, University of Southern California



Figure 2.4: Rural housing in southwest China.

2.5 Building Standards

The changing economic environment in China has led to greatly increased energy use in residential buildings, which has made the energy efficiency of these buildings an important concern from an energy resource and an environmental standpoint. Many new residential buildings are not performing at appropriate levels given the current state of technology. Establishing and enforcing standards requiring that buildings meet certain criteria and performance levels is an issue that needs to be addressed since the performance of these buildings will have important local and global ramifications. China is the second largest consumer of energy in the world, and energy consumption there is expected to continue its upward trend. The fast rate at which new buildings are being constructed presents a tremendous opportunity to minimize some of the negative impacts that come along with the economic prosperity and increased standard of living. Since most of these new buildings are expected to have a fairly long life cycle, any small improvements that can be made to their energy efficiency will have a large impact over their lifetimes.

Glicksman, Norford, and Greden also address building regulations and standards in China [9]. The Chinese Ministry of Construction issued the Energy Conservation Design Standard for New Heating Residential Buildings in 1996, which is both performance- and specification-based.

The standard limits heat transfer coefficients of building features such as windows, walls, and floors, but these limits are significantly higher than the limits in other countries. The authors also note that one of the biggest problems with this standard lies in its enforcement. Numerous political factors along with the fact that there are not enough building inspectors to verify that all new buildings are in compliance contribute to the lack of enforcement of the government's standards. Despite the standards that are in place, the authors note that "Even new buildings still often have little or no insulation in the exterior envelopes, loose single-glazed windows, short material lifetimes, and a disregard for siting to promote wind-driven ventilation." This statement again suggests that some very simple changes in building design and construction can have a significant impact on energy use. Clearly, the issue of standards needs to be addressed in China. Evaluation of current standards is necessary to ensure that they are reasonable and, if followed, will result in acceptable building performance. The enforcement of these standards is a more political issue, but it is equally important to address if the standards are to be meaningful and produce results.

The Leadership in Energy & Environmental Design (LEED) Rating System issued by the U.S. Green Building Council is one of the most well-known voluntary standards for sustainable buildings [16]. Since Chinese standards for buildings are based to some extent on those of the United States, an understanding of the scope and limitations of these policies is important in the quest to create and implement acceptable standards for Chinese buildings. The LEED rating system has a list of criteria, each of which is worth a certain number of points. Once certain prerequisite requirements are met, points are awarded when acceptable documentation is provided to show that a building meets a criterion. Buildings are assigned an overall rating based on the total number of points that are received. Having one set of criteria for all buildings is beneficial in that it establishes a single standard to which one can always refer to see if sustainability features are being given ample consideration. However, there is a drawback since the standard does not allow for adaptation based on differences that invariably come up when buildings are being designed for different purposes and under different circumstances. Still, the range of points that is set up for each rating category allows for some flexibility in the criteria that a building must meet.

The points available under the LEED Rating System are divided into six categories: (1) sustainable sites, (2) water efficiency, (3) energy and atmosphere, (4) materials and resources, (5)

indoor environmental quality, and (6) innovation and design process. All of these issues are important to sustainability, but this review will focus on the energy and atmosphere category.

There are three prerequisite requirements that must be met in the energy and atmosphere category before any points can be awarded. The first prerequisite involves hiring a commissioning authority to help ensure that the building is designed and installed as intended by its buyer. The next prerequisite requires compliance with ASHRAE Standard 90.1 (or the local energy code if it is more demanding). This standard was written for all buildings other than low-rise residential buildings, which fall under ASHRAE Standard 90.2 [1]. Prerequisite 3 requires that no CFC-based refrigerants be used in any new HVAC system. Of these prerequisites, compliance with the ASHRAE standard has the most direct application to energy efficiency, and the following discussion will be of Standard 90.2. The standard sets requirements for maximum values of heat transfer coefficients (i.e. U values) for building walls, windows, roofs, floors, etc. Once these minimum requirements are met, there are two separate paths that can be followed for a building to gain compliance. The first path involves meeting specific requirements for the HVAC and water heating systems of the building. HVAC requirements involve load, ductwork and insulation, equipment specification and installation, control, and efficiency levels. Requirements for the water heating system involve insulation, maximum usage in showers, point-of-service hot water, reuse and recovery, etc. The second path to compliance is a comparison of estimated annual energy cost. Methods for calculating estimated energy costs are given for all of the major utilities. The estimated cost is then compared to a base case building designed to meet the specifications described in the first path to compliance. These two alternatives give some flexibility in the design of a building's energy systems while forcing certain minimum requirements to be met. The basis for much of the LEED Rating System's energy and environmental requirements is a comprehensive ASHRAE standard that has been worked on for many years.

The first credit available in the energy and atmosphere category is to optimize energy performance beyond the requirements set forth in ASHRAE Standard 90.1. If a new building's estimated annual energy cost (computed by the method set forth in the standard) is 15% below the requirement (5% below for existing buildings), one point is awarded. Each further reduction of 5% receives an additional point, up to a maximum of ten points awarded if estimated annual energy cost is 60% below the requirement. The next credit is for using renewable energy sources

such as solar, wind, and geothermal strategies. One, two, or three points are awarded if 5, 10, or 20% of the building's energy comes from on-site renewable energy sources. The third credit awards one point for additional commissioning beyond the prerequisite requirement. To receive this point, an independent design team must be contracted to do several reviews prior to construction. The fourth credit awards one point for installing HVAC and refrigeration equipment that contains no HCFCs or Halons. The fifth credit awards one point for installation of equipment to meter all major energy consuming equipment. Doing so allows for verification that the building is achieving the intended energy performance. The sixth and final credit awards one point for obtaining at least 50% of the building's electricity from renewable sources. Of the seventeen possible credits in the energy and atmosphere category of the LEED Rating System, ten come from optimizing energy performance beyond the standard set by ASHRAE, and another comes from installing metering equipment to ensure that performance is at design levels. The other credits do not directly involve the energy performance of the building, but instead focus on green energy sources, purely environmental considerations, and commissioning.

The primary method by which the LEED Rating System evaluates a building's energy efficiency is through the well-established energy efficiency standard written by ASHRAE. LEED requires that the proper standard be met as a minimum requirement and then awards points for exceeding the standard by certain amounts. The ASHRAE standard/LEED model is a good one to consider for Chinese standards because it includes both performance- and specification-based standards. It allows for flexibility in the design of a building energy system, but at the same time requires that certain minimum standards be met. The idea of specification-based standards to establish a bare minimum requirement seems like a good idea because it would prevent builders from using very cheap insulation and windows simply to cut costs, but the proper minimum value would have to be determined from the available materials in the area and their costs. Performance-based standards beyond the minimum are appealing because they allow for increased flexibility by only requiring a certain level of overall building performance and not of individual system performance. The different types of standards all need to be evaluated in the Chinese context to see if they can be reasonably applied. The LEED rating system and ASHRAE energy standards provide an excellent point of reference on which Chinese building standards can be based, but the specific requirements need to be reevaluated so that they are appropriately applied. The standard needs to be fair, and ensuring that such is the case

requires that consideration be given to economic, material, and political matters in addition to energy efficiency.

In August of 2001, the Chinese Ministry of Construction released a voluntary set of building guidelines known as *Green Guidelines for Sustainable Housing in China*, which are based in part on information from the U.S. Green Building Council and other similar agencies and programs. There are five major categories that are covered in the guidelines: (1) urban environmental planning and design, (2) energy resources and the environment, (3) indoor environmental quality, (4) community water and wastewater management, and (5) materials and resources. These categories are clearly parallel to those in the LEED building rating system. Greden lists the important elements in the energy resources and environment category as energy efficient building design, optimization of energy systems (HVAC), use of renewable energy sources, and environmental impact of energy consumption [10]. The creation of these guidelines is an important step for China on the road to required standards because it begins to get the right people thinking about sustainability issues. The scope of the document seems very similar to the LEED rating system in the areas covered, but it does not give out points for meeting certain criteria. China has used to its advantage the experience that other nations have in taking steps towards sustainability in new buildings. The establishment of the *Green Guidelines* should help pave the road for enforceable standards in the future that will require certain performance levels of new buildings.

2.6 Conclusions

Recent upward trends in the energy consumption of the Chinese residential sector have been the result of economic prosperity. Many new buildings with increasingly large living spaces are being constructed, and their demand for energy is increasing as more people buy large appliances and air conditioners. Since China is the world's largest country and such a significant proportion of its population is moving into new homes, the energy efficiency of these new buildings is an important world concern. The trends in energy use motivate work in many areas, including the development of simple design tools to help architects fully understand the energy consequences of some of their design choices. There are several building rating systems in place in the world, and one of the most well known is the LEED rating system in the United States, which expands on existing standards. In the energy category, the ASHRAE standard on building

energy efficiency is built upon. Together, these two documents provide a valuable reference for a Chinese building standard. However, evaluations and modifications have to be made to make sure that the standard is fair in the Chinese context. Implementation of such a standard may have to be gradual, but setting a standard is the only way to ensure that the new buildings will not put any unnecessary strain on the world's energy resources and the environment. China has already begun to take the first steps with the release of the *Green Guidelines for Sustainable Housing in China* and similar previous documents. These guidelines are voluntary, and the next step is to move towards required, enforced standards.

Chapter 3

Model of a General Building Component

3.1 Introduction

Heat flow through building envelopes is a multi-faceted and extremely complicated process. The outside of the building is exposed to varying temperatures, wind conditions, and amounts of solar radiation. After some amount of time, changes in outdoor conditions make their way to the inside surface of the building, where they can affect the indoor conditions and impose a load on the building's heating or cooling system.

Before presenting the model that will be used for many of the building components, it is helpful to see an overall picture of the building and its interactions with the environment. Figure 3.1 shows the various modes of energy transport that will be considered in the model. Since the program resulting from this work is intended to be used during the preliminary design stages, details about the interior of the building will not be determined, which is why interior walls and other details are not present in the figure. Dotted lines in the figure represent solar (i.e. short wave) radiation. Notice that solar radiation is present on both the outside and inside surfaces of the building since the glazing system transmits some amount of the incident radiation. Solid lines represent conduction either through the building components or, in the case of the slab perimeter, between the building and the surrounding ground. Dashed lines represent some combination of convection and infrared (i.e. long wave) radiation. The block arrows represent the infiltration of outdoor air into the building, which is a critical factor in determining overall building energy consumption. This process is the only one in the figure that is not a heat transfer mechanism, per se. The general model that is derived in this chapter applies to all of the components that are gray in the figure.

In order to approximate the amount energy that will be required to heat and cool a building, the heat transfer through each of many building components must be modeled. These components include the exterior walls, floors, and roof, among others. A general building component consists of several different material layers put together to form a composite

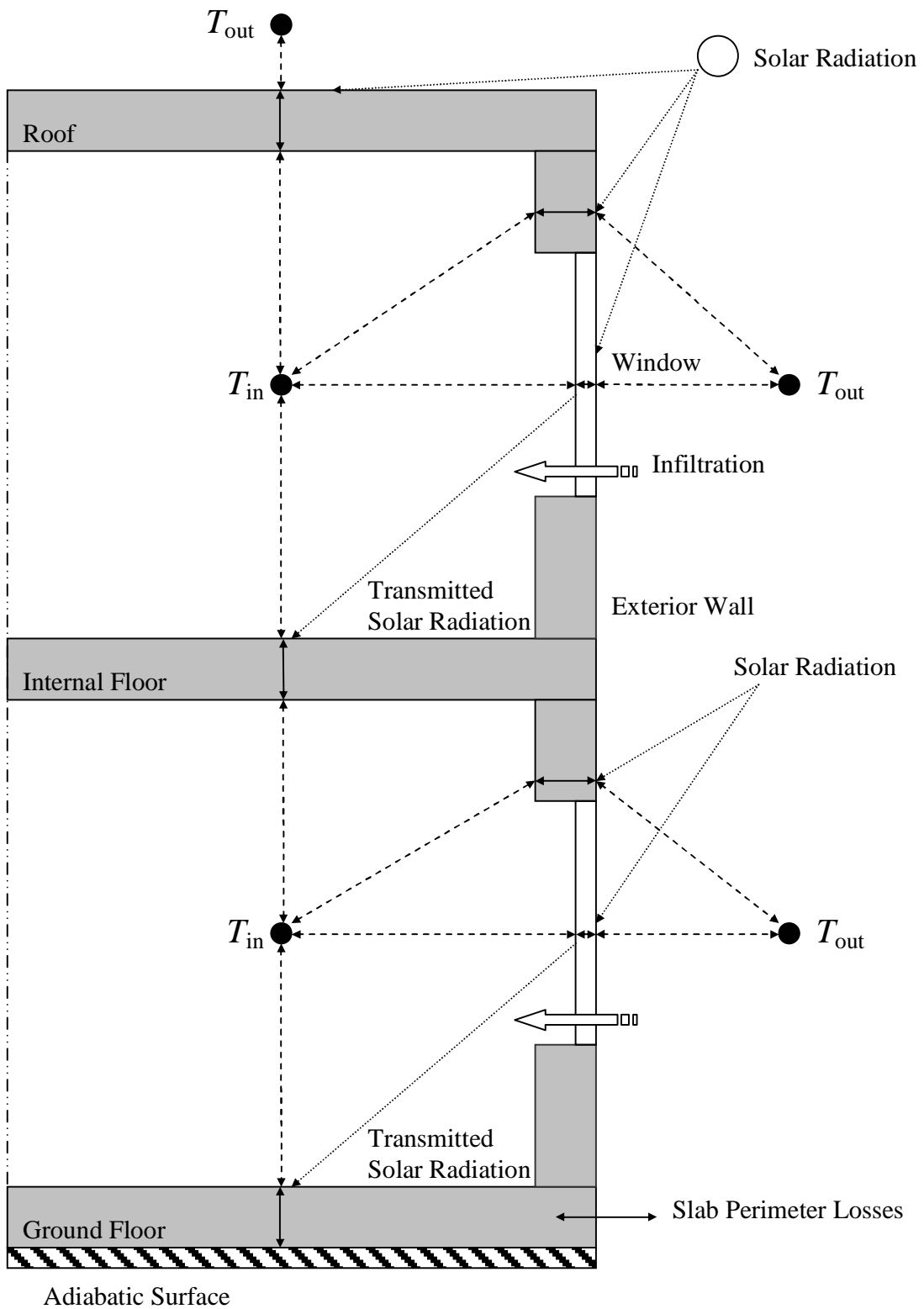


Figure 3.1: Partial building cross section showing forms of energy transport and boundary conditions

structural component, and the aim of this chapter is to develop a model that can be used in this general case. Once the model is developed, it will be applied individually to specific building components in another chapter. One important aspect of the building to which this model does not apply is the glazing system, which is addressed separately in another chapter.

3.2 Finite Difference Methods for Transient Heat Conduction

Buildings are exposed to continuously changing boundary conditions such as outdoor temperature, solar radiation, and wind conditions. Since the building envelope has the capacity to store some amount of heat, i.e. thermal mass, these unsteady boundary conditions are moderated by the envelope and propagate with a time lag. For example, a drop in outdoor temperature may not be felt at the inside surface of a wall for several hours. As a result, steady state calculations will not provide a realistic assessment of building energy requirements.

In general, the thickness of a wall, roof, or floor is much smaller than either of its other two dimensions. Except near the edges, the one-dimensional form of the heat equation provides an accurate approximation of the spatial and temporal dependencies of heat diffusion through the surface:

$$\rho c \frac{\partial T}{\partial t} \approx k \frac{\partial^2 T}{\partial x^2} \quad (3.1)$$

where

ρ = material density

c = material specific heat ($c_p=c_v=c$ for incompressible materials)

k = material thermal conductivity

T = temperature

t = time

x = distance in the direction of material thickness

While analytical solutions to this equation do exist, they are extremely difficult to obtain in the case of heat flow through buildings due to several factors, including (1) unsteady boundary conditions, (2) multiple layers of different materials, and (3) the discrete nature of available weather data.

This problem lends itself well to a numerical finite difference method, which involves dividing the material into small sections and solving for temperatures at some number of discrete

nodes rather than as a continuous distribution. Figure 3.2 shows part of a material layer divided into sections with a node at the center of each section. The slab is infinite in the vertical direction and into the page. Both explicit and implicit methods can be used to write finite difference equations, and a brief comparison of these two methods is presented below.

Explicit methods are good computationally because nodal temperatures at the next time step can be solved for explicitly in terms of the temperatures at the current time step, which are already known. The explicit finite difference equation for node n in Figure 3.2 below is:

$$\rho c \frac{\hat{T}_n - T_n}{\Delta t} \approx k \frac{T_{n-1} - T_n}{\Delta x^2} + k \frac{T_{n+1} - T_n}{\Delta x^2} \quad (3.2)$$

where the hat (^) above a variable means that it is evaluated at time $t + \Delta t$. When both sides of this equation are multiplied by Δx , the left-hand side represents the time rate of change of energy storage of the section surrounding node n (per unit area), and the right-hand side represents the net heat flux into the section (per unit area). Known values are substituted directly into equations to solve for the desired values at the next time step. The main disadvantage of these methods is that the solution can become unstable for certain choices of Δx and Δt . See [11] for a discussion of the stability criteria.

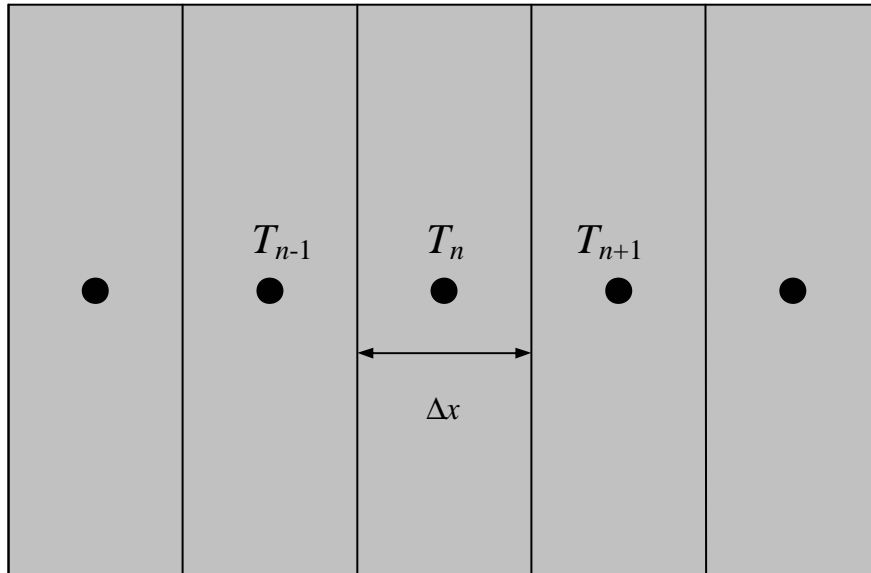


Figure 3.2: Material slab divided into discrete sections with nodes at the center (infinite in directions orthogonal to x)

Implicit methods require greater computational effort than explicit methods because all of the finite difference equations at each time step must be solved simultaneously. The temperature of a node n at the next time step depends on those of its neighbors at the next time step, which are not known ahead of time:

$$\rho c \frac{\hat{T}_n - T_n}{\Delta t} \approx k \frac{\hat{T}_{n-1} - \hat{T}_n}{\Delta x^2} + k \frac{\hat{T}_{n+1} - \hat{T}_n}{\Delta x^2} \quad (3.3)$$

With the extra computational effort required comes a significant advantage—solutions obtained using implicit methods are unconditionally stable. Unconditional stability allows much greater flexibility in choosing the spacing between nodes and the size of the time step. This flexibility can result in a lower overall computation time than the explicit method because many fewer nodes and time steps may be required to solve the problem. Such is the case for building energy simulations, where relatively large spacing between nodes and longer time steps are perfectly acceptable.

Since weather data are typically available for every hour of the year, a time step of one hour is very convenient. This rather large time step renders the Crank-Nicolson method, a compromise between the implicit and explicit methods, a more appropriate choice [7]. Using this method, the finite difference equation takes the form:

$$\rho c \frac{\hat{T}_n - T_n}{\Delta t} \approx \frac{k}{2} \left(\frac{\hat{T}_{n-1} - \hat{T}_n}{\Delta x^2} + \frac{\hat{T}_{n+1} - \hat{T}_n}{\Delta x^2} \right) + \frac{k}{2} \left(\frac{T_{n-1} - T_n}{\Delta x^2} + \frac{T_{n+1} - T_n}{\Delta x^2} \right) \quad (3.4)$$

The Crank-Nicolson form effectively averages the implicit and explicit forms. When the time step is very small, the nodal temperatures do not change very much from one time step to the next, so it is relatively unimportant whether temperatures are evaluated at time t or $t+\Delta t$. When larger time steps are used, more careful consideration must be given to this matter, and an average value is more appropriate. Like the implicit methods, the Crank-Nicolson method requires solving all of the equations simultaneously and is unconditionally stable. Despite their stability, these methods can result in numerically induced oscillations that are physically impossible. This issue is explored and dealt with in a later section.

All of the elements in the model that incorporate thermal mass are based on Equation (3.4). These elements include the exterior walls, ground floor, internal floors (i.e. all floors except the ground floor), and roof. In the following sections, this equation will be generalized to incorporate layers of different materials and various boundary conditions.

3.3 Model for Thermally Massive Building Components

Major building components almost always consist of several layers of different materials. For example, a simple exterior wall may consist of a layer of concrete, a layer of insulation, and a layer of gypsum wall board. Equation (3.4) must be modified so that it can account for nodes completely within a single layer of material, at the interface between two different materials, or at an external boundary of a material. All three cases can be generalized for the exterior walls, ground floor, internal floors, and roof. Even though each surface has unique boundary conditions, the equation still takes a general form that can be used for any surface.

Multiplying both sides of Equation (3.4) by Δx and some minor algebraic manipulation yields a new form used by Spindler that is more easily interpreted [14]:

$$\rho c \Delta x \frac{\hat{T}_n - T_n}{\Delta t} \approx \frac{1}{2} \left(\frac{\hat{T}_{n-1} - \hat{T}_n}{\Delta x/k} + \frac{\hat{T}_{n+1} - \hat{T}_n}{\Delta x/k} \right) + \frac{1}{2} \left(\frac{T_{n-1} - T_n}{\Delta x/k} + \frac{T_{n+1} - T_n}{\Delta x/k} \right) \quad (3.5)$$

Again, the hat (^) means evaluated at time $t+\Delta t$. The left-hand side of this equation represents the time rate of change of the energy stored in section n between time t and $t+\Delta t$ per unit cross-sectional area. Each of the terms on the right-hand side represents an inward heat flux per unit cross-sectional area to section n from one of its neighboring sections. Using the familiar electrical analogy, the temperature difference in the numerator of each term can be thought of as a driving potential for heat flow and the $\Delta x/k$ in the denominator can be thought of as a resistance. The heat fluxes at the beginning and end of the time interval are averaged, and this value is used as the constant value for heat flux throughout the interval.

To simplify notation, Spindler introduced a thermal capacitance, C , and a thermal resistance, R , defined as follows for a given layer [14]:

$$C = \rho c \Delta x = \rho c \frac{LT}{N-1} \quad (3.6)$$

$$R = \frac{\Delta x}{k} = \frac{1}{k} \cdot \frac{LT}{N-1} \quad (3.7)$$

LT is the total thickness of the layer, and N is the number of nodes in the layer. Equation (3.5) then reduces to:

$$C \left(\frac{\hat{T}_n - T_n}{\Delta t} \right) \approx \frac{1}{2} \left(\frac{\hat{T}_{n-1} - \hat{T}_n}{R} + \frac{\hat{T}_{n+1} - \hat{T}_n}{R} \right) + \frac{1}{2} \left(\frac{T_{n-1} - T_n}{R} + \frac{T_{n+1} - T_n}{R} \right) \quad (3.8)$$

This equation is the Crank-Nicolson finite difference approximation used for nodes within a homogeneous material.

Different material layers will typically have different properties, thicknesses, and numbers of nodes. When a node falls at the interface of two different materials, minor modifications to Equation (3.8) are required. Figure 3.3 shows how the nodes are set up at the junction between two dissimilar material layers (both infinite in directions orthogonal to x) and the corresponding electric circuit. Note that the regions surrounding the nodes look the same as before with the exception of node n at the junction. The region surrounding node n is of size

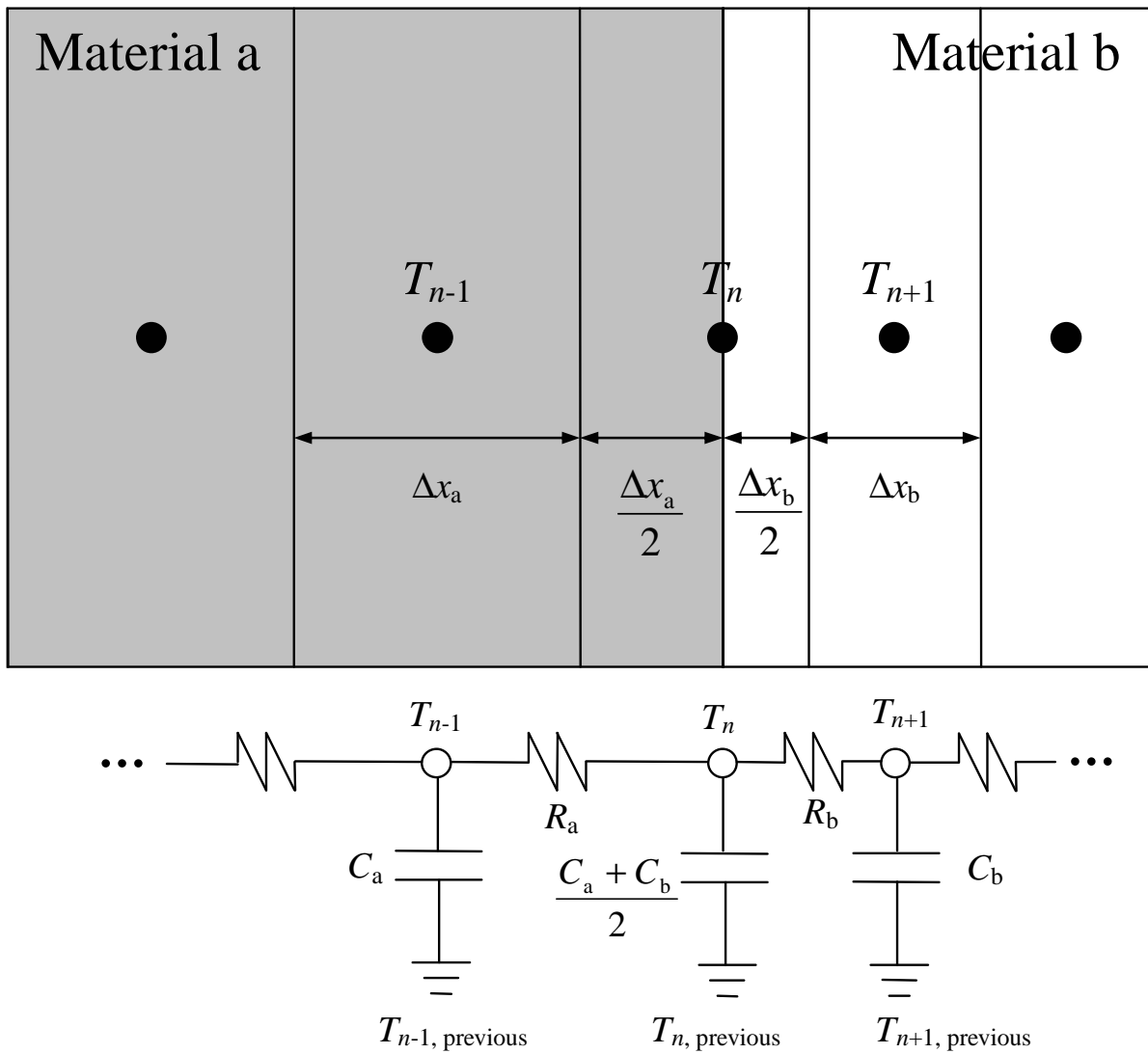


Figure 3.3: Nodal setup at the junction of two dissimilar material layers (infinite in directions orthogonal to x)

$(\Delta x_a + \Delta x_b)/2$. The energy balance for this node in Crank-Nicolson form is given by:

$$\left(\frac{C_a}{2} + \frac{C_b}{2}\right) \frac{\hat{T}_n - T_n}{\Delta t} \approx \frac{1}{2} \left(\frac{\hat{T}_{n-1} - \hat{T}_n}{R_a} + \frac{\hat{T}_{n+1} - \hat{T}_n}{R_b} \right) + \frac{1}{2} \left(\frac{T_{n-1} - T_n}{R_a} + \frac{T_{n+1} - T_n}{R_b} \right) \quad (3.9)$$

The subscripts a and b refer to materials a and b in Figure 3.3. Note that this equation reduces to (3.8) when $C_a = C_b = C$ and $R_a = R_b = R$. Equations (3.8) and (3.9) can be used to step through an arbitrary number of material layers, and they account for all of the nodes present in material layers except for nodes at the outside of the outermost layers, which have unique boundary conditions.

3.4 Simplified Model for Lightweight Building Components

The model presented in the previous section is general, and it can be applied to any material layer in the building. However, the motivation for using nodes in the model was to account for the ability of materials to store heat. In a building whose thermal mass (i.e. ρc , as defined previously) has an important effect on energy flow through the envelope, it is typical to have one or two material layers that account for the vast majority of the thermal mass (e.g. concrete) and others whose thermal mass is very small in comparison (e.g. insulation). If the thermal mass of a material layer is practically negligible, there is no need to have nodes in the layer—it can be modeled as a pure resistance.

One advantage of modeling the lightweight material layers in this manner is that it significantly reduces the number of nodes, thereby reducing the number of simultaneous equations that must be solved. Since the computational effort required to solve simultaneous equations is proportional to the number of nodes to the third power, getting rid of unnecessary nodes saves a good deal of calculation time.

Another advantage of this modeling technique is that it helps avoid numerically-induced oscillations, an undesirable effect that is common among implicit finite difference methods, including the Crank-Nicolson method. Although these methods are unconditionally stable, a low thermal mass can cause the system to be underdamped, which can result in overshoot and oscillations in response to step changes in temperature boundary conditions. This behavior is not physically possible because it would result in a violation of the second law of thermodynamics. Only placing nodes in thermally massive building materials like concrete overdamps the system and avoids this problem, resulting in more realistic building load calculations.

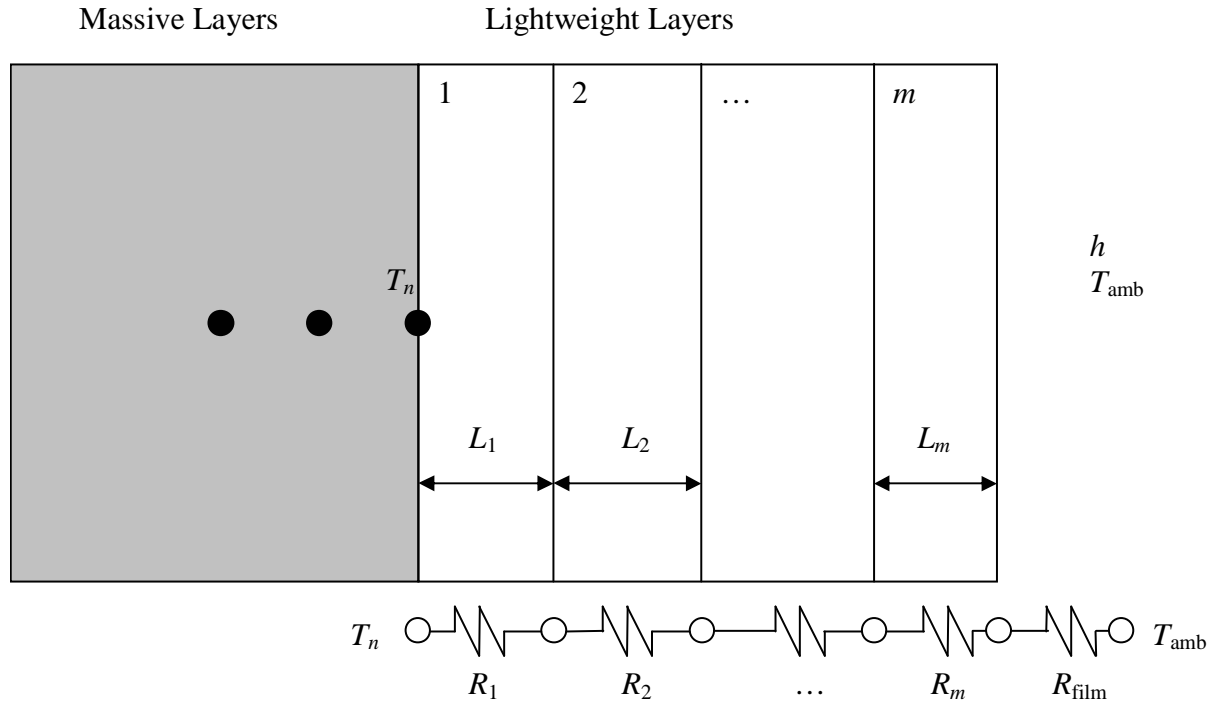


Figure 3.4: Nodal setup approximating lightweight material layers as pure resistances

Figure 3.4 shows the situation with lightweight layers approximated as pure resistances. The resistance per unit area of each layer is equal to the ratio of the layer's thickness to its thermal conductivity and that of the film is simply the inverse of the combined convection and linearized radiation coefficient, h . The value of this coefficient and its use will be discussed in a separate section in the model components chapter. These resistances are all in series, and they can be easily combined. The total resistance of the lightweight (insulating) layers is combined in series with the film resistance to form the total resistance between the temperatures T_n and T_{amb} , as shown in the figure. It is useful to define an effective convection coefficient that encapsulates this total resistance of the material layers and the film:

$$\frac{1}{h_{\text{eff}}} \equiv R_{\text{tot}} = R_{\text{ins}} + R_{\text{film}} = \sum_{i=1}^m \left(\frac{L_i}{k_i} \right) + \frac{1}{h} \quad (3.10)$$

where

h_{eff} = effective convection coefficient

R_{tot} = total resistance of lightweight material layers and air film (per unit area)

R_{ins} = total resistance of the m material layers (per unit area)

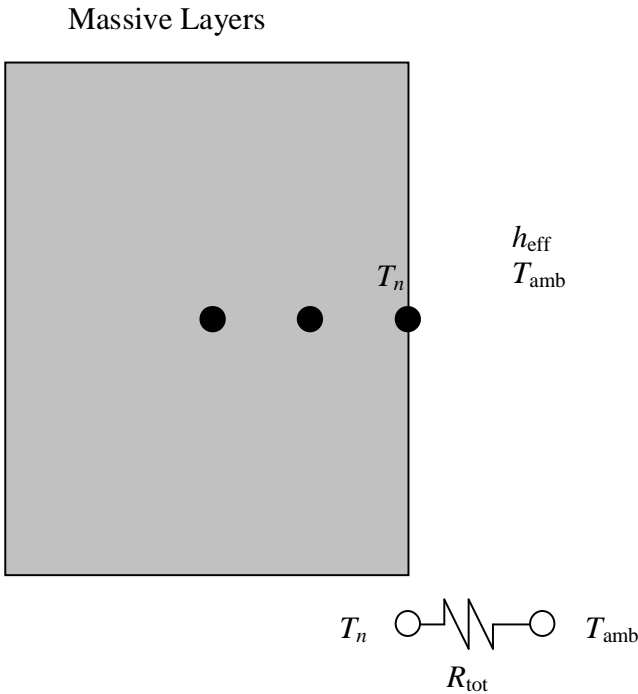


Figure 3.5: Simplified situation lumping all pure resistances into an effective convection coefficient

R_{film} = air film resistance (per unit area)

L_i = thickness of material layer i

k_i = thermal conductivity of material layer i

The simplified situation is shown in Figure 3.5, where the heat exchange between the outermost material node and the surroundings is reduced to a standard convection problem. The heat flux is equal to the product of the effective convection coefficient and the temperature difference between the surface node and the surroundings.

3.5 General Boundary Conditions

The previous section has presented a model that treats material layers with low thermal mass as pure resistances, which simplifies the situation considerably. However, it does introduce one minor complication when it comes to boundary conditions because it is possible to have an incident heat flux at a point where there is no temperature node. Figure 3.6 shows this situation, where Q is an arbitrary incident heat flux (e.g. the amount of solar radiation absorbed by the surface) and T_{amb} is the temperature of the surroundings. This section will derive the general equation that is used for boundary nodes.

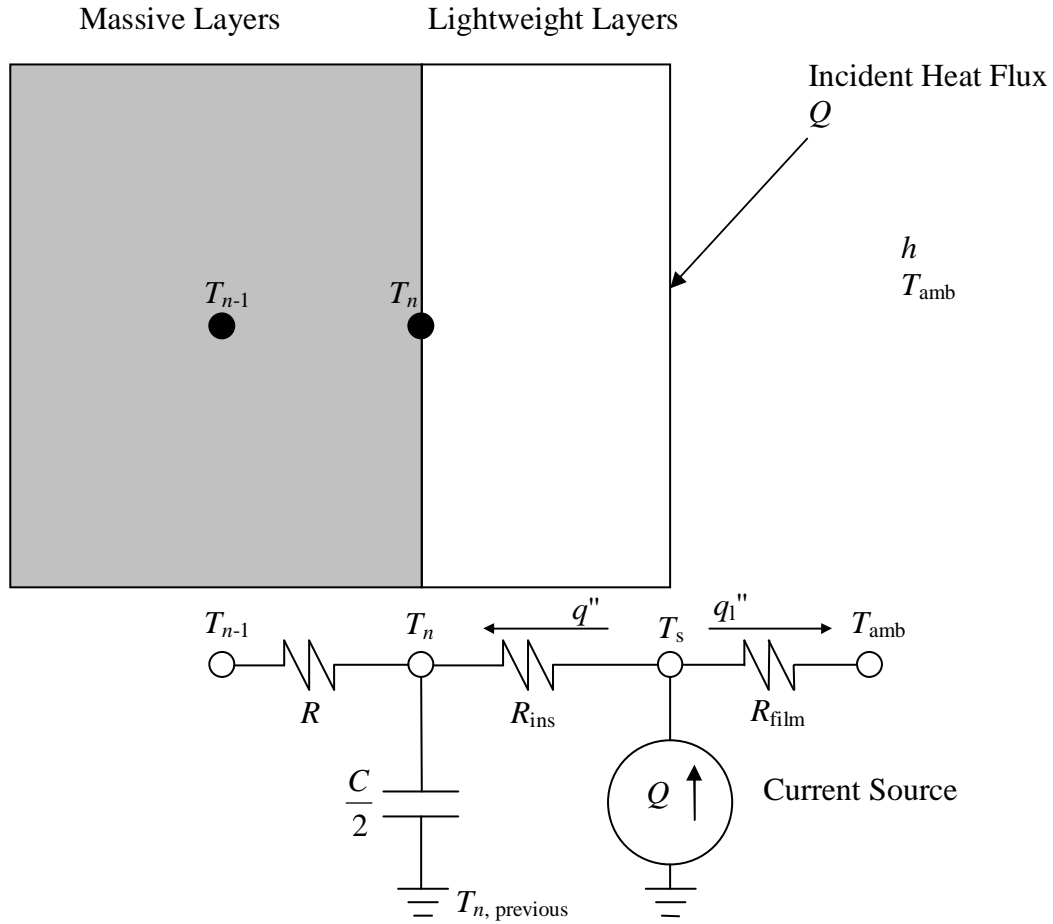


Figure 3.6: Nodal setup with incident heat flux outside of lightweight material layers

Since the lightweight layers are modeled as pure resistances, the net heat flux at the surface (the point with temperature T_s in Figure 3.6) must be equal to zero. In order to write an energy balance for node n , the heat flux into the node from the surroundings, q'' , is needed. An energy balance at the surface gives:

$$q'' = \frac{T_s - T_n}{R_{ins}} = \frac{T_{amb} - T_s}{R_{film}} + Q \quad (3.11)$$

Eliminating the surface temperature and solving for the heat flux gives:

$$q'' = \frac{T_{amb} - T_n + Q \cdot R_{film}}{R_{ins} + R_{film}} \quad (3.12)$$

Note that the denominator is equal to R_{tot} , the total resistance defined previously. This same result can also be obtained by inspection using the principle of superposition from elementary

circuit analysis. With this information, writing the Crank-Nicolson energy balance for node n is straightforward:

$$\frac{C}{2} \left(\frac{\hat{T}_n - T_n}{\Delta t} \right) \approx \frac{1}{2} \left(\frac{\hat{T}_{n-1} - \hat{T}_n}{R} + \frac{\hat{T}_{\text{amb}} - \hat{T}_n + \hat{Q} \cdot R_{\text{film}}}{R_{\text{tot}}} \right) + \frac{1}{2} \left(\frac{T_{n-1} - T_n}{R} + \frac{T_{\text{amb}} - T_n + Q \cdot R_{\text{film}}}{R_{\text{tot}}} \right) \quad (3.13)$$

This equation is the general boundary node equation that is used for all of the layered building components.

One final quantity derived from Figure 3.6 is important—the value of the parameter q_1'' . When the ambient conditions are indoors, this quantity represents the sensible heating (or cooling) load being transferred from the inside air to the given surface (or vice versa) per unit area. The load can be derived in the same way as q'' or by setting the sum of currents entering T_s equal to zero, and the result is:

$$q_1'' = \frac{T_n - T_{\text{amb}} + Q \cdot R_{\text{ins}}}{R_{\text{tot}}} \quad (3.14)$$

This value will be used both in the equation for the indoor air temperature node and for the actual calculation of the loads that are output by the program.

3.6 Assumptions Used in the General Model

This chapter has presented the modeling techniques used by the simulation program at a general level, and several basic assumptions were made. These assumptions are presented here, and other assumptions specific to particular building components will be discussed as the components are presented.

All of the nodal energy balance equations derived in this chapter are based on a discretized version of the one-dimensional heat equation. While there are certainly some multi-dimensional effects when looking at heat transfer through a building envelope, the one dimension considered in the model typically dominates over the vast majority of a building's surface area. Multi-dimensional effects may not always be negligible, but they can be ignored for the purposes of rough approximations of annual energy consumption unless some specific information about two-dimensional effects is known. Discrete finite difference methods are very commonly used when computers are needed to solve differential equations with non-standard boundary conditions. With properly chosen space and time increments, any error introduced by

Table 3.1: Ranges of property values for wood and concrete (see [2], pp. 25.5 ff.)

Material Class	Density Range (kg/m ³)	Thermal Conductivity Range (W/mK)	Specific Heat Range (J/kgK)
Wood (12% moisture)	350-750	0.1-0.2	-
Concrete	320-2400	0.12-2.9	630-960

the discretization is negligible compared to the error introduced by other uncertainties that will be discussed later (e.g. weather data).

Specific property values that go into the model are set based on user input, which is discussed in a separate chapter, but the uncertainty associated with these values is general and applies throughout the model. The uncertainty associated with material property values is significant, and it is influenced by several factors. The first major source of uncertainty in building material property values comes from the fact that there are so many different subclasses of common building materials such as concrete and wood. ASHRAE lists typical thermal properties of common building materials [2], including many different types of wood and concrete. Table 3.1 shows the wide range of property values that can be found within these groups of materials. Note that the thermal conductivity and specific heat of wood are highly dependent on moisture content (which is fixed in the table). Clearly, specifying that a wall is made of concrete does not determine a set of property values that should be used in calculations. For a program with the purpose of providing general guidance to the designer early in the process, some nominal values must be used to avoid confusion. The installation of materials can also affect the property values—there have been experiments showing that installed property values often differ significantly from handbook values. The extent to which the material is exposed to moisture during the building process is one important factor. Material property values account for one of the major sources of uncertainty in the model mainly due to the large range of values that exist for common building materials.

Assuming that lightweight material layers act as pure thermal resistances is another assumption that was made to reduce computation time and avoid numerical noise from being introduced to the simulations. There are several equivalent interpretations when this assumption is made about a given material layer: (1) it has a thermal mass (ρc) equal to zero, (2) it responds instantaneously to any changes in boundary conditions, and (3) all heat flux into the layer must

leave since it cannot store any heat. No real material behaves in exactly this manner. However, many building materials have little enough thermal mass that they respond very quickly to changes in boundary conditions. If the thermal time constant is much less than one hour, the time step used in the program, assuming that the material responds instantly to changes in boundary conditions will have no practical effect on the simulation. The configuration presented in the model also presumes that there are no lightweight material layers in between massive material layers. Although it is certainly possible to account for this situation, no allowance for it is built into the model at this time.

3.7 Summary

The framework for modeling building components has been established in this chapter, and it will be used in dealing with the exterior walls, ground floor, interior floors, and roof of the building. The key results can be seen in three equations. Equation (3.8) describes the heat transfer at a node inside a homogeneous material, and Equation (3.9) does so at the junction of two different materials. Together, they can be used for an arbitrary number of thermally massive material layers that compose a major building component. Equation (3.13) describes the heat transfer at a boundary node, which may or may not have lightweight material layers between it and ambient conditions.

While assumptions specific to individual building components will be presented in turn, several general assumptions apply to all of the building components that are modeled using the presented framework. They include approximating the heat transfer through the building as one-dimensional using finite difference techniques, choosing specific material values that are highly uncertain to use in the model, and modeling material layers with low thermal mass as pure resistances that have no capacity to store heat.

Chapter 4

Outdoor Boundary Conditions

4.1 Introduction

In the previous chapter, a model for a general building component was presented, and energy balance equations for surface nodes were derived using general boundary conditions. In this chapter, the way in which the simulation program obtains values to use as boundary conditions on the outside of the building will be explained. Since climatic conditions are what drive the need for space conditioning in buildings, accurately representing the specific climate at the location of a building is obviously very important to a good model. Measured weather data from typical years are used to approximate the average conditions that will occur at a given location and a given time. Some of the weather data and models to calculate the position of the sun are used to determine the incident solar flux on an arbitrary building surface. Taken as a whole, this information fully specifies the boundary conditions that are needed to run the building energy simulations.

4.2 Weather Data

Accurate weather data are of critical importance to the estimation of heating and cooling loads for a building. The climate in which a building is situated can drastically affect the energy efficiency of a given building design and the sizing of heating and cooling equipment. Two of the most important factors that determine the building loads are outdoor temperature and solar radiation. Weather data are available for many locations throughout the world on an hourly basis, and they usually represent what is called a “typical” meteorological year. The data files often contain vast amounts of information, including outdoor temperature, solar radiation, wind speed and direction, humidity, and so on. The values that are extracted for use in this program are (1) direct normal radiation, (2) diffuse radiation, (3) global radiation received by a horizontal surface, and (4) outdoor temperature. Although several models do exist for estimating values of solar radiation [14], using measured weather data avoids unnecessary modeling and is just as easy to implement. Weather data are available for download from [13] and [15].

There are several possible sources of error associated with using measured weather data even though no real modeling is introduced in doing so. Any physical measurement comes with some degree of uncertainty. Outdoor temperatures can be measured accurately enough that any uncertainty associated with the measurement should be negligible when it comes to yearly load estimations. Measurements of solar radiation, however, are often only good to within $\pm 15\%$, which can be significant. In addition, not every weather station measures solar radiation data, so sometimes the radiation values in data files are merely interpolations of data from other nearby weather stations. The weather stations that collect the data are often located near airports or other areas on the outskirts of cities, and there is no guarantee that local conditions at a building in the city will match those at the weather station. Local temperatures could vary, and vegetation and surrounding buildings could block a significant fraction of the sunlight that would otherwise be present. Solar radiation is one of the predominant factors in estimating the heating and cooling loads for a building, but even using actual past weather data results in a significant amount of uncertainty once measurement error and varying local conditions are accounted for.

4.3 Solar Angles

The position of the sun in the sky is a function of many things, including location on the earth's surface, time of day, and day of the year. In order to determine solar position at a specified time, it must be converted from the time that a clock shows to the time that a solar time sundial shows, known as apparent solar time. This conversion is made by applying two corrections to the local time kept by a standard clock. The equation of time, ET , accounts for the variation in the earth's orbital velocity throughout the year. For computer calculations, its value can be approximated by:

$$ET = 229.2 \left[\begin{array}{l} 0.000075 + 0.001868 \cos(N) - 0.032077 \sin(N) \\ -0.014615 \cos(2N) - 0.04089 \sin(2N) \end{array} \right] \text{min} \quad (4.1)$$

where $N = (n-1)(360/365)$ and n is the day of the year, $1 \leq n \leq 365$ [12]. The second correction to the local time accounts for any difference in longitude between the site in question and the local standard meridian. Local standard meridians are measured every 15° ($360^\circ / 24$ time zones) from the prime meridian, which passes through Greenwich, England. This correction is equal to 4 minutes of time for every degree difference in longitude ($24 \text{ hours} \times 60 \text{ minutes/hour} / 360^\circ$). The time is added for sites to the east of the local standard meridian and subtracted for sites to

the west. The apparent solar time is given by:

$$AST = LST + ET \pm 4(|15 \cdot GMTDiff| - LON) \quad (4.2)$$

where

AST = apparent solar time in minutes after midnight

LST = local standard time in minutes after midnight

ET = equation of time in minutes

$GMTDiff$ = difference in time between local site and Greenwich Mean Time in hours

LON = site longitude in decimal degrees

The last term is added in the western hemisphere (where $GMTDiff$ is negative) and subtracted in the eastern hemisphere (where $GMTDiff$ is positive).

The apparent solar time at a specified location determines a quantity known as the hour angle, HA , which is the angle between two lines projected onto the earth's equatorial plane—a line connecting the center of the earth to that of the sun and a line from the center of the earth to the location where the solar position is desired. The hour angle is simply equal to the difference between solar noon and the apparent solar time converted into degrees of the earth's rotation:

$$HA = \frac{1}{4} |SN - AST| \quad (4.3)$$

where SN = solar noon in minutes after midnight = $12 \times 60 = 720$ and HA is expressed in degrees. The final quantity that is required to calculate the position of the sun is the sun's declination, which varies throughout the year. The declination, δ , is the angle between the line connecting the center of the earth to the center of the sun and a projection of that angle on the earth's equatorial plane. Its value in degrees can be approximated for computer calculations by:

$$\delta = \left[\begin{array}{l} 0.3963723 - 22.9132745 \cos(N) + 4.0254304 \sin(N) - 0.3872050 \cos(2N) \\ + 0.05196728 \sin(2N) - 0.1545267 \cos(3N) + 0.08479777 \sin(3N) \end{array} \right]^\circ \quad (4.4)$$

where N is defined in the same way that it was in Equation (4.1) [12].

Figure 4.1 shows all of the angles that are relevant when determining incident solar flux on an arbitrary surface, including the solar altitude, β , and azimuth, ϕ , that specify the location of the sun. Using the angles determined previously along with the local latitude, L , the solar altitude is calculated from geometry:

$$\sin \beta = \cos L \cos \delta \cos HA + \sin L \sin \delta \quad (4.5)$$

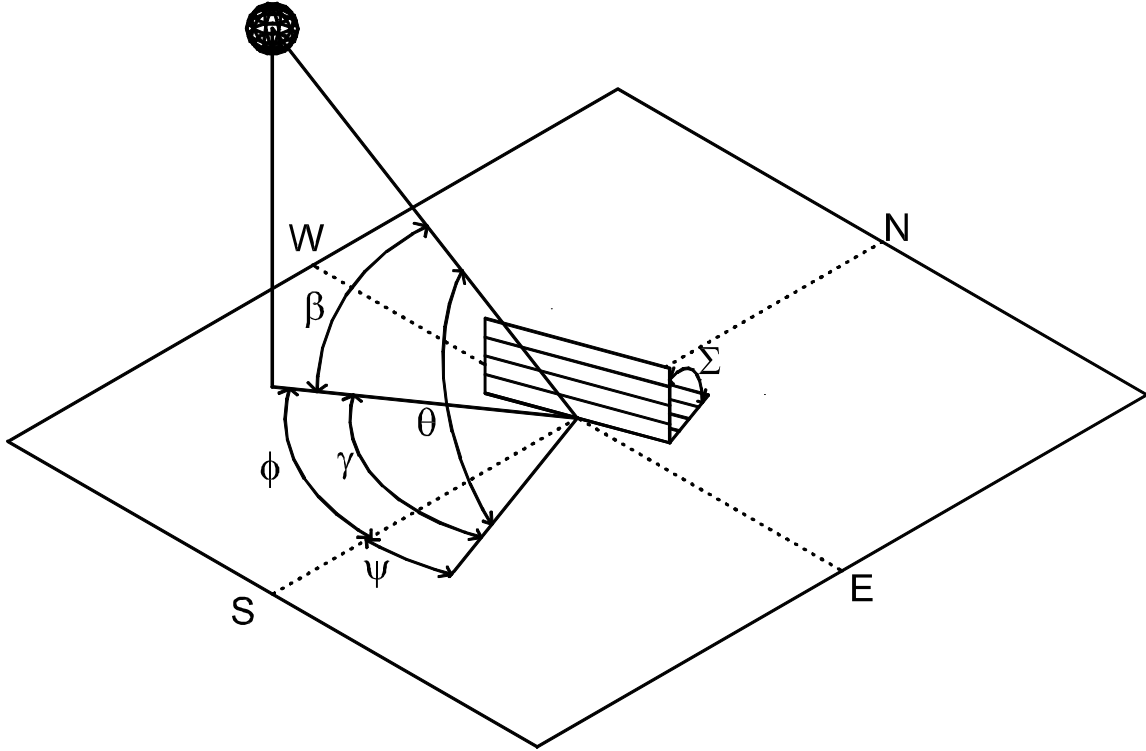


Figure 4.1: Solar angles for an arbitrary surface

The solar azimuth measured from the south can then be computed:

$$\cos \phi = \frac{\sin \beta \sin L - \sin \delta}{\cos \beta \cos L} \quad (4.6)$$

Angles west of south are positive, and angles east of south are negative.

An arbitrary surface can face any direction and be tilted at an angle. The surface azimuth, ψ , is shown in the figure, and it is defined as the angle between true south and a line normal to the surface projected onto the plane of the cardinal directions. The relative azimuth, γ , is simply the difference between the solar azimuth and the surface azimuth ($\phi - \psi$). The incident angle of the sun onto the surface, θ , is calculated from geometry based on these angles:

$$\cos \theta = \cos \beta \cos \gamma \sin \Sigma + \sin \beta \cos \Sigma \quad (4.7)$$

Σ is the tilt angle, which is 0° for horizontal surfaces and 90° for vertical surfaces. Note that for vertical surfaces,

$$\cos \theta = \cos \beta \cos \gamma \quad (4.8)$$

For horizontal surfaces,

$$\cos \theta = \sin \beta \quad (4.9)$$

The angle of incidence will be used in the determination of incident solar flux on a surface.

4.4 Incident Solar Flux

As mentioned previously, the radiation values available in the weather data files are direct normal radiation, diffuse radiation, and global radiation seen by a horizontal surface. One quantity of interest that is used as a boundary condition in the model is the total heat flux that is incident on an arbitrary surface. Direct, diffuse, and ground reflected radiation all contribute to the total.

The direct normal radiation incident on a surface, E_D , depends on the sun's angle of incidence to the surface. When $0^\circ \leq \theta \leq 90^\circ$, it is given by:

$$E_D = E_{DN} \cos \theta \quad (4.10)$$

where E_{DN} is the direct normal radiation from the weather data file. When the incident angle takes on values outside of the stated range, $E_D = 0$.

The total diffuse radiation striking a surface consists of both beam solar radiation that is scattered by the atmosphere and global radiation reflected by the ground in the area surrounding the surface. The incident diffuse radiation scattered from the sky onto the surface is given by:

$$E_{\text{diff,sky}} = E_{\text{diff,horiz}} \left(\frac{1 + \cos \Sigma}{2} \right) \quad (4.11)$$

where

$E_{\text{diff,sky}}$ = incident diffuse radiation scattered from the sky

$E_{\text{diff,horiz}}$ = diffuse radiation from the weather data file

Σ = tilt angle as defined previously

The last term in this equation is the view factor between a tilted surface and the sky, which is equal to 1 for a horizontal surface and 0.5 for a vertical surface. The amount of radiation that is reflected from the ground to a building surface depends on the ground covering near the building. Grass and asphalt, for example, do not reflect in the same way. The ground reflected radiation is given by:

$$E_{\text{diff,ground}} = E_{\text{global,horiz}} \rho_g \left(\frac{1 - \cos \Sigma}{2} \right) \quad (4.12)$$

where

$E_{\text{diff,ground}}$ = incident diffuse radiation reflected from the ground

$E_{\text{global,horiz}}$ = global radiation received by a horizontal surface from the weather data file

ρ_g = ground reflectance

In this equation, the last term is the view factor between a tilted surface and the ground, which is equal to 0 for a horizontal surface and 0.5 for a vertical surface. A typical value for ρ_g is 0.2, and this value is used in the model since specific details about the land surrounding the building are probably unknown at the early design stages.

The total incident heat flux at an outside building surface, $E_{\text{tot,surf}}$, is simply equal to the sum of the three quantities just explained:

$$E_{\text{tot,surf}} = E_D + E_{\text{diff,sky}} + E_{\text{diff,ground}} \quad (4.13)$$

This total value will be used as part of the boundary conditions for the outside surface node of the building components that are exposed to solar radiation, namely the exterior walls and the roof. The quantities explained in this section will also be used to determine the total radiation that passes through the glazing system and into the interior of the building.

4.5 Assumptions

Most of the assumptions made in this chapter relate to the weather data and were discussed earlier. All values extracted on an hourly basis from the weather data files are assumed to be constant over the entire hour to which they correspond. A reflectivity of 0.2 was assumed for the ground surrounding the building, and numerical approximations were made for the equation of time and the solar declination for each day of the year.

Chapter 5

Building Component Models

5.1 Introduction

Previously, a general model was derived which expresses the energy balance of a building surface in finite difference form. In this chapter, that general model will be applied to several specific building components: (1) exterior walls, (2) ground floor, (3) internal floors, and (4) roof. Different techniques used to model other aspects of the building will then be presented. Three energy balance equations derived as part of the general model are repeated here for quick reference since they will be used several times. Equation (3.8) applies to a node inside a homogeneous material layer:

$$C \left(\frac{\hat{T}_n - T_n}{\Delta t} \right) \approx \frac{1}{2} \left(\frac{\hat{T}_{n-1} - \hat{T}_n}{R} + \frac{\hat{T}_{n+1} - \hat{T}_n}{R} \right) + \frac{1}{2} \left(\frac{T_{n-1} - T_n}{R} + \frac{T_{n+1} - T_n}{R} \right) \quad (5.1)$$

Equation (3.9) applies to a node at the junction of two dissimilar materials:

$$\left(\frac{C_a}{2} + \frac{C_b}{2} \right) \frac{\hat{T}_n - T_n}{\Delta t} \approx \frac{1}{2} \left(\frac{\hat{T}_{n-1} - \hat{T}_n}{R_a} + \frac{\hat{T}_{n+1} - \hat{T}_n}{R_b} \right) + \frac{1}{2} \left(\frac{T_{n-1} - T_n}{R_a} + \frac{T_{n+1} - T_n}{R_b} \right) \quad (5.2)$$

Equation (3.13) applies to a boundary node:

$$\frac{C}{2} \left(\frac{\hat{T}_n - T_n}{\Delta t} \right) \approx \frac{1}{2} \left(\frac{\hat{T}_{n-1} - \hat{T}_n}{R} + \frac{\hat{T}_{amb} - \hat{T}_n + \hat{Q} \cdot R_{film}}{R_{tot}} \right) + \frac{1}{2} \left(\frac{T_{n-1} - T_n}{R} + \frac{T_{amb} - T_n + Q \cdot R_{film}}{R_{tot}} \right) \quad (5.3)$$

Since these equations were derived for a general case, they can be readily applied to specific building components by substituting in appropriate values for the general parameters. Of course, parameters such as C and R that were defined for a material layer will take on different numerical values for different building components, but they are calculated in the same way.

5.2 Exterior Walls

The exterior walls account for a large fraction of the building's surface area that is exposed to the outside environment. The makeup of exterior walls varies widely in practice with

typical constructions ranging from lightweight wood frames to dense concrete slabs. The construction and insulation of exterior walls has a tremendous impact on overall building energy performance.

5.2.1 Thermal Model

Figure 5.1 shows the configuration and boundary conditions on both the inside and outside of an exterior wall. Recall that h_{out} is a combined convection and radiation coefficient. Defining it in this manner provides a simple way to account for infrared and long wave radiant exchange between a building surface and its surroundings. The value of h_{out} determines the film resistance, R_{film} , for the exterior surfaces of the building. A more detailed discussion of the specific values used in the program is presented in the section on convection and radiation coefficients.

Equation (5.1) describes the energy balance for an arbitrary node n completely within a material layer, and Equation (5.2) does so at the junction of two material layers. Equation (5.3), with some appropriate substitutions, is used for the outside surface node. Using the

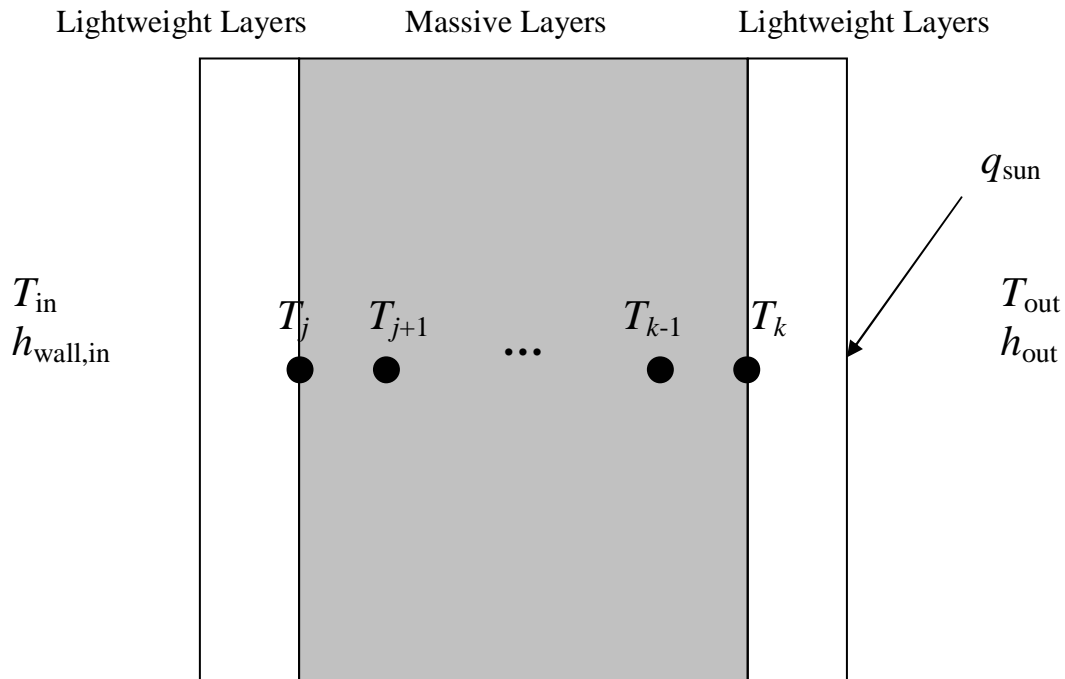


Figure 5.1: Exterior wall schematic showing outdoor and indoor boundary conditions

configuration in the figure, the subscript n in the equation must be replaced by k for this node. The ambient temperature, T_{amb} is equal to the outdoor temperature, T_{out} , which is taken from the weather data files. The arbitrary heat flux, Q , is equal to the solar radiation absorbed by the surface, q_{sun} , given by:

$$q_{\text{sun}} = \alpha E_{\text{tot,surf}} \quad (5.4)$$

where α is the absorptivity of the exterior surface. $E_{\text{tot,surf}}$ is the total incident radiation on the surface that was determined in the chapter on outdoor boundary conditions. A quantity known as the sol-air temperature, $T_{\text{sol-air}}$, is commonly used in the literature when outdoor surfaces are exposed to solar radiation:

$$T_{\text{sol-air}} = T_{\text{out}} + \frac{\alpha E_{\text{tot,surf}}}{h_{\text{out}}} = T_{\text{out}} + \alpha E_{\text{tot,surf}} \cdot R_{\text{film}} \quad (5.5)$$

The sol-air temperature is the temperature which, in the absence of all solar radiation, gives the same heat flux into the surface as the outdoor temperature does in the presence of the incident solar radiation. Using this quantity, Equation (5.3) can be expressed in an alternate form for the outside boundary node of the exterior wall:

$$\frac{C}{2} \left(\frac{\hat{T}_k - T_k}{\Delta t} \right) \approx \frac{1}{2} \left(\frac{\hat{T}_{k-1} - \hat{T}_k}{R} + \frac{\hat{T}_{\text{sol-air}} - \hat{T}_k}{R_{\text{tot}}} \right) + \frac{1}{2} \left(\frac{T_{k-1} - T_k}{R} + \frac{T_{\text{sol-air}} - T_k}{R_{\text{tot}}} \right) \quad (5.6)$$

This equation can be used for the outside boundary node of any exterior surface when the sol-air temperature is properly defined for the surface. Equation (5.3) is also used for the inside surface node. Using the nodes as defined in the figure, the subscript n must be replaced by j , and $n-1$ by $j+1$ (-1 is replaced by +1 since the configuration is a mirror image of that used in the derivation). In this case, T_{amb} is equal to the indoor temperature, T_{in} , and the incident heat flux, Q , is equal to zero. The film resistance is determined by the inside wall combined convection and radiation coefficient, $h_{\text{wall,in}}$.

5.2.2 Assumptions

Several assumptions that apply to the general model were discussed in the general model chapter, and they all apply to the exterior wall model just described. These assumptions include one-dimensional heat transfer, the finite difference approximation, specific material property values, and neglecting all thermal mass of the lightweight material layers. The solar absorptivity of a surface was introduced in this section, and it is another material property value that must

have some assumed value. All of the assumptions in the general model that was derived previously are implicit in the model for the exterior wall since it is based on the general case.

Another important assumption is that all radiation exchange amongst the interior building surfaces is neglected. The inside surfaces of the exterior walls, ground floor, internal floors, roof, and windows are all included in this assumption. One reason motivating this modeling decision is the fact that the configuration of the building's interior is highly uncertain. The layout of an apartment building includes many interior walls, and incorporating radiation heat transfer amongst interior surfaces would need to take these surfaces into account. It is very unlikely that a user in the early design stages would have the details figured out, and attempting to incorporate them into the program would add unnecessary complexity. With the exception of windows, the interior surfaces are often at very similar temperatures, so the effects of radiation between them should be fairly small. Especially for well-insulated buildings, the effects of this assumption on the estimates of annual heating and cooling loads are not significant.

One way that the model attempts to minimize any error due to neglecting radiation exchange amongst interior surfaces is to use combined convection and radiation coefficients for the interior surfaces of the building. In effect, the result is to increase the heat transfer between each surface and the indoor air. The assumption made in so doing is that the interior surfaces radiate to some thermal mass inside the building (e.g. furniture, people, etc.), and the effects are quickly transferred to the inside air. While the approximation is not physically correct since interior surfaces do not radiate to the inside air, it is a reasonable way to reduce the already small error associated with neglecting radiation between the inside surfaces.

As will be discussed in a later section, all of the solar radiation that enters the building through the glazing system is assumed to be absorbed by the floors (both ground and internal). As a result, it is assumed there is no direct or reflected solar radiation strikes the interior surface of the external walls.

5.3 Ground Floor

The ground floor is the component that interacts with the terrain below the building. These interactions are quite complex since the terrain also interacts with the ambient outdoor conditions. Insulation levels around the perimeter of a floor slab can have a significant impact on building energy requirements, especially in one-story buildings.

5.3.1 Thermal Model

Figure 5.2 shows the configuration and boundary conditions on the inside and outside of the ground floor. The model assumes 100 mm slab on grade floors with no basement. Studies have shown that the only significant heat gains or losses through slab on grade floors are through the slab perimeter, which is why the bottom surface of the slab is modeled as adiabatic. Making this surface adiabatic is tantamount to setting the convection coefficient below the slab, $h_{\text{slab,below}}$, equal to zero, which corresponds to an infinite film resistance. Slab perimeter losses are treated as a separate phenomenon resulting in a heating or cooling load on the indoor air, so they have no direct impact on the energy balance equations for the nodes in the slab. The combined convection and radiation coefficient inside the slab, $h_{\text{floor,in}}$, determines the film resistance on that side of the floor.

5.3.1.1 Nodal Energy Balances

Again, Equation (5.1) describes the energy balance for an arbitrary node n completely within a material layer, and Equation (5.2) does so at the junction of two material layers. Equation (5.3) can be used to express the energy balance for the outside surface node at the bottom of the slab. For this node as shown in Figure 5.2, the subscript n must be replaced by j , and $n-1$ by $j+1$. The arbitrary heat flux, Q , is equal to zero and the film resistance is infinite,

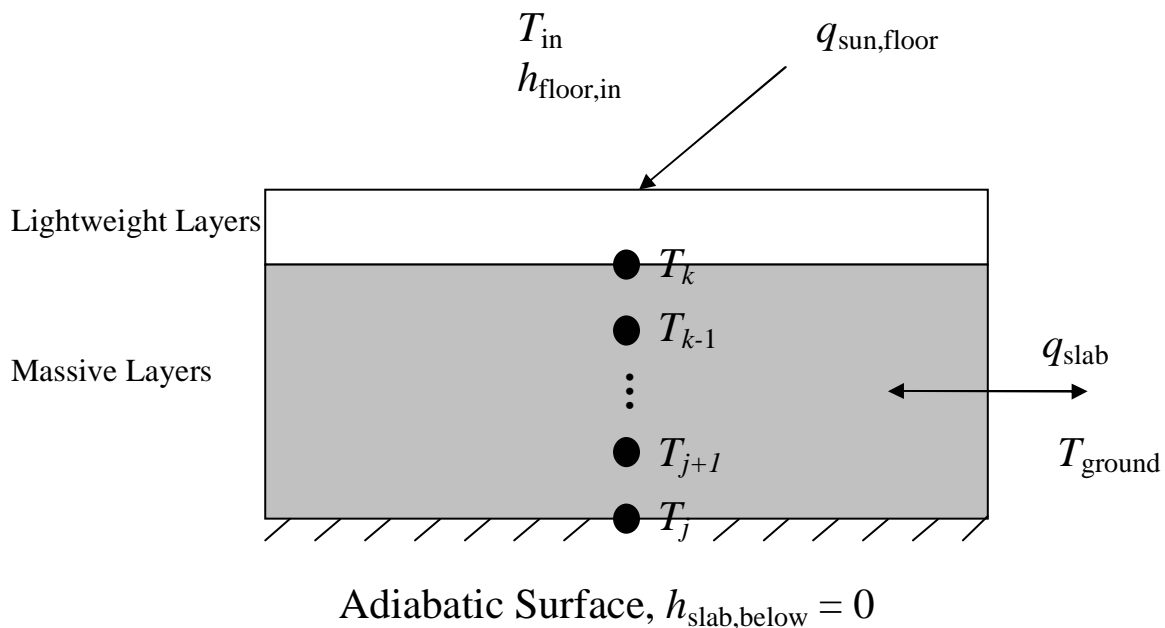


Figure 5.2: Slab on grade floor schematic showing indoor and outdoor boundary conditions

which causes the right hand side of the equation to simplify substantially:

$$\frac{C}{2} \left(\frac{\hat{T}_j - T_j}{\Delta t} \right) \approx \frac{1}{2} \left(\frac{\hat{T}_{j+1} - \hat{T}_j}{R} \right) + \frac{1}{2} \left(\frac{T_{j+1} - T_j}{R} \right) \quad (5.7)$$

Equation (5.3) is also used to write the energy balance at the inside surface node, replacing all instances of the subscript n with k . The ambient temperature, T_{amb} , is equal to the indoor temperature, T_{in} , and the film resistance, R_{film} , is determined using the combined convection and radiation coefficient for the floor, $h_{\text{floor,in}}$. The arbitrary heat flux, Q , is equal to $q_{\text{sun,floor}}$. This quantity is equal to the total amount of solar radiation emitted through the glazing system on a given floor distributed evenly over the entire floor area. It is closely related to the incident solar radiation on each exterior wall, and the determination of its value will be discussed in the section on the glazing system.

5.3.1.2 Slab Perimeter Losses

Heat transfer between a slab on grade floor and the ground is a complex phenomenon. In reality, the effects are multi-dimensional, and the response of the ground temperature, T_{ground} , significantly lags outdoor temperature changes due to its large thermal mass. Studies have shown that the total heat loss is approximately proportional to the perimeter of the slab rather than the area since the perimeter can provide a shorter conduction pathway for heat to flow [2]. Slab perimeter losses (in W rather than W/m^2) are modeled using a standard relationship:

$$q_{\text{slab}} = F \cdot P(T_{\text{in}} - T_{\text{out}}) \quad (5.8)$$

where F is the perimeter loss coefficient and P is the perimeter of the slab. When the indoor temperature is greater (less) than the outdoor temperature, there are losses (gains) through the slab as shown by the arrows in Figure 5.2. Any heat transfer through the slab is assumed to be an instantaneous load on the indoor air and have no effect on the temperature distribution within the slab. ASHRAE (pp. 28.12-13) recommends using a perimeter loss coefficient that depends on three factors: (1) wall construction, (2) the amount of slab perimeter insulation, and (3) the number of heating degree days at the building's locality [2]. A heating degree day is a simple way to express the harshness of a particular climate during the heating season. One heating degree day using a base temperature, B , would mean that the outdoor temperature was one degree below B for one day (or two degrees below B for one-half day, etc). Using hourly weather data, the number of heating degree days, HDD , is easily computed:

Table 5.1*: Perimeter loss coefficients for various heating degree days and perimeter insulation levels in W/mK

Insulation	Heating Degree Days, 18°C Base (K-days/year)		
	≤ 1640	2970	≥ 4130
Uninsulated	1.07	1.17	1.24
R=0.95 K-m ² /W	0.83	0.86	0.97

* Note: Values come from [2], Table 16 on p. 28.13.

$$HDD = \frac{1}{24} \sum_{T_{out} < B} (B - T_{out}) \quad (5.9)$$

A 200 mm block wall is the most similar to the wall constructions used in the program, and the values used for various heating degree days and insulation levels are shown in Table 5.1. The values in the bottom row of the table are used in the program. Linear interpolation is used for degree day values between those in the table. This slab perimeter loss model was created primarily for calculating heating loads, but the same perimeter loss coefficient is used throughout the heating and cooling seasons to approximate heat gains and losses through the slab.

5.3.2 Assumptions

Several assumptions have been made in the model for a slab on grade floor, including some that have already been discussed and some new ones. A 100 mm concrete slab is the assumed geometry for the floor. All of the assumptions discussed in the general model also apply to the ground floor. As discussed in the previous section, all radiation exchange between interior surfaces is neglected in the model.

Three assumptions are made regarding solar radiation that passes through the windows. The first is that all the radiation that enters through the glazing system strikes the floor. Depending on where the window is located, “floor” could be the ground floor or an internal floor. Except at very low solar altitudes, most of the direct normal radiation will hit the floor, but diffuse radiation is likely to be more spread out and strike other interior building surfaces. Accounting for this fact would require detailed knowledge of the building’s interior geometry and specific window configuration, which is probably unknown at the early design stages and would add complexity to the user interface. The second assumption is that all of the incident solar radiation is absorbed by the floor. In reality, the covering on the floor plays a big role in determining how much radiation is absorbed and how much is reflected. A small fraction may actually be reflected back out through the glazing system, but the vast majority will be contained

within the thermal mass of the building. Finally, the solar radiation is assumed to be evenly distributed over the entire floor area. Localized patches of sunlight occur in real situations, but incorporating that into the model would introduce multi-dimensional effects, which have been avoided for computational simplicity. Although the model for dealing with solar radiation that enters the building through the glazing system makes these rudimentary assumptions, it does account for the most its important aspect in terms of building energy consumption—it places all of the radiation on the inside of the building’s thermal mass.

The other assumptions that are made involve modeling the losses through a slab on grade floor. It is assumed that all losses or gains through the ground floor are through the perimeter, so the bottom of the slab is treated as an adiabatic surface. Any losses through the perimeter would result in some multi-dimensional temperature effects, but they are ignored and the load is transferred directly to the indoor air. The perimeter losses are treated as if they have no effect on the nodal temperatures, which are constant over the entire floor footprint.

5.4 Internal Floors

Internal floors consist of every floor in a building above the ground floor. They are exposed to indoor conditions from above and below, and they provide additional thermal mass to help regulate indoor air temperatures.

5.4.1 Thermal Model

Figure 5.3 shows the configuration and boundary conditions of the internal floors. As will be discussed in the section on the indoor air, the entire building is treated as a single zone with the same air temperature. As a result, all of the internal floors have identical configurations and boundary conditions. It is only necessary to set up nodes and equations for one internal floor regardless of how many stories the building has under these simplifying assumptions because its solution can be applied to all of the others.

Equation (5.1) again describes the energy balance for an arbitrary node n completely within a material layer, and Equation (5.2) does so at the junction of two material layers. Equation (5.3) can be used to write the energy balance for the bottom surface node by replacing the subscript n with j and $n-1$ with $j+1$. The ambient temperature, T_{amb} , is equal to the indoor temperature, T_{in} , and the arbitrary heat flux, Q , is equal to zero. The film resistance, R_{film} , is

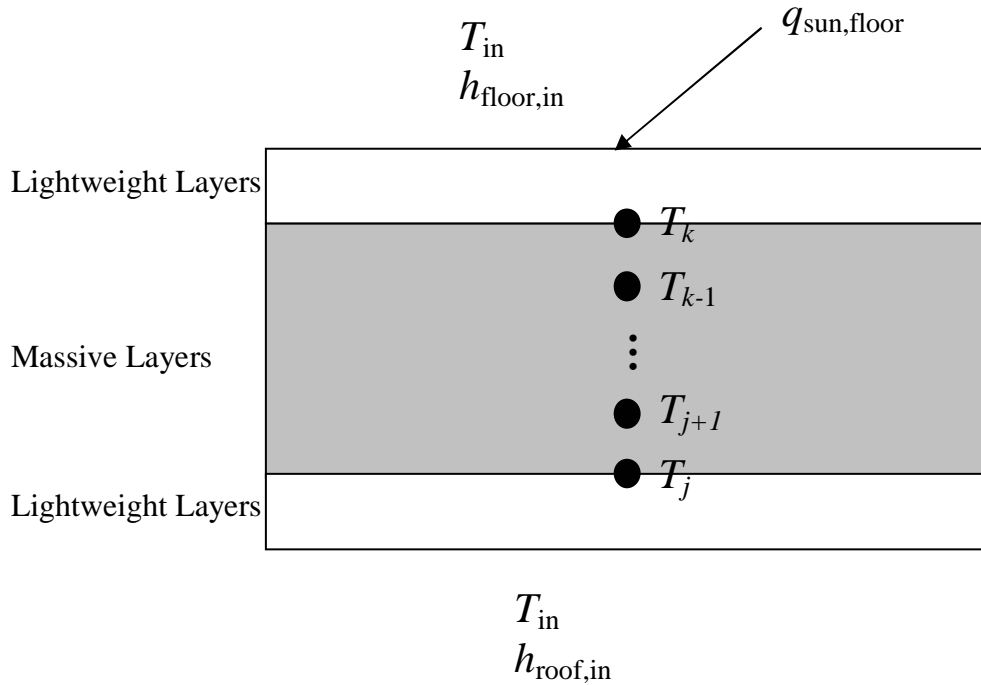


Figure 5.3: Internal floor schematic showing upper (floor) and lower (ceiling) surface boundary conditions

determined by the combined convection and radiation coefficient for the roof and ceiling, $h_{roof,in}$. The equation for the top surface node is identical to that for the top surface node of the ground floor, which was described in the previous section.

5.4.2 Assumptions

All of the assumptions made in the modeling of the internal floors have already been discussed. They are the same as the assumptions for the ground floor, but the ones involving slab perimeter losses are omitted.

5.5 Roof

The roof of a building is another large surface that is exposed to the outdoor environment. A flat or only slightly pitched roof is exposed to a relatively large amount of radiation due to the fact that the surface has a view of the sun almost any time that it is above the horizon. Most rooftops are dark in color and absorb a large fraction of the incident radiation to which they are exposed. This surface is often one of the most difficult to insulate properly, and poor roof insulation can lead to significant degradation of building energy performance.

5.5.1 Thermal Model

Figure 5.4 shows the configuration and boundary conditions on both the inside and outside of the roof. The model assumes a flat roof for simplicity in the user interface, but the possibility for adding a pitch is built in. The combined convection and radiation coefficient is the same as the one used for exterior walls despite the different surface orientation.

Equation (5.1) describes the energy balance for an arbitrary node n completely within a material layer, and Equation (5.2) does so at the junction of two material layers. Again utilizing the concept of the sol-air temperature, as described in the section on exterior walls, Equation (5.6) expresses the energy balance at the outside surface node. For horizontal surfaces, ASHRAE recommends a slight correction to the sol-air temperature:

$$T_{\text{sol-air}} = T_{\text{out}} + \frac{\alpha E_{\text{tot,surf}}}{h_{\text{out}}} - \frac{\epsilon \Delta R}{h_{\text{out}}} \quad (5.10)$$

The surface emissivity, ϵ , is assumed to equal 0.88 for the roof. The other new quantity introduced, ΔR , is equal to the difference between long wave radiation incident on the roof from the sky and other surroundings and radiation emitted by a blackbody at the outdoor temperature.

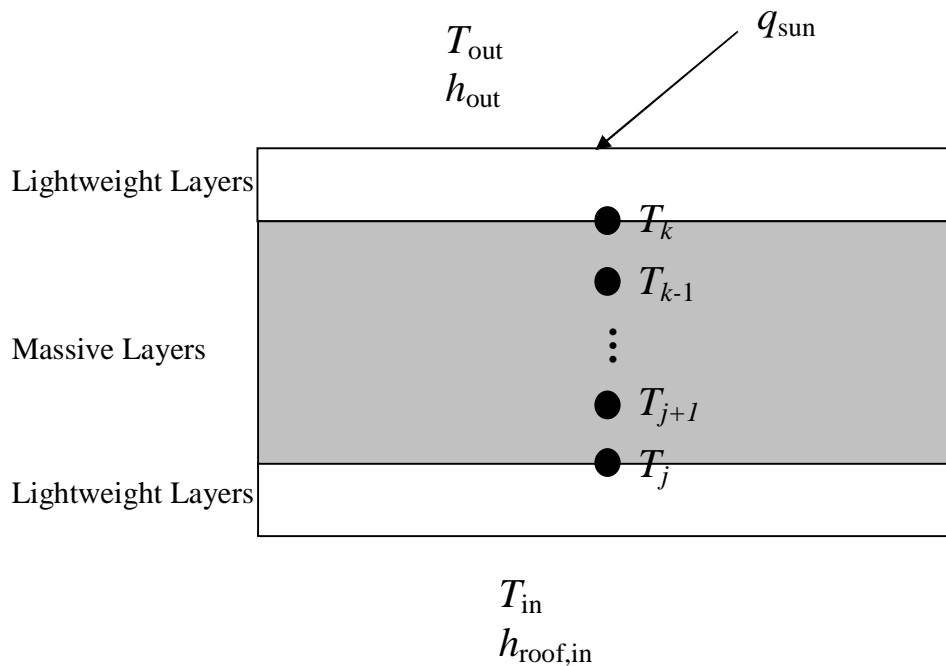


Figure 5.4: Roof schematic showing outside and inside surface boundary conditions

The recommended value for this quantity for a horizontal surface is 63 W/m^2 . For the outdoor film resistance used in the model (which is $34 \text{ W/m}^2\text{-K}$, discussed in a later section), this correction is equal to approximately 1.9°C . The energy balance for the inside surface node is identical to that for the bottom surface node of the internal floors.

5.5.2 Assumptions

All of the assumptions presented with the general model apply to the roof. Like the floors, the roof is assumed to be a concrete slab that is 100 mm thick. The only additional assumptions that were introduced were setting the roof emissivity equal to 0.88 and choosing a value for ΔR , which is equivalent to applying a correction to account for the fact that the sky and surroundings do not radiate in the same manner as a blackbody.

5.6 Glazing System

The glazing system is an integral component of a building's façade because it visually connects the occupants to the outside world and provides natural light to the indoor space. It is also a weak link in terms of thermal isolation from the outside environment because windows typically transmit heat much more readily than even a modestly insulated exterior wall. Poorly installed windows can have another dramatic impact on building energy requirements—they are leaky and allow for excess infiltration of outdoor air. The direction that a window faces strongly affects its exposure to sunlight, which partially determines the amount of solar radiation that it will transmit into the building. Shading both outside and inside the building can also have a strong impact on the amount of solar radiation transmitted into the building. The type of windows used, the quality of their installation, their orientation, and shading are all important factors that affect building energy performance.

5.6.1 Thermal Model

Figure 5.5 shows a typical window in a thermally massive wall. There is a heat flux through the window as a result of the temperature difference between the outside and the inside, and some portion of the incident solar radiation is transmitted through the window. There is also some amount of infiltration of outdoor air through the window, and the discussion of the associated load can be found in the section on indoor air.

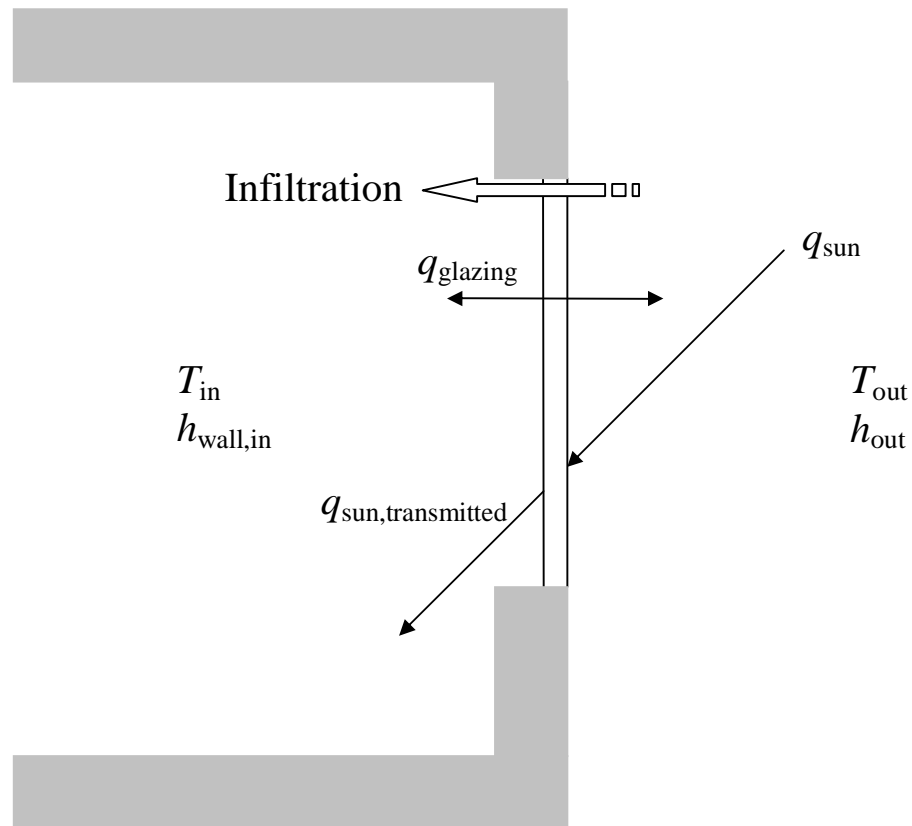


Figure 5.5: Schematic of glazing showing boundary conditions and various energy transport processes

5.6.1.1 Transmission of Heat

Heat transmission through windows is a complex process, especially when multiple panes of glass are used. Conduction through the panes, convection loops in between panes, and radiation exchange from one pane to another all play a role. Different types of window frames also transmit heat differently, and there are multi-dimensional effects near the edges of the window. A glazing does, however, typically have negligible thermal mass, so treating it as a pure resistance is a reasonable assumption.

A common simple model is to use an overall heat transfer coefficient, U , to predict heat transmission through a window. These values typically come from actual measurements of heat transfer through real glazing systems. The overall heat transfer coefficient includes both the glazing itself and the outdoor and indoor film resistances. The heat flux through the glazing to the indoor air, q_{glazing} , is approximated by:

$$q_{\text{glazing}} = U(T_{\text{out}} - T_{\text{in}}) = \frac{T_{\text{out}} - T_{\text{in}}}{R_{\text{film,out}} + R_{\text{glazing}} + R_{\text{film,in}}} \quad (5.11)$$

where R_{glazing} is the resistance of the glazing itself and the two film resistances are those for outside and inside. This quantity is multiplied by the total glazing area in order to obtain the total heat transfer to the indoor air through the system. Values for the overall heat transfer coefficient are tabulated in sources such as ASHRAE for a wide variety of window types and frames. Sometimes “center of glass” and “edge of glass” U values are listed to allow one to account for effects near the edge, but average values are used in this model for simplicity.

5.6.1.2 Transmission of Solar Radiation

The transmission of radiation through a window is an extremely complicated process because the many properties of the window depend on the solar altitude, relative azimuth, and wavelength within the spectrum of solar radiation. The amount of solar radiation that enters the building has two components—the transmitted radiation and the portion of the radiation absorbed by the glazing and later transferred to the indoors via conduction, convection, or radiation. A drastic simplification to the process is required in order to model these important effects in a way that does not require extensive, complicated input from the user.

A quantity known as the solar heat gain coefficient, $SHGC$, is tabulated as a function of incident angle for a wide variety of windows. It represents the total fraction of incident solar radiation that passes through the glazing system and becomes heat gain. Some of the heat gain is in the form of an incident heat flux on interior surfaces, and some is transferred directly to the indoor air after being absorbed by the glazing system. Values of the solar heat gain coefficient are averaged over the entire spectrum of solar wavelengths. The heat flux that becomes heat gain to the building for an unshaded portion of the fenestration system is given by:

$$q_{\text{sun,transmitted}} = SHGC(\theta)(E_{\text{D}})\cos\theta + SHGC_{\text{diff}}(E_{\text{diff,sky}} + E_{\text{diff,ground}}) \quad (5.12)$$

where $SHGC(\theta)$ indicates that the solar heat gain coefficient is a function of the incident angle and $SHGC_{\text{diff}}$ is the value of $SHGC$ for diffuse radiation. Recall from the chapter on outdoor boundary conditions that E_{D} is the incident direct normal radiation, $E_{\text{diff,sky}}$ is the diffuse sky radiation, and $E_{\text{diff,ground}}$ is the diffuse radiation reflected from the ground surrounding the building. As mentioned earlier, all of this transmitted radiation is assumed to strike the floors of the building. The heat flux on the floor for an unshaded glazing is computed by multiplying the

heat flux transmitted through the windows by the total window area and distributing it evenly across the entire floor surface area:

$$q_{\text{sun, floor, unshaded}} = \frac{\sum_{i=1}^4 (A_{\text{window, wall } i} \cdot q_{\text{sun, transmitted}})_{\text{wall } i}}{NF \cdot A_{\text{floor}}} \quad (5.13)$$

where

$q_{\text{sun, floor, unshaded}}$ = incident heat flux on the floor for unshaded windows

$A_{\text{window, wall } i}$ = total area of the windows on one wall of the building

A_{floor} = area of a single floor (equal to the building footprint area)

NF = the number of floors in the building

The implicit assumptions are that there is an equal glazing area on each of the building's floors and that there are no windows on the roof. This model does not account for solar gains through the window frame. Equation (5.13) is valid when the windows are unshaded, but shading devices both outside and inside the building are common. The effects of these shading devices are discussed next.

5.6.1.3 Outdoor Shading

There are numerous shading mechanisms for fenestration products, including overhangs, louvers, sunshades, screens, awnings, other architectural projections, and vegetation. Horizontal projections (i.e. overhangs) and vertical projections are considered in this model. In the northern hemisphere, overhangs can be an effective strategy to reduce cooling loads while having little impact on heating loads, particularly for windows that face south, southeast, or southwest. The relatively high solar altitude in the summer causes long shadows to be cast on the windows, preventing a great deal of direct normal radiation from ever striking the surface. Diffuse radiation incident on the window surface is also reduced since the overhang reduces the window's view of the sky. These effects can substantially reduce cooling loads. Because the solar altitude is relatively low in the winter, only small shadows are cast on the windows during the heating season and minimal solar radiation is blocked. Solar radiation is desirable during the winter because it reduces the heating load.

Figure 5.6 shows two views of a window with both horizontal and vertical projections along with some angles necessary to compute the size of the shadow cast by the projections.

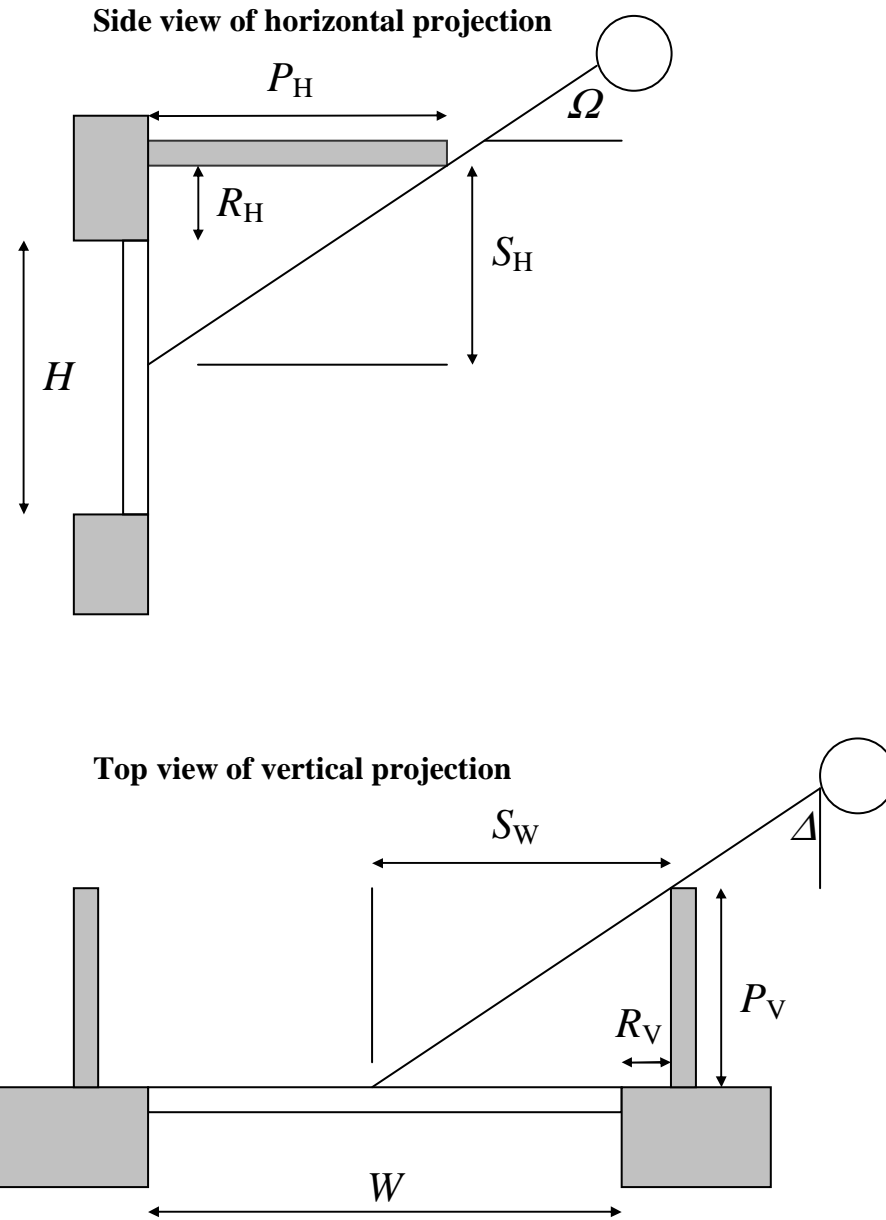


Figure 5.6: Geometry and shadows associated with vertical and horizontal window projections

Diffuse radiation will be incident on the entire window surface at a reduced intensity, but direct normal radiation is only incident on the sunlit portion. The profile angle, Ω , is shown in the figure and given by:

$$\tan \Omega = \frac{\sin \beta \sin \Sigma - \cos \beta \cos \gamma \cos \Sigma}{\cos \theta} \quad (5.14)$$

The angles β , γ , θ , and Σ are the solar altitude, relative azimuth, incident angle, and tilt angle, respectively, as defined previously in the chapter on outdoor boundary conditions. The vertical

projection profile angle, Δ , is also shown in the figure and given by:

$$\tan \Delta = \frac{\sin \gamma \cos \beta}{\cos \theta} \quad (5.15)$$

Both equations are valid whenever the incident angle is between 0° and 90° . Using these angles, the shadow width and height are computed:

$$S_W = P_V |\tan \Delta| \quad (5.16)$$

$$S_H = P_H |\tan \Omega| \quad (5.17)$$

where

S_W = shadow width

S_H = shadow height

P_V = vertical projection length

P_H = horizontal projection length

Finally, the fraction of the window area that is sunlit is computed for a given wall:

$$\frac{A_{\text{sunlit}}}{A_{\text{window, wall } i}} = \frac{[W - (S_W - R_W)][H - (S_H - R_H)]}{W \cdot H} \quad (5.18)$$

where

A_{sunlit} = sunlit window area on a given wall

W = window width

H = window height

R_W = spacing between window and vertical projection

R_H = spacing between window and horizontal projection

Care must be taken to ensure that the quantity inside the left set of brackets in this equation is between zero and W , and the quantity inside the right set of brackets is between zero and H . A sunlit dimension of a window cannot be negative, nor can it be larger than the corresponding total dimension of the window. With very large or very small shadows, Equation (5.18) cannot be used explicitly; the physical limitations just mentioned are enforced instead.

The expression for heat flux that enters the building, $q_{\text{sun,transmitted}}$, remains the same. The only difference is that the direct normal radiation, E_D , is equal to zero for shaded portions of the glazing. The final expression for computing the incident heat flux on the floor of the building accounts for the sunlit and shaded areas of the glazing system, and it will be presented after the model for indoor shading is introduced.

5.6.1.4 Indoor Shading

Indoor shading devices such as Venetian blinds, roller shades, and drapes are extremely common in residential buildings. In addition to some degree of control over sunlight, they also provide privacy and decoration. The interior solar attenuation coefficient, IAC , is a very simple way to account for the effects that some of these shading devices have on the amount of solar radiation that is transmitted through the glazing system. The means for calculating the amount of radiation transmitted to the indoors in the absence of interior shading has already been discussed. This quantity is simply multiplied by an appropriate attenuation coefficient, which is a number between zero and one. An interior shading device with an IAC of 0.80 reduces the total amount of solar radiation entering the space by 20%.

Since an architect is unlikely to have any control over the internal shading devices that are used in a building, Venetian blinds are assumed to be present in all of the building's windows. It is further assumed that these blinds are left open during the heating season ($IAC = 1.0$) and closed 45° during the cooling season ($IAC = 0.75$). Such a blind schedule allows as much solar radiation as possible to enter the building when heat gains are helpful. It also blocks some excess heat during the cooling season but still transmits natural light.

After accounting for both exterior and interior shading, the total solar radiation transmitted through the glazing system can be determined. The heat flux incident on the floor is then calculated by evenly distributing this radiation over the entire floor area of the building:

$$q_{\text{sun, floor}} = \frac{IAC \sum_{\text{walls}} [SHGC(\theta)(E_D \cos \theta)A_{\text{sunlit}} + SHGC_{\text{diff}}(E_{\text{diff, sky}} + E_{\text{diff, ground}})A_{\text{window}}]}{NF \cdot A_{\text{floor}}} \quad (5.19)$$

It is this value that is used as the boundary condition shown in Figure 5.2 and Figure 5.3.

5.6.2 Assumptions

Many assumptions are made in the simplified model presented for the glazing system. Any thermal mass of the windows is neglected when using the overall heat transfer coefficient, U , to model heat transmission. This value is held constant throughout the year, but the outdoor film resistance is actually strongly dependent on the wind conditions, which obviously vary. Tabulated values of U typically assume fairly strong wind conditions, resulting in a “worst case” scenario. Heat transmission through the windows is also assumed to be independent of the

transmission of thermal radiation. In fact, these two processes are coupled. Some amount of thermal radiation incident on a window is absorbed, resulting in a higher temperature of the glass and affecting the magnitude and possibly the direction of heat flux.

The transmission of thermal radiation through windows is modeled using the solar heat gain coefficient, *SHGC*. Although its value is wavelength-dependent, integrated values over the entire solar spectrum are used in the model. As previously discussed, all radiation that enters the building is assumed to be absorbed by the floor. The solar heat gain coefficient is intended to predict the total amount of incident radiation that eventually heats the building, including a portion that is absorbed by the glazing and later transmitted to the space. Some of the absorbed radiation will be transmitted directly to the indoor air rather than to the interior surfaces of the building, but the model assumes that even this portion of the incident solar radiation is absorbed by the floor.

The configuration used to derive the equations for exterior shading is shown in Figure 5.6. Although the configuration includes both horizontal and vertical projections, it is possible for the model to incorporate only one of the two. If only an overhang is used on a building (i.e. a horizontal projection), the assumption is that the projection is very wide compared to the window. Likewise, if only vertical projections are used, the assumption is that they are very tall compared to the window. Although architectural projections reduce the view factor between the window and the sky, this effect is not incorporated into the model. The amount of diffuse sky radiation received at the window surface is modeled the same way with or without projections. Venetian blinds are assumed to be present in all windows, and the interior solar attenuation coefficient is used to model their effects on the amount of solar radiation that is admitted to the building space. This quantity also depends on solar position and wavelength, but these dependencies are ignored. Although the transmittance of solar radiation through windows is inherently complicated, considerable simplification has been made to produce results that are accurate as a first order approximation.

5.7 Indoor Air

Indoor air is the most important factor affecting the thermal comfort of a building's occupants. With the exception of the use of indoor shading devices, the indoor air is the first model component over which the occupant exercises control. The air temperature is typically

controlled by a thermostat, which triggers the heating or cooling system when the temperature drops below or rises above the desired level. The humidity of the air is also important for occupant comfort, but latent loads are not considered in this model.

5.7.1 Thermal Model

Heat is exchanged between the indoor air and all of the building's interior surfaces. As modeled, the heat exchange through the slab perimeter is also with the indoor air. Some amount of outdoor air is mixed with the indoor air due to both ventilation and infiltration. Finally, internal gains from occupants, appliances, and lighting add heat to the indoor air. All of these factors combined can result in a load on the heating or cooling system if additional energy must be added or removed to maintain the air within the desired temperature range. Recall from Equation (3.14) that the net heat transferred to the ambient air from a surface in the general model presented is given by:

$$q_1'' = \frac{T_n - T_{\text{amb}} + Q \cdot R_{\text{ins}}}{R_{\text{tot}}} \quad (5.20)$$

The thermal mass of the indoor air is orders of magnitude lower than those of the massive building components, so the air temperature is assumed to respond instantaneously to set the heat gains equal to the losses. The model assumes that all of the indoor air is well-mixed and at a uniform temperature. In other words, the entire building is treated as a single zone at the same temperature. Recalling that the inverse of R_{tot} is equal to h_{eff} and utilizing the thermal models already presented, the energy balance for the indoor air is given by:

$$\begin{aligned} & \sum_{\text{walls}} \left[h_{\text{eff,wall}} A_{\text{wall}} (\hat{T}_{\text{in}} - \hat{T}_{\text{wall}}) \right] + h_{\text{eff,floor}} A_{\text{floor}} (\hat{T}_{\text{in}} - \hat{T}_{\text{floor}}) + h_{\text{eff,int floor,top}} A_{\text{int floor}} (\hat{T}_{\text{in}} - \hat{T}_{\text{int floor,top}}) \\ & + h_{\text{eff,int floor,bottom}} A_{\text{floor}} (\hat{T}_{\text{in}} - \hat{T}_{\text{int floor,bottom}}) + \hat{q}_{\text{sun,floor}} \left[A_{\text{floor}} \left(\frac{R_{\text{ins,floor}}}{R_{\text{tot,floor}}} \right) + A_{\text{int floor}} \left(\frac{R_{\text{ins,int floor,top}}}{R_{\text{tot,int floor,top}}} \right) \right] \\ & + h_{\text{eff,roof}} A_{\text{roof}} (\hat{T}_{\text{in}} - \hat{T}_{\text{roof}}) + F \times P (\hat{T}_{\text{in}} - \hat{T}_{\text{out}}) + \frac{(\rho c_p)_{\text{air}} V_{\text{air}}}{3600} \times ACH (\hat{T}_{\text{in}} - \hat{T}_{\text{out}}) \\ & + UA_{\text{windows}} (\hat{T}_{\text{in}} - \hat{T}_{\text{out}}) - Q_{\text{gain}} = 0 \end{aligned} \quad (5.21)$$

where

$h_{\text{eff,surface}}$ = effective convection coefficient for the *inside* of a specific surface

A_{surface} = surface area of the inside of a specific surface

A_{windows} = total surface area of all the windows on the building

T_{surface} = temperature of the node closest to the indoor air for a specific surface

$R_{\text{ins,surface}} = R_{\text{ins}}$ (combined resistance of lightweight layers) applied to specific surface

$R_{\text{tot,surface}} = R_{\text{tot}}$ (total resistance of film and lightweight layers) applied to specific surface

$(\rho c_p)_{\text{air}}$ = density multiplied by constant pressure specific heat for air

V_{air} = air volume inside the building

ACH = number of air changes per hour in the building due to ventilation and infiltration

Q_{gain} = internal gains from occupants, appliances, etc. (units of power)

When the temperature is within the allowable range, the heating and cooling systems are inactive, and this equation is used to determine how the indoor temperature changes from hour to hour. When the heating or cooling system is active, the indoor temperature is fixed at the thermostat setting. In this case, the left-hand side will represent the instantaneous heating load. The way in which the program handles switching between these two different regimes will be explained in the section describing the simulation process.

5.7.2 Assumptions

The major assumption made in modeling the indoor air is treating the entire building as a single zone. The larger the building, the more inaccurate this assumption is, but it is still adequate for first order approximations of building heating and cooling requirements. In apartment buildings, there is often control for each individual apartment or, at the very least, for each floor. Treating the entire air volume as well-mixed at a uniform temperature is effectively using an average building air temperature to calculate heat transfer at every surface. Neglecting the thermal mass of the air is another assumption in the model. Reasons for avoiding nodes with very low thermal mass were discussed in the chapter on the general model, and the air is even more lightweight than insulation. The thermal mass of all the items inside the building (e.g. furniture) is also neglected in this formulation.

5.8 Convection and Radiation Coefficients

It has been mentioned that the film resistances in the model are based on combined convection and radiation coefficients. A brief explanation of this modeling technique is presented here, followed by the actual values for the coefficients used in the model.

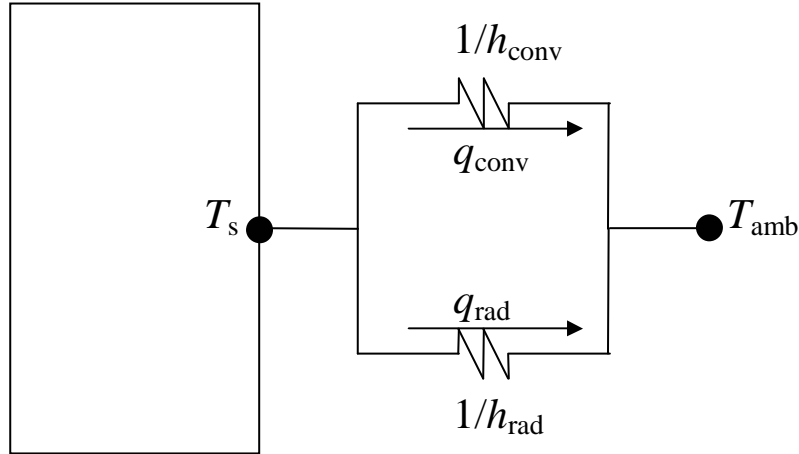


Figure 5.7: Resistances due to convection and radiation between surface and ambient conditions

5.8.1 Thermal Model

A building surface at temperature T_s typically exchanges heat with the surroundings via both convection and radiation. These two mechanisms occur in parallel, and they can be thought of as resistances between the surface and ambient air temperatures, as shown in Figure 5.7. The convection coefficient is defined in terms of the convective heat flux from the surface, q_{conv} , and the temperature difference:

$$q_{\text{conv}} = h_{\text{conv}} (T_s - T_{\text{amb}}) \quad (5.22)$$

Assuming that the surroundings act as a blackbody at ambient temperature, the radiative heat flux from the surface, q_{rad} , depends on the difference of the temperatures to the fourth power:

$$q_{\text{rad}} = \varepsilon \sigma (T_s^4 - T_{\text{amb}}^4) \quad (5.23)$$

where ε is the surface emissivity and σ is the Stefan-Boltzmann constant, which is equal to $5.67 \times 10^{-8} \text{ W}/(\text{m}^2\text{K}^4)$. All temperatures in the radiation equations must be expressed on an absolute (Kelvin) scale. Linearizing this equation is a simplification that allows for the convenient definition of a radiation coefficient:

$$q_{\text{rad}} \approx 4\varepsilon\sigma T_m^3 (T_s - T_{\text{amb}}) = h_{\text{rad}} (T_s - T_{\text{amb}}) \quad (5.24)$$

where T_m is the mean of the other two temperatures. Combining the parallel resistances into a single equivalent resistance gives the combined convection and radiation coefficient, h_{combined} :

Table 5.2* : Film coefficient values used in the model for each surface of interest

Surface	Symbol	Value (W/m²K)
Walls	$h_{\text{wall,in}}$	8.29
Ceilings	$h_{\text{roof,in}}$	6.13
Floors	$h_{\text{floor,in}}$	9.26
Outside Surfaces	h_{out}	34.0

* Note: Values come from [2], Table 1 on p. 25.2

$$h_{\text{combined}} = h_{\text{conv}} + h_{\text{rad}} \quad (5.25)$$

All of the film coefficients presented in the model are of this general form. Note that a pure convection coefficient could still be used by setting the surface emissivity equal to zero. The values used in the program for each of the surfaces were taken from [2], and they are shown in Table 5.2.

5.8.2 Assumptions

Linearizing the expression for radiative heat flux from a surface is an approximation that is appropriate for the purposes building energy simulations. The error introduced by this approximation grows with the temperature difference between the surface and its surroundings, which is relatively small as far as buildings are concerned. The outside surface is assumed to exchange radiation with a virtual blackbody at the ambient temperature. This assumption introduces a small amount of error when a building surface is radiating to the night sky. It has already been mentioned that radiation exchange between interior surfaces of the building is not considered in this model. Using a combined convection and radiation coefficient rather than a pure convection coefficient for the inside building surfaces results in an increased amount of heat exchange between the interior surfaces and the indoor air. The reason for including radiation and reducing the film resistance involves thermal mass inside the building that has not been accounted for in any other way. The assumption is that the interior surfaces will radiate to the furnishings and other objects inside the building, which are approximately at the indoor temperature. These objects will then quickly come into thermal equilibrium with the air. Although the interior building surfaces do not really radiate to the indoor air, making this assumption is a fairly realistic and simple way to deal with radiation from these surfaces.

5.9 Simulation Using the Model Components

Once model parameters are fixed based on input from the user and the boundary conditions are obtained from a weather data file, all of the modeling presented thus far produces an equal number of equations and unknown nodal temperatures. These equations can be rearranged by moving all temperatures at time $t+\Delta t$ to the left hand side and all other terms to the right hand side. After grouping like terms, the equations take the following form:

$$\mathbf{A}\hat{\mathbf{T}} = \mathbf{B}\mathbf{T} + \mathbf{C} \quad (5.26)$$

where

\mathbf{A} = coefficient matrix for the temperatures at the next time step

\mathbf{B} = coefficient matrix for the temperatures at the current time step

\mathbf{C} = vector collecting all constant terms

$\hat{\mathbf{T}}$ = vector of unknown nodal temperatures at the next time step

\mathbf{T} = vector of known temperatures at the current time step

Steady state temperatures using weather data for the first hour of the year are used as initial conditions (i.e. the vector \mathbf{T} for the first hour of the simulation). With values for \mathbf{T} substituted into the equation, the problem reduces to a simple set of linear equations.

The general procedure for a simulation involves solving for the nodal temperatures at successive time steps. The unknown temperatures are obtained by solving the system of equations. The temperatures just obtained are then substituted into the vector \mathbf{T} , and the process is repeated, allowing the simulation to march forward in time. The most computationally efficient method of solving such a system of equations is LU decomposition, and this method is the one used by the program. The matrix \mathbf{A} can be decomposed once and used to solve the system for any vector on the right hand side of the equation. The simulation runs for every hour of the year, and it typically completes in less than two seconds on a 950 MHz computer, which is modest by 2004 standards.

Up to this point, there has been no mention of the thermostat settings and the role that they play in the simulation. Figure 5.8 shows an example of the relationship between the upper and lower thermostat set points, fixed and floating air temperatures, and loads. Currently, the range of acceptable indoor temperatures is set to 18°C-26°C. When the indoor air temperature is

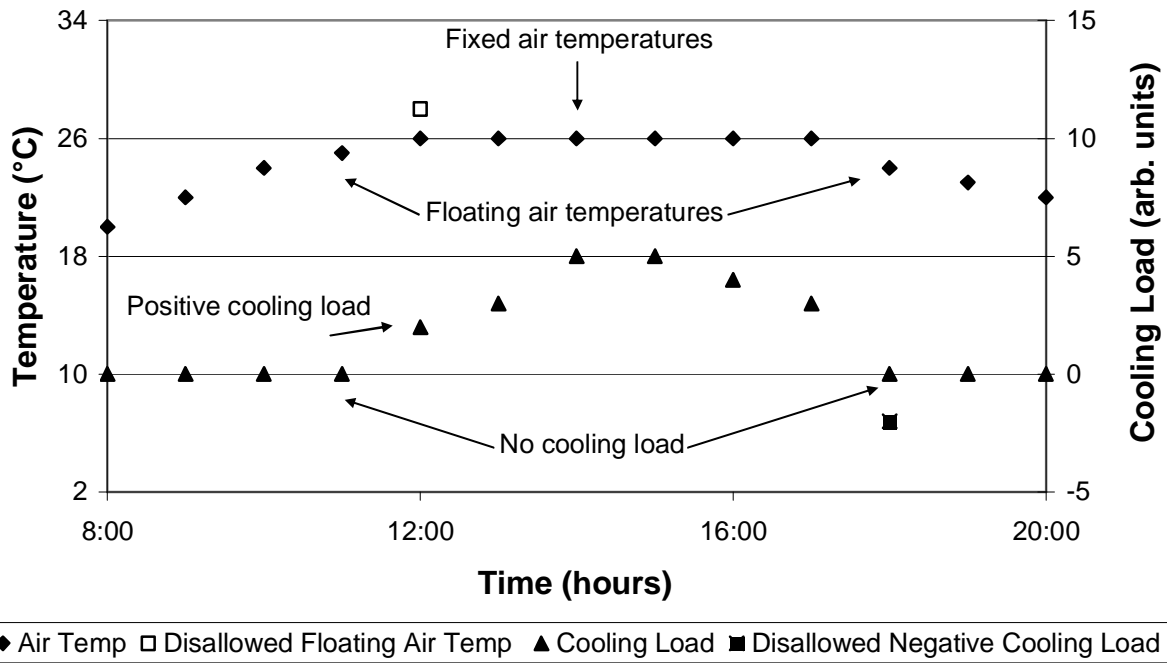


Figure 5.8: Sample day showing periods of both fixed air temperatures with loads and floating air temperatures with no loads

within that range, it is allowed to float freely by including it as a variable in the system of equations. There is no load on the heating or cooling system in this situation. When the solution to the system of equations yields an indoor temperature outside of the acceptable range, the approach used by Spindler is taken [14]. The simulation reverts to the temperatures from the previous time step and fixes the indoor temperature at the appropriate thermostat setting. The upper thermostat setting is used when the indoor temperature floats above the allowable range (typically in the cooling season), and the lower setting is used when it floats below the allowable range (typically in the heating season). This action removes one equation (the energy balance for the indoor air temperature node) and one unknown (the indoor air temperature) from the system. Some new constant terms are introduced to the right-hand side of the equation since a fixed value is substituted for the indoor air temperature. Nodal temperatures are then obtained by solving this slightly modified system, and loads are calculated from the left-hand side of Equation (5.21). Using this equation, a positive quantity represents a heating load, and a negative quantity represents a cooling load. The simulation continues in this manner until a *heating* load is obtained at the *upper* thermostat setting or a *cooling* load is obtained at the *lower* thermostat setting. Such an occurrence indicates that the indoor air temperature should be allowed to float

freely. This process continues, switching between fixed and floating indoor air temperature as appropriate, until the end of the year is reached.

As an example, consider a summer day like the one in Figure 5.8 that begins with the cooling system turned off and an indoor temperature within the allowable temperature range. At some point in the day, continuing to allow the indoor temperature to float would result in an air temperature above the upper limit of the allowable range. When that happens, the cooling system activates and fixes the indoor temperature. The program approximates this behavior by reverting to the temperatures at the previous time step and fixing the indoor air temperature at 26°C. New nodal temperatures are then calculated using the fixed air temperature, and they are used to compute the cooling load. There continues to be a load on the cooling system throughout the hottest part of the day. When outdoor conditions cool down in the evening and comfortable conditions can be maintained without the aid of the cooling system, the indoor temperature is again allowed to float. In this case, maintaining the indoor temperature at 26°C would impose a load on the *heating* system (i.e. a negative cooling load). A heating load at the upper thermostat setting is the cue for the program to switch back to floating indoor air temperatures. It would be nonsensical for the heating system to turn on in order to maintain the 26°C indoor temperature when lower temperatures are within the allowable range.

Since the behavior of occupants cannot be accurately predicted, an assumption about when the windows of a building are open must be made. Assuming that the windows of a residential building are always closed usually results in unrealistically high cooling loads. The only difference in the model when the windows are open is that an increased air change rate, *ACH*, is used. The specific numerical values of the air change rates used in the program are discussed in the next chapter. The simulation runs with open windows for hours in the cooling season during which the outdoor temperature is within the comfortable range (i.e. between the upper and lower thermostat settings). This assumption is not completely realistic because occupants are not always at home to open and close windows as the outdoor temperature varies. However, making the assumption provides more accurate estimates of cooling loads because people tend to leave their windows open when the outdoor air temperature is comfortable rather than using the air conditioning system. The simulation procedure for switching between fixed and floating indoor air temperatures remains the same regardless of whether or not the windows are open.

5.10 Summary

The general model that was derived in a previous chapter has been applied to several building components—the exterior walls, ground floor, internal floors, and roof. Thermally massive material layers were divided into discrete sections with nodes at the center, and lightweight layers were treated as purely resistive. Different modeling techniques which neglect the effects of thermal mass were used for the glazing system and indoor air. All of the building component models were synthesized, resulting in a system of equations that can be solved to obtain temperatures at each node for every hour of the year. Finally, the procedure that the program uses to run the hourly simulations was described, which allows for both fixed and floating indoor air temperatures.

Chapter 6

Model Parameters and the User Interface

6.1 Introduction

In the preceding chapters, the thermal models for each building component used in the program have been presented, and the way in which these components are synthesized to run hourly simulations and calculate loads has been described. The values of most of the model parameters were left unspecified because they are set based on input from the user. In this chapter, the options available in the user interface and the parameters that they set in the model will be described. Some parameter values are not influenced by the options selected by the user, and these fixed values will be presented after the interface is explained.

The primary goal of this program is to provide the user with rough estimates of building energy use and to show the energy-related consequences of certain important design decisions. One of the biggest challenges in developing a user interface for a simulation program of this sort is the tradeoff between simplicity and available options to the user. The target user of this program is an architect without extensive knowledge of energy-related issues in the early stages of the design process. While there are numerous parameter values that go into the model, it is unlikely that such a user would want to specify something like the emissivity of an exterior wall surface. The approach taken in developing the interface was to keep it as simple as possible. Some inputs, such as location and size of the building, are required to run a simulation and must be provided by the user. Because this type of input essentially defines the context of the problem, making presumptions about it does not make sense. Aside from these defining features, the user is only presented with choices over which they are likely to have some degree of control and that are important to the building's overall energy consumption. As such, many of the parameter values presented in this chapter represent nominal values. For example, the user can specify a double-glazed window, but he or she cannot specify a double-glazed window with green tinted glass and an aluminum frame. Keeping the number of choices to a minimum helps avoid information overload, and it also decreases the likelihood that a user will become frustrated

trying to figure out how to use the program and abandon it altogether. The hope is that, if useful information can be obtained with a minimal learning curve, the design tool is more likely to be used and help the architect make sustainable design choices.

Figure 6.1 shows a screen shot of the program's user interface. The input and output portions are both visible at the same time, allowing the user to see results almost immediately after saving a building scenario. The results for up to four building scenarios can be shown at the same time, allowing for a side-by-side comparison of different cases. For example, the user could compare a base case building with single-glazed windows to other cases with double- and triple-glazed windows directly. Notice that the input portion of the interface is divided into several groups (not all of which are visible in the screen shot). The various values that must be chosen by the user will be explained by group in the following sections.

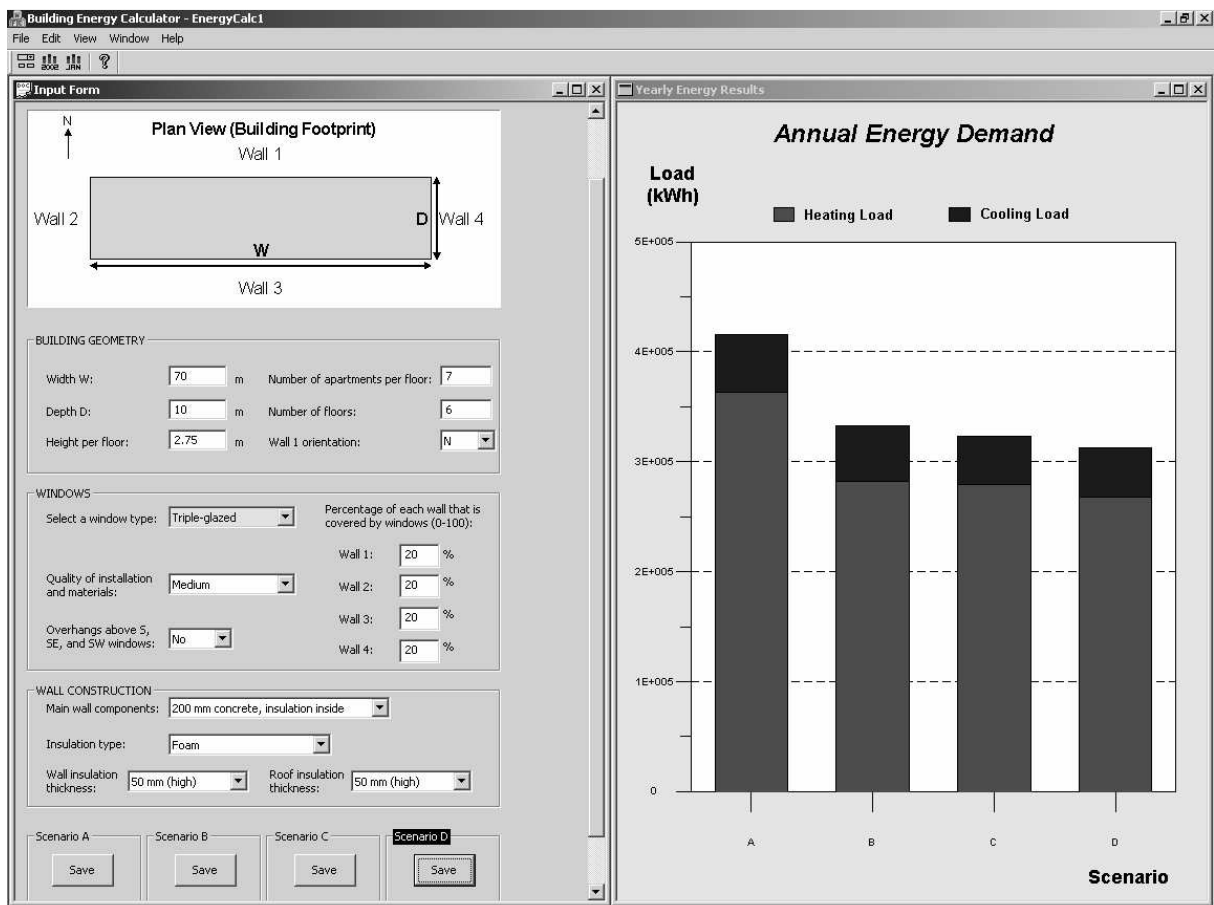


Figure 6.1: Screen shot of the program's user interface

6.2 Location Group—Select a City

The climate of the area in which a building is located is what drives the need for space conditioning—the outdoor temperature is not always at a level that people deem comfortable. In the city selection input, there is a list of cities for which weather data are available. The city selected should be either the city where the building is located or the one with the most comparable climate because the selection determines which weather data file is used to run the simulations. In addition, heating and cooling seasons are defined for each city based on an examination of average monthly temperatures. Months with average temperatures below 18°C are considered to be in the heating season. The need to distinguish between the heating and cooling seasons will become clear when air changes are discussed later in this chapter.

6.3 Building Geometry Group

6.3.1 Variables Defining Building Size: Width, Depth, Height per Floor, and Number of Floors

Depending on the design requirements, the size of an apartment complex may range from a small, one-story building to a large, multi-story building. Figure 6.2 shows the graphic that is used in the program to help the user specify some of the geometric parameters for the building. Notice that the program assumes a rectangular footprint. The width, W , and depth, D , of the building footprint and the height per floor of the building, HPF , are input in meters. Together

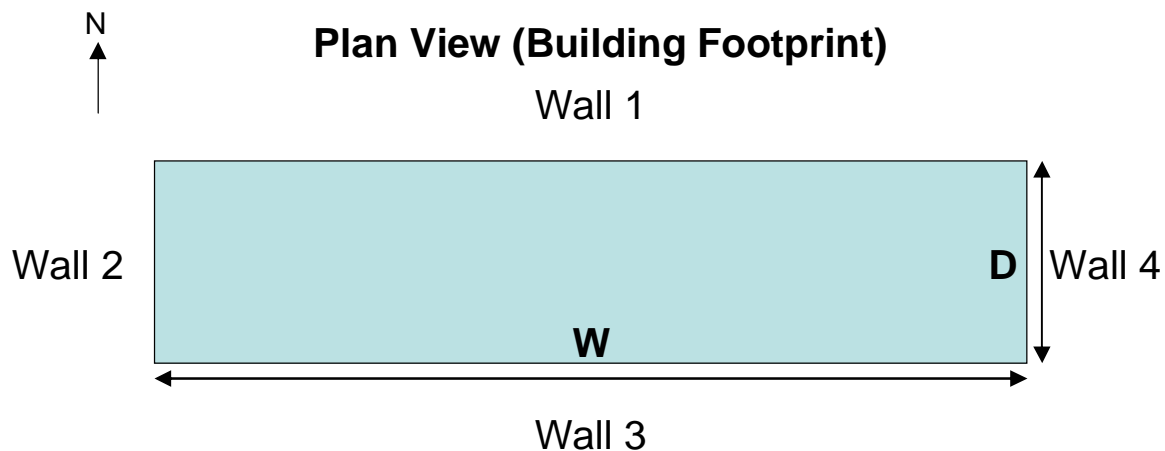


Figure 6.2: Graphic from user interface explaining building geometry

with the number of floors, NF , these parameters fully specify the size of each relevant building surface. The floor area is simply taken as the product of the width and depth of the footprint:

$$A_{\text{floor}} = W \times D \quad (6.1)$$

This value applies to the ground floor and each internal floor. The slab perimeter is given by:

$$P = 2(W + D) \quad (6.2)$$

The total surface area of each exterior wall, including the wall and its windows, is calculated by multiplying the height of the building by either the width or depth, depending on which wall in the figure is of interest:

$$A'_{\text{wall 1}} = A'_{\text{wall 3}} = W \times HPF \times NF \quad (6.3)$$

$$A'_{\text{wall 2}} = A'_{\text{wall 4}} = D \times HPF \times NF \quad (6.4)$$

The prime (') symbols in these equations are to distinguish the total surface area of each exterior wall, including the wall and its windows, from the portion that is strictly wall material and does not include windows. The wall numbers in the subscripts refer to the labels in Figure 6.2. Although the specified values are technically outside building dimensions, they are also used as the inside dimensions in calculating wall areas. In other words, the overlap between two walls is not subtracted from the inside surface area. Finally, the air volume inside the building, V_{air} , is computed from the user-specified dimensions:

$$V_{\text{air}} = W \times D \times HPF \times NF \quad (6.5)$$

Recall that all of these quantities are used in the energy balance for the indoor air temperature node and in calculating heating and cooling loads. All of the other energy balances are on a per unit area basis, and the size of the building does not enter into the picture.

6.3.2 Number of Apartments per Floor

The number of apartments per floor multiplied by the number of floors gives the total number of apartments in the building, which is used to estimate the internal gains that add heat to the indoor air. Recall that solar gains are modeled separately. The internal gains are highly uncertain at the preliminary design stages of a building, but they are an important factor in determining cooling loads and must be estimated. The assumption made in the program is that, on average, each apartment has two people giving off 67 W each and an appliance load of 250 W. The total internal gains, Q_{gain} , are therefore estimated to be 384 W/apartment multiplied by the

total number of apartments, and this value is held constant throughout the year. In reality, the gains would vary throughout the course of a day as people come to and go from an apartment, but attempting to account for occupancy schedules is beyond the scope of this program.

6.3.3 Wall 1 Orientation

The amount of sunlight that a building receives depends on its orientation. The wall 1 orientation input allows the user to select an orientation for the building in any of the cardinal or intermediate directions. The value specified by the wall 1 orientation input is the direction that an outward normal vector from “Wall 1” in Figure 6.2 would point. Whenever the selection is changed, the compass arrow in the upper left hand corner of the figure is automatically rotated to point the appropriate way. The selection sets the appropriate surface azimuth, ψ , between -180° and $+180^\circ$ for each of the four walls in the model (south = 0° , east = -90° , west = $+90^\circ$, etc.). The angle between each of the walls is assumed to be 90° .

6.4 Windows Group

6.4.1 Window Type

Using windows with multiple panes of glass can significantly enhance the insulating quality of the glazing system while still allowing ample sunlight to enter the building. The window type input allows the user to select from windows that are single-glazed, double-glazed, double-glazed with a low emissivity coating, and triple-glazed. The selection determines both the overall heat transfer coefficient for the window, U , and the solar heat gain coefficient, $SHGC$. Table 6.1 shows the values used in the program for each choice, which are taken from [2].

Table 6.1: Window overall heat transfer coefficients and solar heat gain coefficients from ASHRAE

Description	ID*	U_1^{**} (W/m ² K)	U_2^{***} (W/m ² K)	$SHGC(\theta)$						
				0°	40°	50°	60°	70°	80°	diffuse
Single-glazed	1a	6.12	7.24	0.86	0.84	0.82	0.78	0.67	0.42	0.78
Double-glazed	5a	3.42	4.62	0.76	0.74	0.71	0.64	0.50	0.26	0.66
Double-glazed, low e	17a	2.89	4.05	0.65	0.64	0.61	0.56	0.43	0.23	0.57
Triple-glazed	29a	2.60	3.80	0.68	0.65	0.62	0.54	0.39	0.18	0.57

* ID refers to the ID used in [2]. See Table 4 on p. 30.8 and Table 13 on p. 30.26

** Overall heat transfer coefficient for aluminum frame with thermal break

*** Overall heat transfer coefficient for aluminum frame without thermal break

Notice that there are two overall heat transfer coefficients listed in the table. One of them, U_1 , is used for aluminum frames with a thermal break, and the other, U_2 , is used for aluminum frames without a thermal break. Which of these two values is set in the model depends on the quality of installation and materials input, as discussed in the next section. For the solar heat gain coefficient, linear interpolation is used when the incident angle falls between the tabulated values.

6.4.2 Quality of Installation and Materials

The amount of care taken in the installation of windows can have a large impact on building energy consumption. Windows installed by unskilled workers or without appropriate attention may allow excess infiltration of outdoor air. The quality of the windows themselves may also be sub-par, causing them to transmit heat more readily than they would otherwise. The quality of installation and materials input allows the user to select between high (airtight), medium, and low (leaky) quality installation. The selection fixes the air change rate when windows are closed in the building. Different air change rates are used during the heating and cooling seasons because wind speeds and air leakage tend to be higher during the winter months. Table 6.2 shows the number of air changes per hour (*ACH*) used in the program, including both ventilation and infiltration, in both seasons for the different qualities of window installation. These values are loosely based on those found in Tables 7 and 8 on p. 28.4 of [2], but they are modified to reflect the fact that construction standards in China are not yet as high as they are in the United States. When the outdoor air is at a comfortable temperature, opening the windows can be an alternative to using an air conditioning system, particularly during the cooling season. When the windows are open, the program assumes 6.0 air changes per hour in the building.

In the previous section, two different overall heat transfer coefficients were listed for each type of window. When high or medium quality is selected, the value for the window having an aluminum frame with a thermal break (U_1) is used. When low quality is selected, the higher value for the window having an aluminum frame with no thermal break (U_2) is used. The

Table 6.2: Air changes per hour for different qualities of window installation

Installation Quality	Heating Season <i>ACH</i>	Cooling Season <i>ACH</i>
High (airtight)	2.0	1.5
Medium	1.0	0.70
Loose (leaky)	0.50	0.50

wide range of values for both the air changes and the overall heat transfer coefficients indicates that the type and quality of a building's windows as well as the effectiveness of the installation are very important in terms of building energy requirements.

6.4.3 Overhangs above S, SE, and SW Windows

Properly designed exterior shading of windows can reduce cooling loads in a building with minimal impact on heating loads. At this time, the only option in the user interface involving exterior shading is a yes or no option to put overhangs (i.e. horizontal projections) above windows that face south, southeast, and southwest. Setting the input to yes assumes that there are overhangs above all windows on walls facing any one of the three directions mentioned. In the spirit of keeping things simple for the user, a typical geometry is assumed for the window and the overhang. Figure 6.3 shows a side view of the configuration. The window width, W , is into the page in this figure. The following parameter values are used:

$W = 0.90$ m (window width)

$H = 1.50$ m (window height)

$P_H = 0.60$ m (horizontal projection length)

$R_H = 0.40$ m (spacing between window and horizontal projection)

Although the possibility to include them was built into the model, vertical projections are not used at this time (i.e. the vertical projection length, P_V , is zero). When the overhang input is set

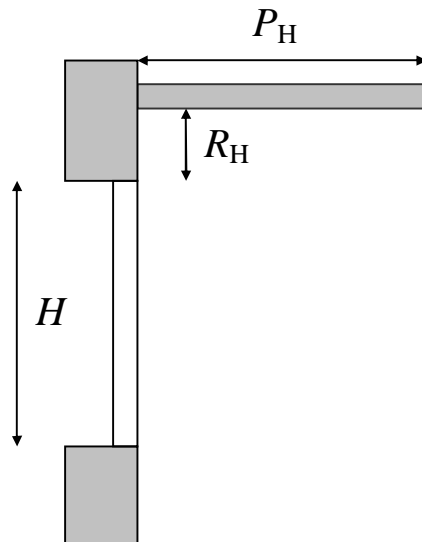


Figure 6.3: Geometry of window and overhang (side view)

to no, both the vertical and horizontal projections have zero length. The exterior shading portion of the model then has no effect on the simulation.

6.4.4 Wall 1-4 Window Percentage

Windows are seldom distributed evenly among the walls of a building. Putting a relatively large glazing area on the south side of a building is often a good strategy for passive solar heating in the winter months. The window percentage inputs allow the user to specify the window area on each wall as a percentage of the total wall surface area, which was calculated in the section on variables defining building size. Note that 25% is entered as 25 rather than 0.25. The total window area for each wall is equal to the total wall surface area multiplied by the appropriate fraction:

$$A_{\text{window, wall 1}} = A'_{\text{wall 1}} \left(\frac{WP_{\text{wall 1}}}{100} \right) \quad (6.6)$$

where $WP_{\text{wall 1}}$ is the window percentage for wall 1. The rest of the total surface area consists of the actual wall materials:

$$A_{\text{wall 1}} = A'_{\text{wall 1}} \left(1 - \frac{WP_{\text{wall 1}}}{100} \right) \quad (6.7)$$

It is this final wall area that is used when computing the heat transfer from the inside wall temperature node to the indoor air.

6.5 Wall Construction Group

6.5.1 Main Wall Components

Wall constructions in buildings range from lightweight wood frames to dense concrete slabs, and the thermal mass of the walls affects energy flow through the building envelope. Concrete construction is extremely prevalent in China since it is one of the most readily available materials, so the available options in the program focus on this type of construction. The choices presented to the user include both 200 and 300 mm concrete slab walls with the primary insulation layer either inside or outside of the concrete. The complete wall composition, from inside to outside, for each of the 200 mm concrete wall constructions is shown in Table 6.3. The only difference between these options and the 300 mm concrete options is the thickness of the

Table 6.3: Exterior wall composition (from inside to outside) for 200 mm concrete options in the interface

Wall composition for 200 mm concrete, insulation inside selection					
Material	Layer Classification	Number of Nodes, N	Layer Thickness, LT	Thermal Conductivity, k	Thermal Mass, ρc
			(m)	(W/m-K)	(J/m ³ -K)
Gypsum	Lightweight	0	0.0127	0.16	0.
Plywood	Lightweight	0	0.010	0.11	0.
Insulation	Lightweight	0	See insulation input description		0.
Concrete	Massive	5	0.200	1.3	1.98×10^6
Wall composition for 200 mm concrete, insulation outside selection					
Material	Layer Classification	Number of Nodes, N	Layer Thickness, LT	Thermal Conductivity, k	Thermal Mass, ρc
			(m)	(W/m-K)	(J/m ³ -K)
Gypsum	Lightweight	0	0.0127	0.16	0.
Plywood	Lightweight	0	0.010	0.11	0.
Concrete	Massive	5	0.200	1.3	1.98×10^6
Insulation	Lightweight	0	See insulation input description		0.
Sheathing	Lightweight	0	0.0095	0.090	0.

concrete layer. As discussed in the modeling chapters, the lightweight layers do not have nodes or a thermal mass since they are modeled as pure resistances. The thickness and conductivity of the insulation layers depend on other options in this input group, which are discussed next.

6.5.2 Insulation Type

There are many different types of insulation that are used in buildings, and they have varying levels of performance. Foam insulation is the most common type in buildings that have concrete frames. The insulation type input allows the user to choose between four different types of insulation, and the selection sets the thermal conductivity, k , for the primary insulation layer. The available options are foam (0.025 W/m-K), glass fiber (0.036 W/m-K), loose fill cellulose (0.042 W/m-K), and cement fiber slabs (0.074 W/m-K). These values were taken from Table 4 on p. 25.5 of [2].

6.5.3 Wall Insulation Thickness

Properly insulating the exterior walls of a building is one of the most critical steps towards achieving an energy-efficient building. The wall insulation thickness input allows the

user to set the thickness of the primary insulation layer anywhere from 0-100 mm in increments of 10 mm. This value is used in conjunction with the thermal conductivity of the insulation, as determined in the previous section, to determine the resistance of the insulation layer, R_{ins} , that is used in the model.

6.5.4 Roof Insulation Thickness

It is not uncommon for builders to make insulation in the exterior walls a major focus, but insulation in the roof is often neglected or given little attention. This behavior can result in a substantial increase in heating and cooling loads in the building. In order to demonstrate this effect, the roof insulation thickness input allows the user to set the thickness of the primary roof insulation layer independent of the wall insulation thickness. The available options cover the same range of 0-100 mm in increments of 10 mm. The insulation type for the roof is assumed to be the same as it is for the exterior walls.

6.6 Other Model Parameters

In order to limit the amount of required input information, several model parameters not yet mentioned in this chapter take on assumed values that the user cannot influence through the interface. The roof, ground floor, and internal floors are all assumed to be 100 mm concrete slabs with the same material properties as the concrete in the exterior walls. The roof insulation layer is placed inside the concrete layer, and a layer of gypsum wall board (identical to that in the exterior wall compositions) is inside the insulation. The roof is also assumed to be flat, so its tilt angle, Σ , is equal to zero. The exterior walls are all assumed to be perpendicular to the ground, making the tilt angle of these surfaces equal to 90° . The internal floors have no insulation, but they have the same gypsum layer below the concrete. The absorptivity of solar energy, α , of each exterior building surface is assumed to be 0.6, and the emissivity, ε , is 0.88, both nominal values for concrete. The interior solar attenuation coefficient, IAC , is assumed to be 1.0 during the heating season and 0.75 during the cooling season.

6.7 Program Output

After saving a building scenario, the heating and cooling loads are output in bar graph format. The graphs can be viewed on a yearly or monthly basis. The loads are shown in

kilowatt-hours (kWh), and the values represent the loads associated with heating and cooling the indoor air. There are a number of other figures that could be shown instead, and it is important to understand what the output values represent and what they do not. The loads on the indoor air do not account for efficiency of the heating and cooling equipment, nor do they consider efficiency in getting the primary fuel source to the building (e.g. electric transmission losses, power plant efficiency, etc.). If one were concerned with cost, the efficiency of the equipment used would need to be factored in to determine total billed consumption, and if one had environmental concerns, the efficiency of moving from a primary fuel source (e.g. coal) all the way to heating and cooling energy would need to be considered. These numbers are all interrelated, but they represent different points in the energy supply chain. Since the purpose of the program is to encourage designs with lower energy consumption, the most important point is that different scenarios can be directly compared relative to one another. Putting efficiencies and costs into the equation only results in scaling, so the relative ranking of scenarios in terms of *heating and cooling* energy would not change. Heating and cooling loads may scale differently, however, which could conceivably change the relative ranking of *total* energy consumption.

This page is intentionally left blank.

Chapter 7

Simulation Results and Model Validation

7.1 Sample Simulation Results

In order to demonstrate the results of the energy simulations and give the reader a better feel for the intended use of the program, some sample simulation results will be presented in this section. A single-story apartment building with seven living units will be used as a base case building. Results from three different sets of simulations will be shown, all of which use the base case as a starting point and examine the effects of one particular model parameter. The three parameters varied in the simulations are window type, quality of window installation and materials, and wall insulation thickness.

7.1.1 Base Case Building

The base case is a single-story building in Atlanta, GA that contains seven apartments with 100 m² of floor area each. The walls are 200 mm concrete constructions with double-glazed windows over 20% of their area. Foam insulation with a thickness of 50 mm is used in the walls and roof. The complete set of user interface selections for the base case building is shown in Table 7.1. In all of the results that follow, this base case building is called Scenario A.

Table 7.1: User interface selections for the base case building

Input	Value	Input	Value
City	Atlanta, GA	Window type	Double-glazed
Width W	70 m	Quality of installation and materials	Medium
Depth D	10 m	Overhangs	No
Height per floor	2.75 m	Wall 1 window %	20 %
Apartments per floor	7	Wall 2 window %	20 %
Number of floors	1	Wall 3 window %	20 %
Wall 1 orientation	N	Wall 4 window %	20 %
Main wall components	200 mm concrete, insulation inside		
Insulation type	Foam	Wall insulation thickness	50 mm
Roof insulation thickness	50 mm		

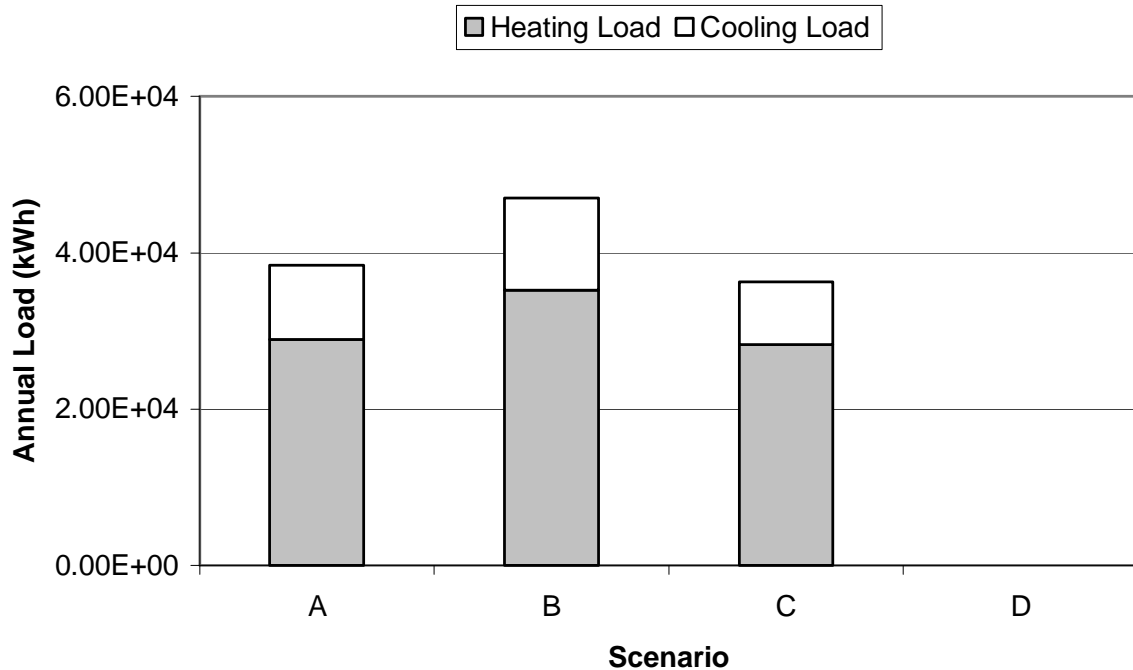


Figure 7.1: Loads resulting from simulations of the base case building with varied window types: single-glazed (Scenario B), double-glazed (Scenario A), and triple-glazed (Scenario C).

7.1.2 Simulation Set 1: Varied Window Types

This set of simulations might be run by an architect who wants to get a feel for the energy savings associated with replacing single-glazed windows with windows that have a higher insulating value in a design. Only the window type input is varied from the base case, and the values used are single-glazed (Scenario B), double-glazed (Scenario A, base case), and triple-glazed (Scenario C). Figure 7.1 shows the results of the simulations in a bar graph very similar to the one produced by the program. For this particular building, upgrading from single-glazed to double-glazed windows reduces total annual heating and cooling loads by nearly 20%, and a much smaller incremental savings is realized by upgrading from double-glazed to triple-glazed windows.

7.1.3 Simulation Set 2: Varied Quality of Window Installation and Materials

This set of simulations demonstrates the importance of using windows of a reasonable quality installed by trained professionals. Only the quality of window installation and materials

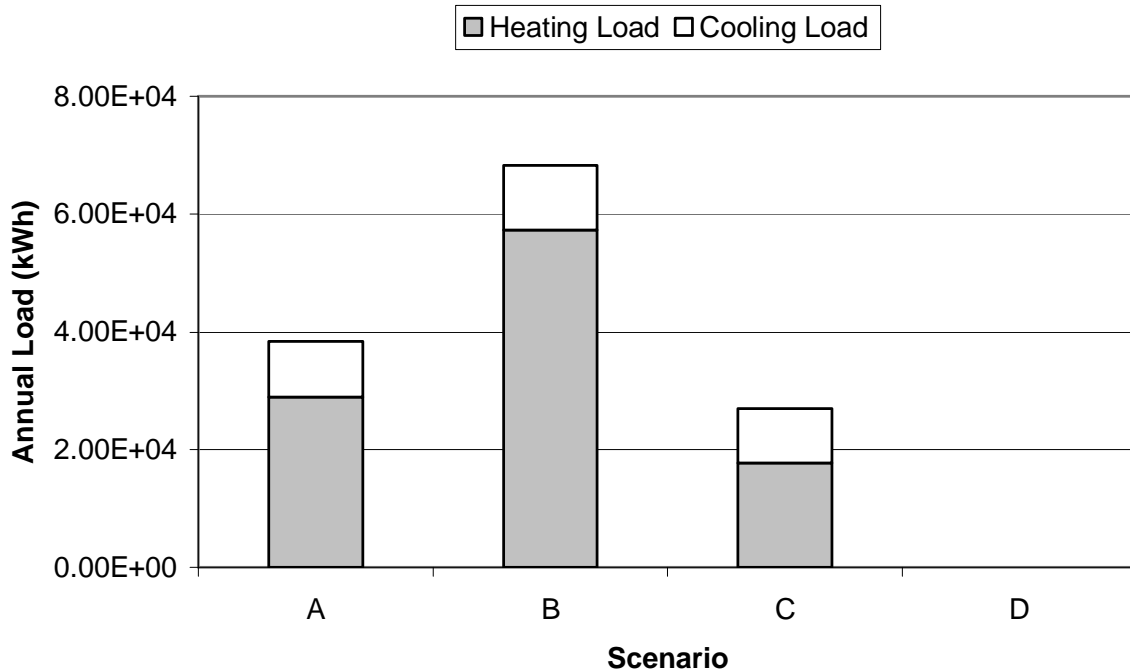


Figure 7.2: Loads resulting from simulations of the base case building with varied qualities of window installation and materials: low (Scenario B), medium (Scenario A), and high (Scenario C).

input is varied from the base case, and the values used are low (Scenario B), medium (Scenario A, base case), and high (Scenario C). Figure 7.2 shows the annual heating and cooling loads resulting from the simulations. If the base case building is constructed with a low quality of window installation and materials instead of medium, the yearly loads increase by nearly 80%. This dramatic effect is due mainly to the high air infiltration rate associated with low quality installation. A further reduction of about 30% can be realized with a high quality installation. This area of building design and construction is one of the biggest opportunities to improve building energy efficiency in developing countries without substantial cost increases.

7.1.4 Simulation Set 3: Varied Wall Insulation Thickness

This set of simulations quantifies the energy savings that can be achieved through increased amounts of wall insulation. Foam insulation is used in each case; only the wall insulation thickness input is varied from the base case. The various thicknesses simulated are 0 mm (Scenario B), 20 mm (Scenario C), 50 mm (Scenario A, base case), and 100 mm (Scenario D). Figure 7.3 shows the simulated annual heating and cooling loads for each case. Adding a modest 20 mm of insulation to an uninsulated concrete slab in this particular building reduces

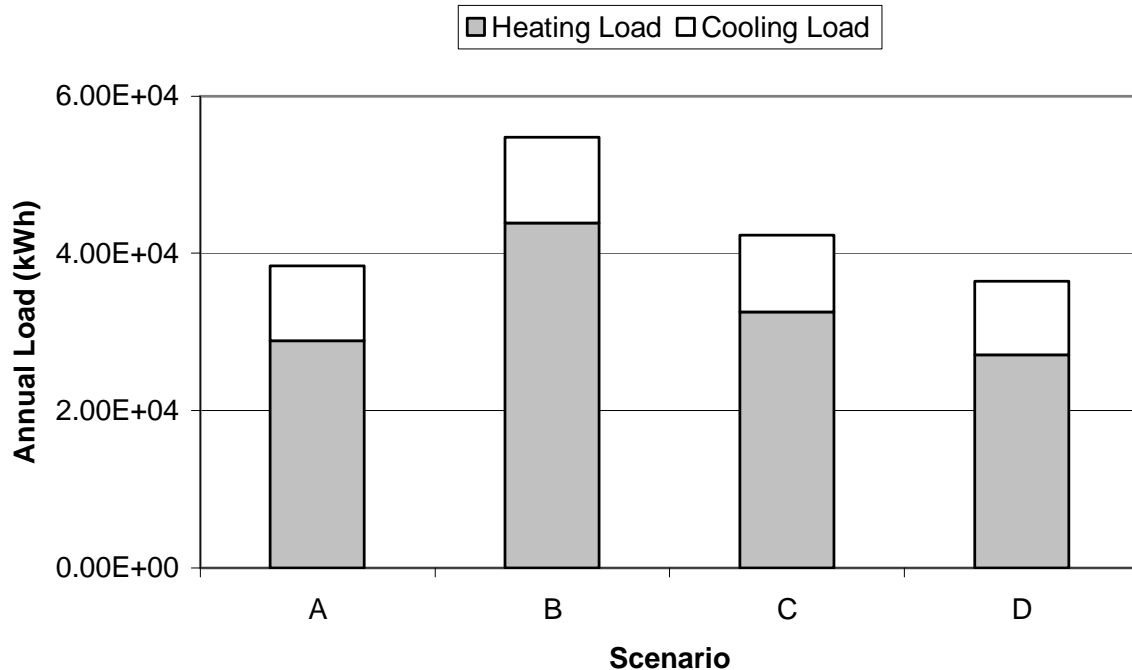


Figure 7.3: Loads resulting from simulations of the base case building with varied wall insulation thicknesses: 0 mm (Scenario B), 20 mm (Scenario C), 50 mm (Scenario A), and 100 mm (Scenario D).

total loads by nearly 25%. Additional insulation has a less dramatic impact, but can still reduce loads substantially. Uninsulated concrete walls are common among many relatively new constructions in China, and substantial energy savings can be achieved by adding a very modest amount of cheap insulation.

7.2 Model Validation: Comparison to Energy-10 Simulations

In order to ensure that the new program produces reasonable results, several building cases were simulated in both the new program and an existing program called Energy-10 (version 1.6.02). Energy-10 was developed by the National Renewable Energy Laboratory (NREL), and like the new program, it is intended to provide basic guidance early in the design process of a building. It has been used fairly widely and has undergone testing similar to that of other government programs like DOE-2. One main difference between Energy-10 and the new program is the level of detail in the user interface—many of the assumptions made in the new program are required as input into Energy-10. For example, details like occupancy schedules, HVAC equipment selection and sizing, lighting, etc. are all included in the user interface of Energy-10. A brief comparison of the simulation results will be presented in this section.

7.2.1 Base Case Building in Energy-10

The base case building used in the comparison is essentially the same as the one described in Table 7.1. In order to compare the results of the simulations in different climates, each case was run for Boston, MA (where heating loads are dominant) and Phoenix, AZ (where cooling loads are dominant). Most of the parameter values discussed in previous chapters could be entered directly, but there are a few points that should be made about entering the building into Energy-10.

Each material used in Energy-10 must have a density and a specific heat associated with it. As discussed previously, material layers classified as lightweight in the new program are treated as pure resistances, which is equivalent to a zero product of density and specific heat. To avoid simulation errors, typical property values were entered for the lightweight layers in Energy-10. Table 7.2 shows the values entered for each material, which are taken either from Table 4 on p. 25.5 of [2] or the Energy-10 library. For concrete, note that the product of density and specific heat is equal to 1.98×10^6 , which is the value used for the thermal mass of concrete in the new program. Other layer properties are identical to those presented earlier.

The model for windows in Energy-10 accounts for effects that the frame has on heat transmission through windows. The U value for both the glass and the frame were set equal to $3.4 \text{ W/m}^2\text{K}$, the same value used in the new program for double-glazed windows. The opaque width of the frame was set to 1 mm to minimize its effects on heat transmission, and the glazing area was set equal to 20% of the wall area for each wall. The solar heat gain coefficient, *SHGC*, cannot be entered as a function of incident angle in Energy-10; only the value at normal incidence is entered. Based on a reading of the product documentation, it is believed that Energy-10 does adjust this value for different incident angles, but specific details about how the adjustment is made are unclear. The solar heat gain coefficient entered was 0.76, the value

Table 7.2: Material property values used for base case building in Energy-10

Material	Density, ρ (kg/m^3)	Specific Heat, c (J/kgK)
Gypsum	800	1090
Plywood	540	1210
Concrete	2240	883.9
Insulation (foam)	40.04	1214.1
Sheathing	160.18	837.3

corresponding to normal incidence in the new program. The “glazing type” selected was 2003, which is double clear glass. Properties for this input that are not accessible to the user are used by Energy-10 to make any adjustments to the solar heat gain coefficient.

The perimeter loss coefficient, F , entered was 0.8844 for the Boston cases and 0.83 for the Phoenix cases, which are the same values computed by the new program based on the number of heating degree days resulting from the appropriate weather data files.

Interior partitions can be entered into Energy-10 to add thermal mass to the inside of the building. The effective area of such partitions was set to zero to eliminate any effects that they have on the simulations.

Energy-10 determines the amount of infiltration into the building based on two additive components, an effective leakage area and a constant air change rate. The effective leakage area was set to zero and the constant air change rate was set equal to 0.5. These settings should result in a constant air change rate of 0.5 ACH throughout the entire year. In order for the new program to simulate the same situation, the air change rate for open windows was temporarily changed from 6.0 to 0.5, effectively keeping the windows closed all year.

The HVAC system selected was a package terminal air conditioner (PTAC) with electric resistance (ER) heat. The efficiency of the heater was set to 100% and the air conditioner coefficient of performance was set to 1.0. The sensible ratio for the air conditioner was set to 1.0 to exclude latent effects. These settings should presumably equate the heating and cooling *energy* used in the building with the sensible heating and cooling *loads* in the zone. It should be noted that some strange behavior was encountered as Energy-10 automatically sized the HVAC equipment. The automatic sizing sometimes resulted in simulation errors and inconsistent results, so sizing by trial and error was performed until the errors did not occur.

There are many categories for internal gains available in Energy-10. Everything was set equal to zero except for the “other” category, which was set equal to a constant value of 3.84 W/m² for every hour of the year. For the base case building dimensions, this value corresponds to the 384 W/apartment used in the new program.

7.2.2 Description of Buildings Simulated

Five different cases were run using the new program and Energy-10 in both the Boston and Phoenix climates, all of which use the base case as a starting point. The five cases are listed

below, and any differences between a case and the base case are mentioned in the description:

1. Base case
2. Base case rotated 90° (i.e. bigger walls face E-W rather than N-S)
3. No windows, no infiltration, no internal gains, no solar radiation
4. No windows, no solar radiation
5. No windows

Since many of the changes made in these cases cannot be changed via the user interface of the new program, the source code was temporarily altered to simulate the desired situation. As mentioned above, the possibility of opening windows was removed from the new program to achieve a constant air change rate throughout the year. For Case 4, the effects of solar radiation were removed from Energy-10 by setting the solar absorptivity of each surface equal to zero.

7.2.3 Simulation Results

Results of the five simulation cases described above run in both the new program and Energy-10 are shown in Table 7.3. All of the deviations in the table are expressed as percentages of the Energy-10 loads. The total deviation column expresses the total deviation in heating and cooling loads as a percentage of the total heating and cooling load from Energy-10:

$$\text{Total Deviation} = \frac{|HL_{E10} - HL_{NP}| + |CL_{E10} - CL_{NP}|}{HL_{E10} + CL_{E10}} \quad (7.1)$$

Table 7.3: Comparison of loads simulated by new program and Energy-10 for various cases

Boston Cases							
Case	Program Heating Load	E-10 Heating Load	Deviation	Program Cooling Load	E-10 Cooling Load	Deviation	Total Deviation
	(GJ)	(GJ)	(%)	(GJ)	(GJ)	(%)	(%)
1	169	152	11.0	43.4	54.4	20.3	13.5
2	178	162	9.7	60.4	75.1	19.6	12.8
3	165	161	2.6	0.0	0.0	0.0	2.6
4	197	200	1.5	1.18	0.756	56.1	1.7
5	180	163	10.2	6.07	18.1	66.5	15.9
Phoenix Cases							
1	7.05	2.77	154.3	266	324	17.9	19.0
2	10.2	5.54	84.0	318	383	16.9	17.9
3	32.3	31.0	4.2	38.7	41.6	6.9	5.8
4	26.6	25.2	5.6	95.2	111	13.9	12.4
5	19.4	11.1	75.0	127	195	34.8	37.0

where

HL = heating load

CL = cooling load

Subscript NP refers to new program

Subscript E10 refers to Energy-10

Unfortunately, the output available from Energy-10 makes it very difficult to pinpoint the main source of differences between the load predictions of the two programs. No attempt will be made to determine which program is “more correct” in each case. Different models, both with many uncertainties, were used, and data from real buildings would be needed to determine which is more accurate.

The Boston heating loads calculated by the two programs all agree within 11%, and the Phoenix cooling loads, with one exception, agree within 20%. These results indicate that the new program shows good agreement with Energy-10 with respect to the dominant load in each case. Although some of the Boston cooling loads and Phoenix heating loads calculated by the new program differ significantly from those calculated by Energy-10, these loads typically make up a very small portion of the total loads. For example, the Phoenix heating loads for Case 1 differ by over 150%, but those loads are more than an order of magnitude smaller than the cooling loads for the same case. Although the relative difference is high in this particular case, the absolute difference is quite small. It is for this reason that the total deviation metric, which considers the deviations as a fraction of the total load, was created.

With one exception, the total deviations are all less than 20%, which is reasonable considering all of the uncertainties associated with the early design stage models of a building. Uncertainties associated with solar radiation data, site shading, occupant behavior with regard to opening windows, etc. easily amount to more than the differences between the two programs. Considering the primary purpose of the new program—to provide basic guidance about building energy use to an early stage designer—this level of discrepancy is acceptable. The purpose of this comparison was to show that the new program gives results comparable to those of another existing building simulation tool, and these simulations show that to be true.

Chapter 8

Conclusions and Recommendations for Future Work

The main result of the work presented in this thesis is a new software tool that provides guidance early in the design process to architects who are interested in creating more energy-efficient buildings. Residential buildings in developing countries, particularly China, are the primary focus of the tool because there are extremely large markets for new buildings and substantial opportunities for efficiency improvements in this sector. The hope is that quantifying the dramatic reduction in energy consumption that comes along with the implementation of simple measures, such as more insulation and better windows, will encourage more sound building design choices.

In order to predict the energy required to heat and cool a building, many aspects of the building had to be modeled. First, a general model was developed to approximate the heat transfer through a thermally massive building component. This model, which accounts for both a material's resistance to heat flow and thermal storage capacity, was then applied to specific building surfaces. Other aspects of the building that are not characterized by the general model were treated separately. Since the program is intended to be used early in the design process when most aspects of the building are still uncertain, many simplifying assumptions were made in the model. Weather data were used to determine the appropriate outdoor boundary conditions, including temperatures and amounts of solar radiation. All of these components were then synthesized to form a model for the entire building. The new program runs simulations using this model to calculate the heating and cooling loads in the building over the course of a typical meteorological year.

Special care was taken in the development of the user interface of the program to ensure that it is easy to learn and use. One of the main differences between the new program and existing simulation tools is that it requires extremely limited input to run a simulation. While the approach taken by most programs is that more options are better because they give the user more flexibility, the new program was developed with the belief that too many options will confuse the

user who is in the early stages of a building design. By limiting the input to a small set of the most important design variables, the attention of the architect and developer is focused on a few of the things they can do that will have the most significant impact on the energy performance of their buildings. This focus is particularly important in developing countries, where walls with no insulation, very leaky windows, and other poor practices are prevalent. The interface further caters to the needs of architects in these countries by including typical local wall constructions and materials as options. Although the model developed is capable of dealing with a large number of parameters that could be entered by a user, the approach taken in developing the program's user interface was to include only pertinent options over which the architect is likely to have some degree of control.

To ensure that the new program yields results similar to those of an existing building energy simulation tool that has been tested, a comparison with Energy-10 was performed. Loads calculated by the two programs typically agreed within 20%, which is reasonable considering the numerous sources of uncertainty involved in the models used by both programs.

As it stands, the program is well-suited for rough approximations of annual energy use in a building, but there are several aspects of the model that could be improved or expanded to include a wider variety of cases. Perhaps most importantly, more building footprints should be included in the interface to allow for shapes more complicated than the simple rectangular footprint that is currently assumed. Instead of having predetermined floor plans, an interactive interface allowing the user to dynamically create the plan of their choice is another option. The floor model could be expanded to include basements and underground walls in addition to slab on grade floors. The nodal model presented can be expanded to allow for multiple zones if that feature is ever desired. Finally, the shading algorithm should be made more sophisticated so that it accounts for the building's latitude when determining typical overhang geometries.

The user interface was designed to be simple and easy to use, but it could be useful to include a set of advanced options for users who want more control. These options should be located in a menu rather than directly on the input form to avoid clutter, and they should have default values so that users who are not interested do not even have to think about them. Examples of advanced options may be desired thermostat set points, more detailed specification of internal gains, and window shading options. Alternatively, a separate user interface could be developed using the same model for more advanced users who want more control over model

parameters. These users may also desire more detailed output, such as the contribution of each individual building component to the annual loads or hourly simulation results. Although the program was designed with a target audience in mind, the model is general enough that it can be expanded to interest a wider audience.

Finally, the program needs to be successfully deployed in developing countries so that it can be used by its intended audience. Deployment is probably best achieved through contacts in the governments and architecture firms of these countries. More extensive documentation and an interactive on-line help system should be created to aid in teaching architects to use the program.

This page is intentionally left blank.

References

- [1] ASHRAE. 1993. *ANSI/ASHRAE Standard 90.2, Energy-Efficient Design of New Low-Rise Residential Buildings*. Atlanta: American Society of Heating, Refrigerating, and Air Conditioning Engineers, Inc.
- [2] ASHRAE. 2001. *ASHRAE Handbook—Fundamentals*. Atlanta: American Society of Heating, Refrigerating, and Air Conditioning Engineers, Inc.
- [3] BP Amoco. 2003. *Statistical Review of World Energy*.
<http://www.bp.com/centres/energy/energy/index.asp>
- [4] China Online. 1997. Vernacular Architecture in Historic Chinese Cities.
<http://chineseculture.miningco.com/cs/chinahousing/#m>
- [5] *China Statistical Yearbook 2001*. 2001. Beijing: China Statistical Publishing House.
- [6] Cordero, Elizabeth. 2001. *Sustainability in Architecture*. MS Thesis. Massachusetts Institute of Technology, Cambridge, MA. pp. 45-61.
- [7] Crank, J. and P. Nicolson. 1947. A Practical Method for Numerical Evaluation of Solutions of Partial Differential Equations of the Heat-Conduction Type. *Proceedings of the Cambridge Philosophical Society*, 43:50-67.
- [8] Energy Information Administration. 2004. *International Energy Data*. U.S. Department of Energy. Washington, DC. <http://www.eia.doe.gov/emeu/international/energy.html>
- [9] Glicksman L.R., L.K. Norford, and L.V. Greden. 2001. Energy Conservation in Chinese Residential Buildings: Progress and Opportunities in Design and Policy. *Annual Review of Energy and Environment*, 26:83-115.
- [10] Greden, Lara. Personal communication. Update to building codes in China. October 3, 2002.
- [11] Incropera, F.P. and D.P. DeWitt. 1996. *Fundamentals of Heat and Mass Transfer*. 4th ed. New York: John Wiley & Sons, Inc. pp. 248-263.
- [12] McQuiston F.C., J.D. Parker, and J.D. Spitler. 2000. *Heating, Ventilating, and Air Conditioning: Analysis and Design*. 5th ed. New York: John Wiley & Sons, Inc. pp. 164-166.
- [13] National Renewable Energy Laboratory, Renewable Resource Data Center. Typical Meteorological Year 2 data files. http://rredc.nrel.gov/solar/old_data/nsrdb/tmy2/

- [14] Spindler, Henry C. 1998. *Residential Building Energy Analysis: Development and Assessment of a Simplified Model*. MS Thesis. Massachusetts Institute of Technology, Cambridge, MA. pp. 24 ff., 41 ff., 97 ff.
- [15] U.S. Department of Energy. Energy Efficiency and Renewable Energy Building Technologies Program. EnergyPlus Energy Simulation Software Weather Data files. http://www.eere.energy.gov/buildings/energyplus/cfm/weatherdata_int.cfm
- [16] U.S. Green Building Council. 2002. *Leadership in Energy & Environmental Design Green Building Rating System for New Construction and Major Renovations (LEED-NC)*, Version 2.1. <http://www.usgbc.org>.

Appendix A

Nomenclature

Quantities without units listed are dimensionless.

A	coefficient matrix for unknown nodal temperatures at the next time step in the system of energy balance equations ($\text{W}/\text{m}^2\text{K}$)
A_{floor}	surface area of the ground floor and each of the internal floors (m^2)
$A_{\text{int floor}}$	total surface area of all internal floors combined, $A_{\text{floor}}(NF-1)$ (m^2)
A_{roof}	surface area of the roof (m^2)
A_{sunlit}	surface area of the windows on a given wall unshaded by projections (m^2)
A_{wall}	surface area of a wall excluding its windows (m^2)
$A'_{\text{wall } i}$	total surface area wall i including its windows (m^2)
A_{window}	surface area of the windows on a given wall (m^2)
A_{windows}	total surface area of all the windows on a building (m^2)
$A_{\text{window, wall } i}$	surface area of the windows on wall i (m^2)
ACH	air changes per hour in the building (hr^{-1})
AST	apparent solar time in number of minutes after midnight (min)
B	coefficient matrix for known nodal temperatures at the current time step in the system of energy balance equations ($\text{W}/\text{m}^2\text{K}$)
B	base temperature used in degree day calculations ($^{\circ}\text{C}$)
c	specific heat for an incompressible substance (J/kgK)
c_p	constant pressure specific heat (J/kgK)
C	vector collecting all constant terms in the system of energy balance equations (W/m^2)
C	capacitance of a given material layer introduced to simplify notation, equal to the product of density, specific heat, and nodal spacing ($\text{J}/\text{m}^2\text{K}$)
C_a	capacitance of material layer a ($\text{J}/\text{m}^2\text{K}$)
C_b	capacitance of material layer b ($\text{J}/\text{m}^2\text{K}$)
D	depth of the building footprint input by the user (m)

E_D	total direct normal radiation incident on a surface (W/m^2)
E_{DN}	total direct normal radiation on a surface perpendicular to the sun's rays from weather data file (W/m^2)
$E_{diff,ground}$	total ground reflected radiation (assumed diffuse) incident on a surface (W/m^2)
$E_{diff,horiz}$	total diffuse radiation on a horizontal surface from weather data file (W/m^2)
$E_{diff,sky}$	total diffuse radiation from the sky incident on a surface (W/m^2)
$E_{global,horiz}$	total direct and diffuse radiation received by a horizontal surface from weather data file (W/m^2)
$E_{tot,surf}$	total direct and diffuse radiation incident on a surface (W/m^2)
ET	value of the equation of time for a given day (min)
F	slab perimeter loss coefficient (W/mK)
$GMTDiff$	difference between the local standard time and Greenwich Mean Time (hr)
h	a general combined convection and radiation coefficient (W/m^2K)
$h_{combined}$	combined convection and radiation coefficient (W/m^2K)
h_{conv}	convection coefficient (W/m^2K)
h_{eff}	a general effective convection coefficient which accounts for both film resistance and purely resistive insulation layers (W/m^2K)
$h_{eff,floor}$	effective convection coefficient for inside surface of the floor (W/m^2K)
$h_{eff,int floor,top}$	effective convection coefficient for top surface of internal floors (W/m^2K)
$h_{eff,int floor,bottom}$	effective convection coefficient for bottom surface of internal floors (W/m^2K)
$h_{eff,roof}$	effective convection coefficient for the inside surface of roof (W/m^2K)
$h_{eff,wall}$	effective convection coefficient for the inside surface of exterior walls (W/m^2K)
$h_{floor,in}$	combined convection and radiation coefficient for the inside surface of the ground floor (W/m^2K)
h_{out}	combined outdoor convection and radiation coefficient (W/m^2K)
h_{rad}	linearized radiation coefficient (W/m^2K)
$h_{roof,in}$	combined convection and radiation coefficient for the inside surface of the roof (W/m^2K)
$h_{slab,below}$	combined convection and radiation coefficient below the slab (W/m^2K)
$h_{wall,in}$	combined convection and radiation coefficient for the inside surface of the exterior walls (W/m^2K)

HA	hour angle (degrees)
H	height of window used in projection calculations (m)
HPF	height per floor of the building entered by the user (m)
HDD	heating degree days calculated from weather data ($^{\circ}\text{C}\cdot\text{day}$)
IAC	interior solar attenuation coefficient used for internal shading
k	thermal conductivity of a material (W/mK)
L	site latitude of the building (rad)
LON	site longitude of the building (rad)
LST	local standard time at the building in minutes after midnight (min)
LT	total thickness of a material layer (m)
m	total number of lightweight layers on a given side of a given building surface
N	total number of nodes in a given material layer
NF	total number of floors in the building input by the user
P	perimeter of the slab on grade floor (m)
P_H	length of the horizontal projection (overhang) above a window (m)
P_V	length of the vertical projection on both sides of a window (m)
q''	net heat flux through the surface exposed to ambient conditions (which may be a lightweight layer) to the outermost node of a building surface (W/m^2)
q_l''	net heat flux to the indoor air from a building surface (W/m^2)
q_{conv}	heat flux between a surface and ambient conditions due to convection (W/m^2)
q_{rad}	heat flux to or from a surface due to radiation (W/m^2)
q_{glazing}	heat flux through the glazing (W/m^2)
q_{slab}	heat transfer through the slab on grade floor (W)
q_{sun}	total solar heat flux absorbed by a surface (W/m^2)
$q_{\text{sun, floor}}$	total solar heat flux transmitted by the entire glazing system absorbed by the floor and distributed evenly across its entire area (W/m^2)
$q_{\text{sun, floor, unshaded}}$	total solar heat flux transmitted by the entire glazing system with no interior or exterior shading that is distributed evenly across the floor area (W/m^2)
$q_{\text{sun, transmitted}}$	solar heat flux transmitted by the windows on a given wall (W/m^2)
Q	arbitrary heat flux incident on a surface (W/m^2)
Q_{gain}	internal gains in the building (W)

R	resistance of a given material layer introduced to simplify notation, equal to the ratio of nodal spacing to thermal conductivity ($\text{m}^2\text{K/W}$)
R_a	resistance of material layer a ($\text{m}^2\text{K/W}$)
R_b	resistance of material layer b ($\text{m}^2\text{K/W}$)
R_H	spacing between the top of a window and a horizontal projection (m)
R_W	spacing between the side of a window and a vertical projection (m)
R_{film}	film resistance, including convection and radiation ($\text{m}^2\text{K/W}$)
$R_{\text{film,out}}$	outside film resistance, including convection and radiation ($\text{m}^2\text{K/W}$)
$R_{\text{film,in}}$	inside film resistance, including convection and radiation ($\text{m}^2\text{K/W}$)
R_{glazing}	resistance of a glazing, excluding outside and inside film resistances ($\text{m}^2\text{K/W}$)
R_{ins}	resistance of all lightweight layers on a given side of a given building surface ($\text{m}^2\text{K/W}$)
$R_{\text{ins,int floor}}$	resistance of all lightweight layers on top surface of an internal floor ($\text{m}^2\text{K/W}$)
$R_{\text{ins,floor}}$	resistance of all lightweight layers on top surface of ground floor ($\text{m}^2\text{K/W}$)
R_{tot}	total resistance of lightweight layers and film on a given side of a given building surface ($\text{m}^2\text{K/W}$)
$R_{\text{tot,int floor}}$	total resistance of the top side of an internal floor ($\text{m}^2\text{K/W}$)
$R_{\text{tot,floor}}$	total resistance of the top side of the ground floor ($\text{m}^2\text{K/W}$)
S_H	height of the shadow cast by a window projection (m)
S_W	width of the shadow cast by a window projection (m)
$SHGC$	solar heat gain coefficient of a window
$SHGC(\theta)$	solar heat gain coefficient for direct radiation as a function of incident angle
$SHGC_{\text{diff}}$	solar heat gain coefficient for diffuse radiation
SN	constant time representing solar noon in minutes after midnight (720 min)
t	time (sec)
\mathbf{T}	vector of known nodal temperatures at the current time step from the system of energy balance equations ($^{\circ}\text{C}$)
$\hat{\mathbf{T}}$	vector of unknown nodal temperatures at the next time step from the system of energy balance equations that is solved for by LU decomposition ($^{\circ}\text{C}$)
T	temperature of a node ($^{\circ}\text{C}$)
T_{amb}	ambient temperature ($^{\circ}\text{C}$)

T_{ground}	temperature of the ground surrounding the slab on grade floor ($^{\circ}\text{C}$)
T_{floor}	temperature of the innermost surface node of the ground floor ($^{\circ}\text{C}$)
T_{in}	temperature of the indoor air ($^{\circ}\text{C}$)
$T_{\text{int floor,top}}$	temperature of the top node of the interior floors ($^{\circ}\text{C}$)
$T_{\text{int floor,bottom}}$	temperature of the bottom node of the interior floors ($^{\circ}\text{C}$)
T_j	temperature of a surface node arbitrarily labeled j ($^{\circ}\text{C}$)
T_{j+1}	temperature of a node $j+1$, which is adjacent to node j ($^{\circ}\text{C}$)
T_k	temperature of a surface node arbitrarily labeled k ($^{\circ}\text{C}$)
T_{k-1}	temperature of a node $k-1$, which is adjacent to node k ($^{\circ}\text{C}$)
T_m	mean of surface and ambient temperatures used in linearized radiation coefficient (K)
T_n	temperature of an arbitrary node n ($^{\circ}\text{C}$)
T_{n-1}	temperature of a node $n-1$, which is adjacent to node n ($^{\circ}\text{C}$)
T_{n+1}	temperature of a node $n+1$, which is also adjacent to node n ($^{\circ}\text{C}$)
T_{out}	outdoor temperature from weather data files ($^{\circ}\text{C}$)
T_{roof}	temperature of the innermost surface node of the roof ($^{\circ}\text{C}$)
T_s	temperature of some surface s exposed to ambient conditions ($^{\circ}\text{C}$)
$T_{\text{sol-air}}$	sol-air temperature of a surface ($^{\circ}\text{C}$)
T_{wall}	temperature of the innermost surface node of an exterior wall ($^{\circ}\text{C}$)
U	overall heat transfer coefficient for the windows ($\text{W}/\text{m}^2\text{K}$)
U_1	overall heat transfer coefficient for window with an aluminum frame with a thermal break ($\text{W}/\text{m}^2\text{K}$)
U_2	overall heat transfer coefficient for window with an aluminum frame without a thermal break ($\text{W}/\text{m}^2\text{K}$)
V_{air}	volume of air in the building (m^3)
W	width of window used in projection calculations (m)
W	width of the building footprint input by the user (m)
$WP_{\text{wall } i}$	percentage of wall i that is covered by windows as input by the user (%)
x	spatial dimension in the direction of the material thickness (m)
\wedge	above a variable indicates that it is evaluated at time $t + \Delta t$

α	solar absorptivity of a material
β	solar altitude angle (rad)
γ	relative azimuth angle of a surface (rad)
δ	solar declination for a given day of the year (degrees)
Δ	vertical projection profile angle used in shading calculations (rad)
Δt	time step, set to 3600 seconds (1 hour) in the program (sec)
ΔR	difference between long wave radiation incident on a surface from the sky and other surroundings and radiation emitted by a blackbody at ambient temperature (W/m^2)
Δx	nodal spacing within a material layer (m)
ε	emissivity of a surface
θ	incident angle of direct normal solar radiation on a surface (rad)
ρ	density of a material (kg/m^3)
ρ_g	ground reflectivity
$(\rho c_p)_{\text{air}}$	density multiplied by constant-pressure specific heat for air ($\text{J}/\text{m}^3\text{K}$)
σ	Stefan-Boltzmann constant, $5.67 \times 10^{-8} \text{ W}/\text{m}^2\text{K}^4$
Σ	surface tilt angle (0° for horizontal surfaces, 90° for vertical) (rad)
ϕ	solar azimuth angle (rad)
ψ	surface azimuth angle (rad)
Ω	profile angle used in shading calculations (rad)

Appendix B

Summary of Parameter Values

Parameters not listed here are calculated using these values and equations in the text.

Constant Values

B	= 18°C
$h_{\text{floor,in}}$	= 9.26 W/m ² K
h_{out}	= 34 W/m ² K
$h_{\text{slab,below}}$	= 1 x 10 ⁻⁶ W/m ² K
$h_{\text{wall,in}}$	= 8.29 W/m ² K
H	= 1.50 m
IAC	= 0.75
k	= 0.16 W/mK for gypsum layers = 0.11 W/mK for plywood layers = 1.3 W/mK for concrete layers = 0.090 W/mK for sheathing layers
LT	= 0.0127 m for gypsum layers = 0.010 m for plywood layers = 0.0095 m for sheathing layers = 0.100 m for concrete layers in the roof, ground floor, and internal floors
N	= 5 for massive layers = 0 for lightweight layers
P_H	= 0.6 m (on windows with overhangs selected, = 0 otherwise)
P_V	= 0 m
R_H	= 0.4 m (on windows with overhangs selected, = 0 otherwise)
R_W	= 0 m
SN	= 720 min
W	= 0.90 m (window width)

α	= 0.6
Δt	= 3600 sec (= 1 hr)
ΔR	= 63 W/m ²
ε	= 0.88
ρ_g	= 0.2
ρc	= 1.98 x 10 ⁶ J/m ³ K for concrete layers = 0. J/m ³ K for all lightweight layers
$(\rho c_p)_{\text{air}}$	= 1207.2 J/m ³ K (= 1.2 kg/m ³ x 1006 J/kgK)
σ	= 5.67 x 10 ⁻⁸ W/m ² K ⁴
Σ	= $\pi/2$ rad (90°) for walls = 0 rad (0°) for the roof

Values Read from Weather Data Files (based on city selected by user)

E_{DN} (every hour of year)

$E_{\text{diff,horiz}}$ (every hour of year)

$E_{\text{global,horiz}}$ (every hour of year)

$GMTD_{\text{diff}}$

L

LON

T_{out} (every hour of year)

Values Directly Entered by User

D

$Floors$

HPF

LT for wall insulation layers

LT for roof insulation layers

NF

Number of apartments per floor (no symbol used)

W (width of building footprint)

$WP_{\text{wall } i}$ (for $i = 1, 2, 3, 4$)

Values Set Based on User Input

- ACH* = 2.0 hr⁻¹ for low quality installation and materials in the heating season
 = 1.0 hr⁻¹ for medium quality installation and materials in the heating season
 = 0.50 hr⁻¹ for high quality installation and materials in the heating season
 = 1.5 hr⁻¹ for low quality installation and materials in the cooling season
 = 0.70 hr⁻¹ for medium quality installation and materials in the cooling season
 = 0.50 hr⁻¹ for high quality installation and materials in the cooling season
 = 6.0 hr⁻¹ when windows are open with any quality in either season
- F* = 0.83 W/mK for 1640 heating degree days/year
 = 0.86 W/mK for 2970 heating degree days/year
 = 0.97 W/mK for 4130 heating degree days/year
 = linearly interpolated value for in between values
- k* = 0.025 W/mK for foam insulation layers
 = 0.036 W/mK for glass fiber insulation layers
 = 0.042 W/mK for loose fill cellulose insulation layers
 = 0.074 W/mK for cement fiber slab insulation layers
- LT* = 0.200 m for concrete layers in 200 mm wall constructions
 = 0.300 m for concrete layers in 300 mm wall constructions
- Q_{gain}* = 384 W/apartment x number of apartments per floor x *NF*
- SHGC* =

Window Type	Incident Angle						
	0°	40°	50°	60°	70°	80°	diffuse
Single-glazed	0.86	0.84	0.82	0.78	0.67	0.42	0.78
Double-glazed	0.76	0.74	0.71	0.64	0.50	0.26	0.66
Double-glazed, low e	0.65	0.64	0.61	0.56	0.43	0.23	0.57
Triple-glazed	0.68	0.65	0.62	0.54	0.39	0.18	0.57

- U* = *U*₁ for medium or high quality of installation and materials
 = *U*₂ for low quality of installation and materials
- U*₁ = 6.12 W/m²K for single-glazed windows
 = 3.42 W/m²K for double-glazed windows

U_2

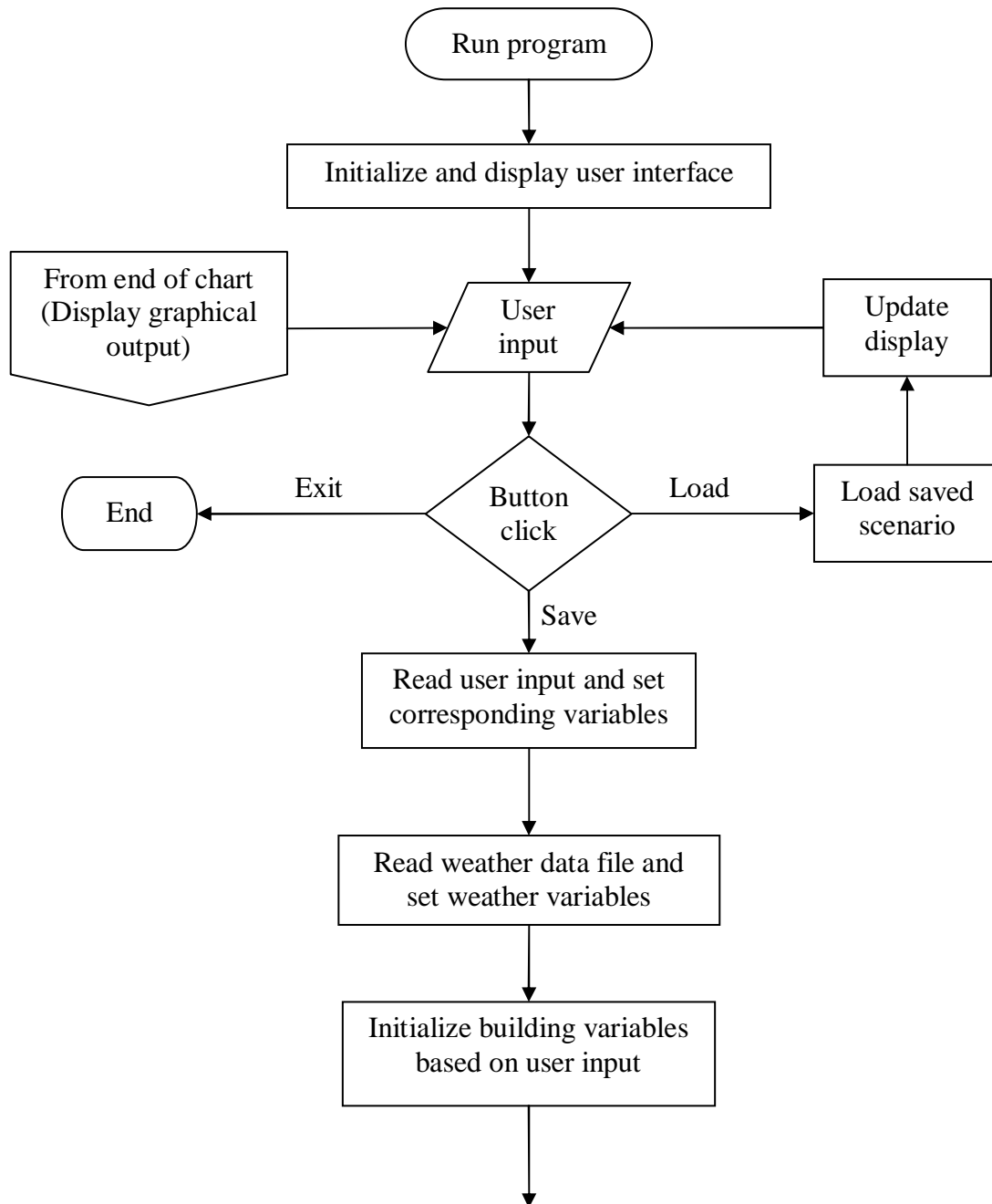
- = 2.89 W/m²K for double-glazed windows with low-e coating
- = 2.60 W/m²K for triple-glazed windows
- = 7.24 W/m²K for single-glazed windows
- = 4.62 W/m²K for double-glazed windows
- = 4.05 W/m²K for double-glazed windows with low-e coating
- = 3.80 W/m²K for triple-glazed windows

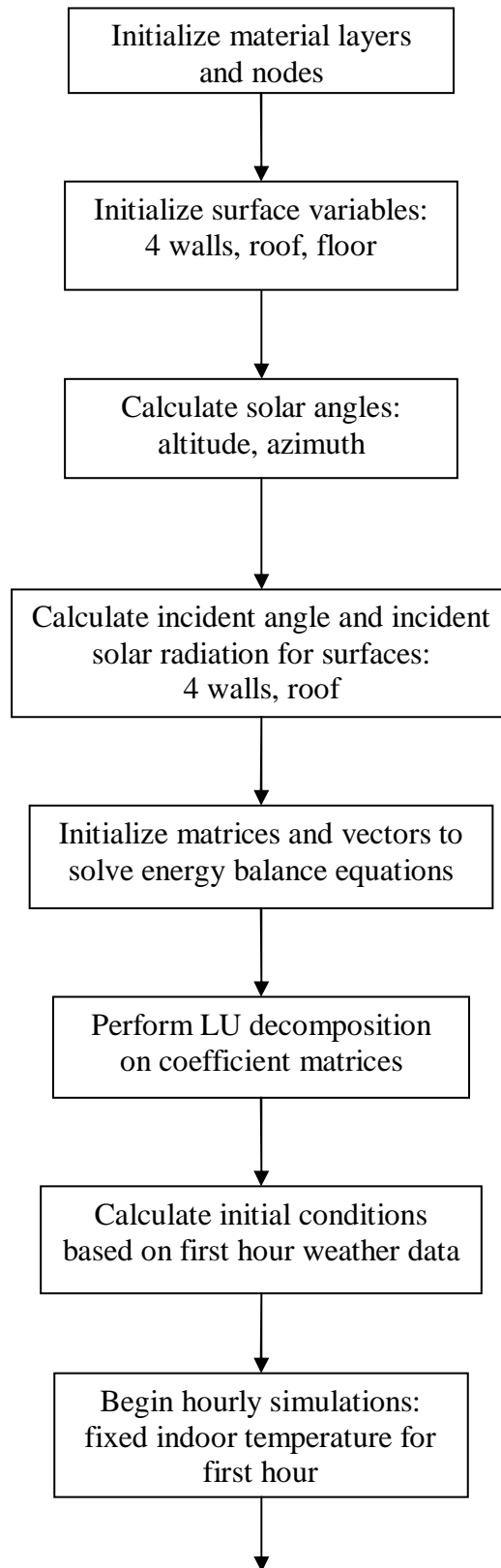
ψ

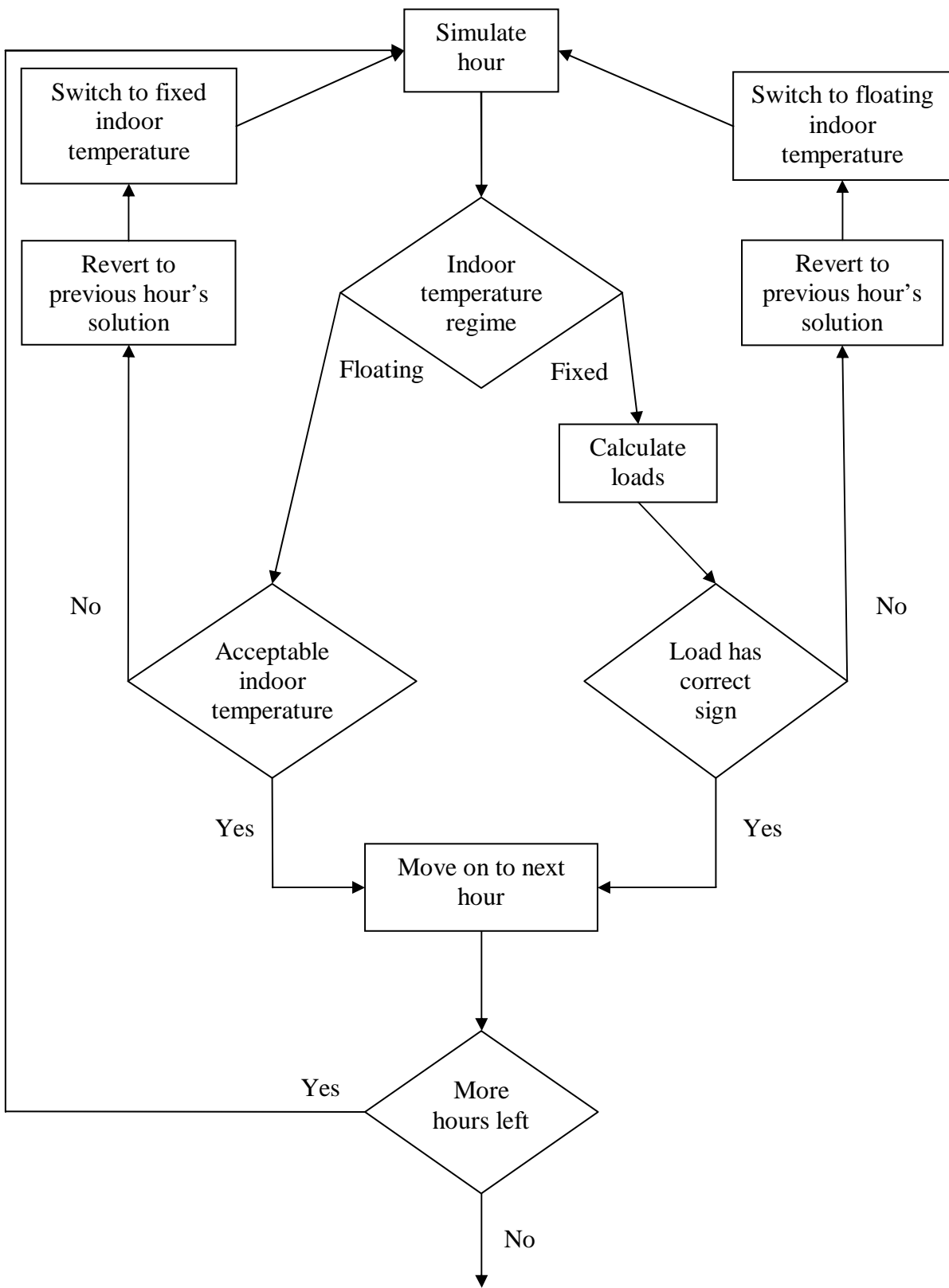
- = 0 rad (0°) for S facing surfaces
- = $\pi/4$ rad (45°) for SW facing surfaces
- = $\pi/2$ rad (90°) for W facing surfaces
- = $3\pi/4$ rad (135°) for NW facing surfaces
- = π rad (180°) for N facing surfaces
- = $-3\pi/4$ rad (-135°) for NE facing surfaces
- = $-\pi/2$ (-90°) for E facing surfaces
- = $-\pi/4$ rad (-45°) SE facing surfaces

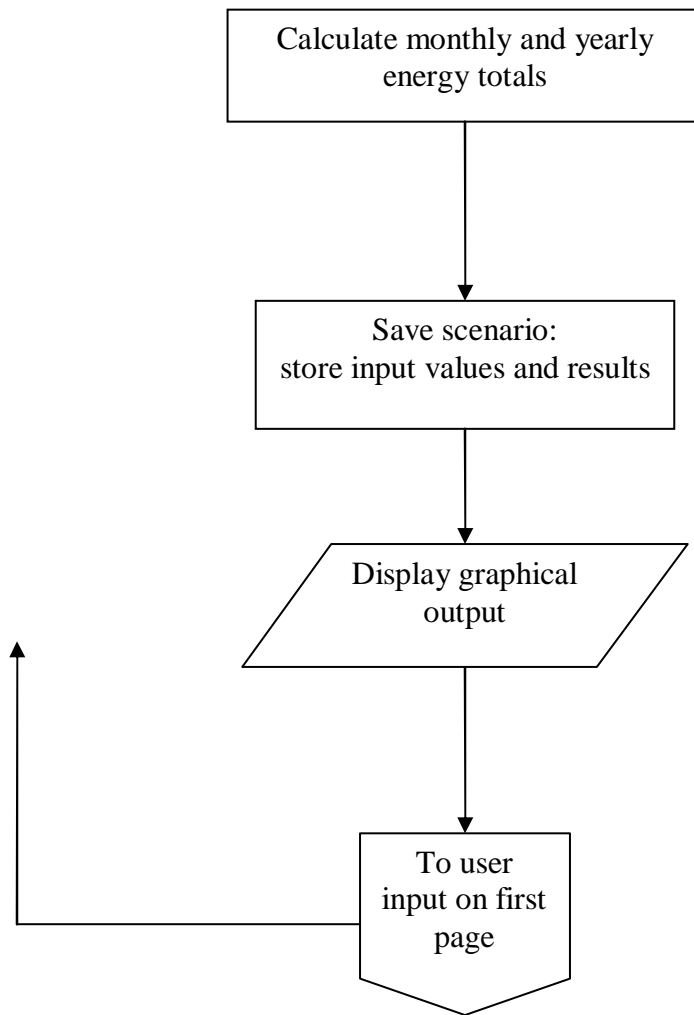
Appendix C

Program Flowchart









Appendix D

Notes on Program Source Code

The program was created using the Microsoft® Visual Studio® .NET development environment in the C++ programming language. Several classes are used in the program implementation, some of which were created automatically by the framework to allow for standard Windows® functionality. There are two classes that perform all of the calculations in the back end of the program:

class CBuilding—This class incorporates everything that defines a building in the program, including variables for all the building surfaces, user inputs, weather data, energy results, etc. and most of the functions that perform calculations. Material layers and the setup of the nodes are also handled in this class. The class is defined in the file Building.h.

class CSurface—This class defines a building surface, such as the exterior wall, and performs calculations unique to that surface. Examples include incident solar angle and exterior shading calculations. The class is defined in the file Surface.h.

The majority of the work on the user interface can be seen in three additional classes:

class CEnergyCalculatorView—Along with the resource files, this class defines and handles the input form view of the program. The class is defined in the file EnergyCalculatorView.h.

class CGraphView—This class defines and handles the yearly bar graph view of the program. The class is defined in the file GraphView.h.

class CMonthlyGraphView—This class defines and handles the monthly bar graph view of the program. The class is defined in the file MonthlyGraphView.h.

The bar graph views in the program were created with the aid of the Generic Logic Toolkit (<http://www.genlogic.com>). In order to view or modify the template files (which have a .g extension), the GLG Graphics Builder is required. If the source code is to be recompiled, the GLG C++ library file is required. Both of these can be purchased from the Generic Logic web

site. Neither of these items are required to run the compiled program, but they are needed if modifications to this part of the user interface are to be made.

The model that has been presented in this thesis is implemented into the program through the two classes that make up the back end of the program. The member variables and functions that make up these classes will now be described. If a variable was used explicitly in the model formulation, its symbol is shown at the end of the variable description. Variables with no units listed are dimensionless. The name of the file in which each function is implemented is listed at the end of its description for reference.

class CBuilding

Variables of type double

airVolume—volume of all the air inside the building, V_{air} (m^3)

aptDimensionA—width of the building footprint entered by user, W (m)

aptDimensionB—depth of the building footprint entered by user, D (m)

coolingDD—number of cooling degree days in the year ($^{\circ}\text{C}\text{-day}$)

gmtOffset—difference in time between building locality and Greenwich Mean Time, GMTDiff (hr)

h_eff_floor_in—effective convection coefficient on the inside surface of the ground floor, $h_{\text{eff, floor}}$ ($\text{W}/\text{m}^2\text{K}$)

h_eff_lumped_bottom—effective convection coefficient on the bottom surface of an internal floor, $h_{\text{eff, int floor, bottom}}$ ($\text{W}/\text{m}^2\text{K}$)

h_eff_lumped_top—effective convection coefficient on the top surface of an internal floor, $h_{\text{eff, int floor, top}}$ ($\text{W}/\text{m}^2\text{K}$)

h_eff_roof_in—effective convection coefficient on the inside surface of the roof, $h_{\text{eff, roof}}$ ($\text{W}/\text{m}^2\text{K}$)

h_eff_roof_out—effective convection coefficient on the outside surface of the roof, h_{eff} ($\text{W}/\text{m}^2\text{K}$)

h_eff_wall_in—effective convection coefficient on the inside surface of the exterior walls, $h_{\text{eff, wall}}$ ($\text{W}/\text{m}^2\text{K}$)

h_eff_wall_out—effective convection coefficient on the outside surface of the exterior walls, h_{eff} ($\text{W}/\text{m}^2\text{K}$)

heatingDD—number of heating degree days in the year, HDD ($^{\circ}\text{C}\text{-day}$)
 heightPerFloor—height of each floor of the building entered by the user, HPF (m)
 internalGains—total internal gains from occupants, appliances, etc., Q_{gain} (W)
 latitude—latitude of the city chosen by user from the weather data file, L (decimal degrees)
 longitude—longitude of the city chosen by user from the weather data file, LON (decimal degrees)
 monthlyCoolingEnergy[$NUMMONTHS$]—array to store the total cooling energy for each month of the year after it has been solved for (J)
 monthlyHeatingEnergy[$NUMMONTHS$]—array to store the total heating energy for each month of the year after it has been solved for (J)
 openWindowACH—number of air changes per hour, ACH , when the windows are open (hr^{-1})
 perimeterLossCoeff—slab perimeter loss coefficient, F (W/mK)
 slabPerimeter—perimeter of the slab on grade floor, P (m)
 solarAttenCoeff—interior solar attenuation coefficient, IAC
 summerACH—number of air changes per hour, ACH , for the summer months (hr^{-1})
 wall1WindowPercentage—percentage of wall 1 that is covered by windows, $WP_{\text{wall 1}}$ (%)
 wall2WindowPercentage—percentage of wall 2 that is covered by windows, $WP_{\text{wall 2}}$ (%)
 wall3WindowPercentage—percentage of wall 3 that is covered by windows, $WP_{\text{wall 3}}$ (%)
 wall4WindowPercentage—percentage of wall 4 that is covered by windows, $WP_{\text{wall 4}}$ (%)
 winterACH—number of air changes per hour, ACH , for the winter months (hr^{-1})
 yearlyCoolingEnergy—stores the total cooling energy for the entire year after it has been solved for (J)
 yearlyHeatingEnergy—stores the total heating energy for the entire year after it has been calculated (J)

Variables of type double*

rhs—pointer to array storing the right-hand side of the energy balance equations in the floating indoor air temperature regime, $\mathbf{BT}+\mathbf{C}$ (W/m^2)
 rhsFixedT—pointer to array storing the right-hand side of the energy balance equations in the fixed indoor air temperature regime, $\mathbf{BT}+\mathbf{C}$ (W/m^2)
 temp—pointer to array storing most recent set of nodal temperatures, $\hat{\mathbf{T}}$ ($^{\circ}\text{C}$)

tempPrevious—pointer to array storing the previous set of nodal temperatures, T ($^{\circ}\text{C}$)

Variables of type double**

matrixCooling—pointer to two-dimensional array storing the coefficients for the unknown set of nodal temperatures at the next time step in the system of energy balance equations when the indoor air temperature is floating in the cooling season, \mathbf{A} ($\text{W}/\text{m}^2\text{K}$)

matrixCoolingFixedT—pointer to two-dimensional array storing the coefficients for the unknown set of nodal temperatures at the next time step in the system of energy balance equations when the indoor air temperature is fixed in the cooling season, \mathbf{A} ($\text{W}/\text{m}^2\text{K}$)

matrixHeating—pointer to two-dimensional array storing the coefficients for the unknown set of nodal temperatures at the next time step in the system of energy balance equations when the indoor air temperature is floating in the heating season, \mathbf{A} ($\text{W}/\text{m}^2\text{K}$)

matrixHeatingFixedT—pointer to two-dimensional array storing the coefficients for the unknown set of nodal temperatures at the next time step in the system of energy balance equations when the indoor air temperature is fixed in the heating season, \mathbf{A} ($\text{W}/\text{m}^2\text{K}$)

matrixOpenWindows—pointer to two-dimensional array storing the coefficients for the unknown set of nodal temperatures at the next time step in the system of energy balance equations when the indoor air temperature is floating and the windows are open, \mathbf{A} ($\text{W}/\text{m}^2\text{K}$)

Variables of type HourArray

airChangeEnergy—load to the indoor air due to air changes over a given hour (J)

diffHorRad—diffuse solar radiation received on a horizontal surface from the weather data file, $E_{\text{diff,horiz}}$ (W/m^2)

dirNormRad—direct normal solar radiation on a surface perpendicular to the sun's rays from the weather data file, E_{DN} (W/m^2)

globalHorRad—total direct and diffuse radiation received by a horizontal surface from the weather data file, $E_{\text{global,horiz}}$ (W/m^2)

lumpedMassEnergy—total load to the indoor air from the interior floors over a given hour (J)

outsideTemp—outside temperature for each hour of the year, T_{out} ($^{\circ}\text{C}$)

radiationOnFloor—total solar heat flux transmitted by the glazing system and absorbed by the floor, $q_{\text{sun,floor}}$ (W/m^2)

slabLossEnergy—energy transfer through the slab on grade floor over a given hour, q_{slab} (W)
totalEnergy—total load to the indoor air from all sources over a given hour (J)

Variables of type int

“User choice” in this section indicates an integer corresponding to an index of the selection chosen from a list box. This index is used to set another variable to the appropriate value.

airChangeChoice—user choice for quality of installation and materials
aptPerFloor—number of apartments on each floor of the building
cityChoice—user choice for city in which the building is located
floorNodes—total number of nodes in all of the ground floor layers
insulationThicknessChoice—user choice for insulation thickness
insulationTypeChoice—user choice for insulation type
lumpedMassNodes—total number of nodes in all of the interior floor layers
nodesPerWall—total number of nodes in all of the exterior wall layers
numFloorLayers—number of layers in the ground floor
numLumpedMassLayers—number of layers in the interior floors
numOfFloors—number of floors in the building input by the user
numRoofLayers—number of layers in the roof
numWallLayers—number of layers in the exterior walls
overhangChoice—user choice for overhangs above S, SE, and SW facing windows
roofInsulationChoice—user choice for roof insulation thickness
roofNodes—total number of nodes in all of the roof layers
seasonChangeAtHour[2]—indicates the two hours of the year at which the season changes
 from heating to cooling or vice versa for the selected city
totalNodes—total number of nodes in the building
wallChoice—user choice for wall construction
wall1DirectionChoice—user choice for wall 1 orientation
windowChoice—user choice for type of windows

Variables of type int*

indxCooling—pointer to index vector used in LU decomposition of matrixCooling

indxCoolingFixedT—pointer to index vector used in LU decomposition of
matrixCoolingFixedT

indxHeating—pointer to index vector used in LU decomposition of matrixHeating

indxHeatingFixedT—pointer to index vector used in LU decomposition of
matrixHeatingFixedT

indxOpenWindows—pointer to index vector used in LU decomposition of
matrixOpenWindows

Variables of type bool

east—true if selected city is in the eastern hemisphere (based on longitude from data file)

heatInJanuary—true if January is part of the heating season for the selected city

north—true if selected city is in the northern hemisphere (based on latitude from data file)

slabInsulation—true if the slab on grade floor has perimeter insulation 0.95 K-m²/W

Variables of type CSurface*

pFloor—pointer to the floor surface variable

pRoof—pointer to the roof surface variable

pWall1—pointer to the wall 1 surface variable

pWall2—pointer to the wall 2 surface variable

pWall3—pointer to the wall 3 surface variable

pWall4—pointer to the wall 4 surface variable

Variables of type LayerProperties

The data type LayerProperties contains material properties, thickness, and number of nodes for a thermally massive layer

floorLayers[maxLayers]—array to store the properties of the floor layers

lumpedMassLayers[maxLayers]—array to store the properties of the interior floor layers

roofLayers[maxLayers]—array to store the properties of the roof layers

wallLayers[maxLayers]—array to store the properties of the exterior wall layers

Variables of type InsulationLayer

The data type `InsulationLayer` stores the layer thickness and thermal conductivity for a lightweight layer.

`floorInside[maxLayers]`—array to store properties of the lightweight layers inside the ground floor

`roofInside[maxLayers]`—array to store properties of the lightweight layers inside the roof

`roofOutside[maxLayers]`—array to store the properties of the lightweight layers outside the roof

`lumpedThermalMassBottom[maxLayers]`—array to store the properties of the lightweight layers below the interior floors

`lumpedThermalMassTop[maxLayers]`—array to store the properties of the lightweight layers above the interior floors

`wallInside[maxLayers]`—array to store the properties of the lightweight layers inside the exterior walls

`wallOutside[maxLayers]`—array to store the properties of the lightweight layers outside the exterior walls

Functions of type void

`calculateNodeTempsAndLoads()`—contains all of the logic for running the simulations.

This function switches between fixed and floating indoor air temperatures, heating and cooling seasons, etc. It also calls the functions to set up the matrices and LU decomposition. Implemented in `LoadCalcs.cpp`

`calculateLoads(int i, double ACHterm, double slabF)`—called after the nodal temperatures are calculated when the indoor temperature is fixed to calculate the load on the indoor air.

Implemented in `LoadCalcs.cpp`

`calculateSolarAngles(HourArray altitude, HourArray azimuth)`—calculates the solar altitude and azimuth for each hour of the year at the building locality. Implemented in `Building.cpp`

`calculateTotalEnergy()`—called from outside of the class to start the calculation process. It calls functions to calculate incident solar radiation on each surface, then calls `calculateNodeTempsAndLoads`, and finally fills the variables that store the total energy values. Implemented in `Building.cpp`

`copyVector(int n, double copyFrom[], double copyTo[])`—simply copies a given number of elements from one vector into another vector. Implemented in `LoadCalcs.cpp`

`fillCoefficientMatrix(double** coeffMatrix, double ACHterm, double slabF)`—sets up the coefficient matrix based on layer information and the energy balance equations. Implemented in `Matrices.cpp`

`fillRhsVector(int index, double ACHterm, double slabF, double iac)`—sets up the right-hand side vector for floating indoor temperatures based on layer information and the energy balance equations. Implemented in `Matrices.cpp`

`fillRhsVectorFixedT(int index, double T_in, double iac)`—fills the right-hand side vector for fixed indoor temperatures based on layer information and the energy balance equations. Implemented in `Matrices.cpp`

`findInitialNodeTemps()`—calculates steady state nodal temperatures based on outdoor conditions for the first hour of the year to use as a starting point in the simulation. Implemented in `Matrices.cpp`

`getWeatherData(int cityChoice)`—parses the weather data file. Implemented in `Building.cpp`

`initialize()`—sets up surfaces, layer information, and other variables based on values input by the user. Implemented in `Building.cpp`

`LU(double** A, int n, int* piv)`—performs LU decomposition. Implemented in `LU-Decomp.cpp`

`setValues(int inCityChoice, int inWindowChoice, double inAptDimA, double inAptDimB, double inHeightPerFloor, double inWall1WindowPercentage, double inWall2WindowPercentage, double inWall3WindowPercentage, double inWall4WindowPercentage, int inAptPerFloor, int inNumOfFloors, int inWall1DirectionChoice, int inAirChangeChoice, int inOverhangChoice, int inWallChoice, int inInsTypeChoice, int inIntThickChoice, int inRoofInsulationChoice)`—sets variables whose values come directly from user input. Implemented in `Building.cpp`

`solve(double** LU_, int n, int* piv, double b[])`—solves the system of energy balance equations for the current right hand side vector using the already decomposed matrix. Implemented in `LU-Decomp.cpp`

Functions of type double

These functions all grant “read-only” access to private variables from outside the class.

getDiffHorRad(int i)—accesses diffHorRad[i]. Implemented in Building.h

getDirNormRad(int i)—accesses dirNormRad[i]. Implemented in Building.h

getGlobalHorRad(int i)—accesses globalHorRad[i]. Implemented in Building.h

getMonthlyCoolingEnergy(int i)—accesses monthlyCoolingEnergy[i]. Implemented in Building.h

getMonthlyHeatingEnergy(int i)—accesses monthlyHeatingEnergy[i]. Implemented in Building.h

getOutsideTemp(int i)—accesses outsideTemp[i]. Implemented in Building.h

getYearlyCoolingEnergy()—accesses yearlyCoolingEnergy. Implemented in Building.h

getYearlyHeatingEnergy()—accesses yearlyHeatingEnergy. Implemented in Building.h

class CSurface

Variables of type double

absorptivity—solar absorptivity of the surface, α

emissivity—emissivity of the surface, ε

groundViewFactor—view factor between the surface and the ground

shgc[7]—solar heat gain coefficient for incident angles of 0°, 40°, 50°, 60°, 70°, 80°, and diffuse radiation, $SHGC(\theta)$ and $SHGC_{diff}$

surfaceAngle—surface orientation angle (S = 0°, E = -90°, W = 90°, N = 180°, etc.), ψ (decimal degrees)

surfaceArea—total area of the surface excluding windows, various A terms (m^2)

tiltAngle—tilt angle of the surface (horizontal = 0°, vertical = 90°), Σ (decimal degrees)

viewFactor—view factor between the surface and the sky

windowArea—area of the surface covered by windows, A_{window} (m^2)

windowU—overall heat transfer coefficient for the windows on the surface, U (W/m^2K)

Variables of type HourArray

incidentAngle—incident angle of the sun on the surface, θ (decimal degrees)

incidentDiffRad—incident diffuse radiation on the surface, $E_{\text{diff,ground}} + E_{\text{diff,sky}}$ (W/m^2)

incidentNormalRad—incident direct normal radiation on the surface, E_D (W/m^2)

solAirTemp—sol-air temperature at the surface, $T_{\text{sol-air}}$ ($^{\circ}\text{C}$)

tanHorProjAng—tangent of the horizontal projection angle on the surface, $\tan \Omega$

tanVertProjAng—tangent of the vertical projection angle on the surface, $\tan \Delta$

wallEnergy—load to the indoor air from the surface (J)

windowEnergy—load to the indoor air from the glazed portion of the surface, q_{glazing} (J)

Variables of type bool

windowOverhangs—true if the surface has overhangs above its windows

Functions of type void

calculateIncidentAngles(const HourArray altitude, const HourArray azimuth)—
computes the incident angle of the sun on the surface for each hour of the year.

Implemented in Surface.cpp

calculateSolarRad()—calculates incident normal and diffuse radiation on the surface as well
as the sol-air temperature for each hour of the year. Implemented in Surface.cpp

setVariables(double inSurfaceAngle, double inTiltAngle, double inAbsorptivity, double
inEmissivity, double inWindowU, double inShgc[], double inWindowArea, double
inSurfaceArea, bool inWindowOverhangs)—sets the necessary variables for the walls
and roof. This function is called from CBuilding::initialize(). Implemented in Surface.cpp

setVariables(double inSurfaceArea)—sets the necessary variables for the ground floor.

This function is called from CBuilding::initialize(). Implemented in Surface.cpp

Functions of type double

interpolateSHGC(int index)—calculates the solar heat gain coefficient to use by linear
interpolation when the incident angle is between the values given in shgc[7]. Implemented
in Surface.cpp

sunlitWindowArea(int index)—calculates the portion of the window area that is sunlit (as
opposed to in the shade). The effects of overhangs are incorporated through this function.
Implemented in Surface.cpp

Sequence of function calls when a Save button is clicked

CBuilding::setValues, CBuilding::initialize, CBuilding::calculateTotalEnergy

Obtaining the Program and Contact Information

At the time of this writing, the permanent location of the program has not been determined. Check for a link at <http://chinahousing.mit.edu>. To request a copy of the source code or ask questions about any problems obtaining the program, please use the email addresses below:

Author: jysmith@alum.mit.edu

Dr. Leon Glicksman, thesis supervisor: glicks@mit.edu